GEMS & GEMOLOGY

VOLUME XXXII FALL 1996

THE QUARTERLY JOURNAL OF THE GEMOLOGICAL INSTITUTE OF AMERICA

GEMS & GEMOLOGY

FALL 1996 VOLUME 32 NO. 3

TABLE OF CONTENTS

pg. 159

pg. 176

pg. 187

pg. 209

153 **EDITORIAL**

Opening Pandora's Black Box
Richard T. Liddicoat, Editor-in-Chief

154 **LETTERS**

FEATURE ARTICLES

156 **De Beers Natural versus Synthetic Diamond Verification Instruments**
Christopher M. Welbourn, Martin Cooper, and Paul M. Spear

170 **Introduction to Analyzing Internal Growth Structures: Identification of the Negative *d* Plane in Natural Ruby**
Christopher P. Smith

186 **Russian Flux-Grown Synthetic Alexandrite**
Karl Schmetzer, Adolf Peretti, Olaf Medenbach, and Heinz-Jürgen Bernhardt

REGULAR FEATURES

203 **1996 Challenge Winners**
204 **Gem Trade Lab Notes**
214 **Gem News**
223 **Book Reviews**
225 **Gemological Abstracts**

ABOUT THE COVER: Responding to trade concerns about the possible commercial availability of cuttable-quality synthetic diamonds, De Beers researchers in Maidenhead, England, have developed two types of machines—the DiamondSure and the DiamondView—to separate natural from synthetic diamonds. These new instruments are the focus of the lead article in this issue, by Christopher Welbourn, Martin Cooper, and Paul Spear.

The natural-diamond rings shown here contain round brilliants weighing a total of 5.19 ct (top), 4.38 ct (left), 5.36 ct (bottom), and (right) 6.78 ct with a 3.49 ct yellow emerald-cut diamond. Courtesy of Hans D. Krieger, Idar-Oberstein, Germany.

Photo © Harold & Erica Van Pelt—Photographers, Los Angeles, CA.

Color separations for Gems & Gemology *are by Effective Graphics, Compton, CA. Printing is by Cadmus Journal Services, Baltimore, MD.*

ISSN 0016-626X

GEMS & GEMOLOGY

SUBSCRIPTIONS

Subscriptions in the U.S.A. are priced as follows: $59.95 for one year (4 issues), $149.95 for three years (12 issues). Subscriptions sent elsewhere are $70.00 for one year, $180.00 for three years.

Special annual subscription rates are available for all students actively involved in a GIA program: $49.95, U.S.A.; $60.00, elsewhere. Your student number *must* be listed at the time your subscription is entered.

Single issues may be purchased for $15.00 in the U.S.A., $18.00 elsewhere. Discounts are given for bulk orders of 10 or more of any one issue. A limited number of back issues of *G&G* are also available for purchase.
Please address all inquiries regarding subscriptions and the purchase of single copies or back issues to the Subscriptions Department.

To obtain a Japanese translation of *Gems & Gemology*, contact the Association of Japan Gem Trust, Okachimachi Cy Bldg., 5-15-14 Ueno, Taito-ku, Tokyo 110, Japan. Our Canadian goods and service registration number is 126142892RT.

MANUSCRIPT SUBMISSIONS

Gems & Gemology welcomes the submission of articles on all aspects of the field. Please see the Guidelines for Authors in the Summer 1996 issue of the journal, or contact the editor for a copy. Letters on articles published in *Gems & Gemology* and other relevant matters are also welcome.

Gems & Gemology is published quarterly by the Gemological Institute of America, a nonprofit educational organization for the jewelry industry, 1660 Stewart Street, Santa Monica, CA 90404.

Postmaster: Return undeliverable copies of *Gems & Gemology* to 1660 Stewart Street, Santa Monica, CA 90404.

OPENING PANDORA'S BLACK BOX

· *Richard T. Liddicoat, Editor-in-Chief*

In this era of increasingly sophisticated synthetic materials and forms of enhancement, gemologists need every possible weapon in their testing arsenal. To this end, this issue of *Gems & Gemology* offers two articles relating to new methods of identification. One describes two instruments designed by De Beers researchers to help identify synthetic diamonds. These instruments successfully address a need and desire for quick, easy, and reliable diamond testing in a fast-paced, competitive world. Thus, they represent a growing trend in gemology toward "black box" methodology, which can be practiced with a minimum of skill and technical knowledge. Although such instruments provide a great service to our industry, there are some problems for which no "black box" may ever be available, that to date have been solved only by using expensive instrumentation in a well-staffed laboratory. Foremost among these are the separation of some natural and synthetic rubies, sapphires, and emeralds. The second article, by the Gübelin Laboratory's Christopher Smith, involves an identification technique that may seem esoteric to some readers, but is actually closer to "grass roots" gemology. Internal growth-structure analysis (that is, analysis of features such as twinning and crystal planes within a cut natural or synthetic stone that reflect its distinctive growth history) requires relatively little new equipment. It does, however, call for the unique talents of the professional gemologist.

There are many levels of need among gemologists. Those operating in a well-financed testing laboratory may have the resources and space to consider X-ray, ultraviolet, infrared, and Raman spectroscopy—and/or other systems costing $100,000 or more. A well-equipped electron microprobe can cost over a million dollars. Most gemologists, however, have neither the finances nor the space to consider much more than a binocular microscope, refractometer, polariscope, desk-model spectroscope, and a few other relatively small and inexpensive items. As recently as the middle of this century, amateur gemologist Count E. C. R. Taaffe recognized that he had something hitherto unknown—the first taaffeite—using only a loupe and other rudimentary equipment. He lacked even a refractometer.

Although any gemologist with access to extensive testing instrumentation may benefit from internal growth-structure analysis, it is of particular value to the gemologist in the office, the jewelry store, the small laboratory. First introduced to gemology by Karl Schmetzer, its advantage is that it requires only a binocular microscope and a few accessories that can be purchased or even created by modifying equipment on hand. Such a method may require extensive and time-consuming "jury-rigging" (at relatively minor expense), but it can yield information as essential as that provided by the most sophisticated instrumentation. However, it depends heavily on the most important of all gemological tools: the gemologist's own knowledge, skill, and meticulous practice in testing.

We can be thankful whenever a veritable "black box" is designed to meet one of our testing challenges. But when none is available, there is no substitute for creative gemology. ❑

LETTERS

THE OBSERVATION OF MAGNETISM IN SYNTHETIC DIAMOND

"A Chart for the Separation of Natural and Synthetic Diamonds," by J. Shigley et al. [Winter 1995, pp. 256–264] is one of the jewelry trade's most useful reference aids. The article dealt with the range of indicator tests available to the jeweler/gemologist, one of which is magnetism. The article spawned two responses, which were published in the Spring 1996 "Letters" section (p. 63). Both Dr. Hanneman's original letter and the reply by GIA Gem Trade Laboratory Vice-President Tom Moses describe methods for observing magnetism in a gemstone, but both have their drawbacks.

Suspending a gemstone on a fine thread, and bringing a powerful magnet close, does enable observation of the slightest magnetic response, but great care is required, inasmuch as just the observer's breathing can induce movement of the stone. Attaching the specimen to the thread with Blu-Tack or Stik-Tack is courting disaster, for both products induce a magnetic response!

In my 1992 Tucson lectures on the magnetism test, I suspended an elastic band from the thread, and the band acted as a cradle to support the stone. In 1995, I demonstrated two tests, using a ring set with a De Beers experimental synthetic diamond. In one test, I simply tied a fine thread through the ring shank and brought the magnet close; in the second test, I floated the ring on a polystyrene raft in a small basin of water. In both cases, the ring was drawn to the magnet. Australian gemologist Rod Brightman suspends the rare-earth magnet and brings the jewel close.

In my experience, these tests work for most of the known synthetic diamonds, including those from De Beers, General Electric, and Russia. However, I have not observed any such response in Sumitomo synthetic diamonds.

Dr. Jeff Harris, at Glasgow University, indicated that the iron sulphide minerals pyrrhotite and pentlandite would show a magnetic response in a natural diamond, and together we observed the slightest of responses from such mineral inclusions in natural diamond when the stone was floated on a tiny (5 × 5 mm) polysterene raft. Fortunately for the gemologist, such inclusions are black, and they are almost always accompanied by stress fractures that are also filled with black mineral films. (Metallic inclusions in synthetic diamonds do not exhibit stress fractures.) Even when large, such natural inclusions produce only the slightest response. In contrast, the synthetic's inclusions induce a distinct response even when they are dust-like. When such inclusions are large, an unset synthetic diamond may jump 6 mm or more off a surface to reach the rare-earth magnet.

Readers might also like to know of a synthetic diamond demonstration last November at the Seattle (Washington) chapter of the GIA Alumni & Associates and the Canadian Gemmological Association Conference. A faceted blue synthetic diamond (courtesy of De Beers) phosphoresced for at least 12 hours after 30 minutes' exposure to shortwave ultraviolet radiation. Subsequent carefully controlled observations showed that the phosphorescence lasted 11 days!

ALAN HODGKINSON
Ayrshire, Scotland

Editor's note: We contacted Mr. Moses, who had mentioned Blu-Tack in his Spring 1996 issue reply to Dr. Hanneman's letter. He confirmed that he has seen a magnetic reaction in some Blu-Tack, but only when the Blu-Tack is noticeably dirty or discolored, in which case it should be replaced.

MORE ON THE HISTORY OF DIAMOND SOURCES

It was with great pleasure that I read the two-part article "A history of diamond sources in Africa" [Winter 1995 and Spring 1996, pp. 228–255 and 2–30, respectively]. Dr. Janse did an excellent job of condensing the most important historical events that have taken place during the more than 130 years since the first diamond finds were made in South Africa.

For those *G&G* readers with an avid interest in the early years of South Africa's development following the initial diamond finds, I would like to add a reference to Dr. Janse's extensive bibliography: *South Africa's City of Diamond: Mine Workers and Monopoly Capitalism in Kimberley, 1867–1895*, by Dr. William H. Worger [Yale University Press, New Haven and London, 330 pp.]. I found it to be a fascinating factual account of the hardships experienced by those involved in the diamond industry during this formative period. It also looks at the impact of the diamond discoveries on South Africa, and Kimberley in particular, both culturally and economically.

I highly recommend this book to any gemologist, jeweler, or hobbyist who is intrigued by the history and development of the diamond industry.

CHRISTOPHER P. SMITH
Manager of Laboratory Services
Gübelin Gemmological Laboratory
Lucerne, Switzerland

In Reply

I thank Christopher Smith for his kind words about my articles. I have a copy of Dr. Worger's book in my library and, although the socio-economic background of early diamond mining was beyond the scope of my papers, I agree that this provides an excellent overview. For further information in this area, I would add *Capital and Labour in the Kimberley Diamond Fields 1871–1890*, by Dr. Robert V. Turrell [Cambridge University Press, New York and London, 1987, 297 pp.], and the more readable *Kimberley, Turbulent City*, by Brian Roberts [O. Phillip, Cape Town, in Association with the Historical Society of Kimberley and the Northern Cape, 1976, 413 pp.].

I take this opportunity to thank the many readers for their complimentary remarks on these articles.

A. J. A. JANSE, PH.D.
Archon Exploration Pty Ltd
Perth, Australia

CORRECTION

In the article "Russian Demantoid, Czar of the Garnet Family," by W. R. Phillips and A. S. Talantsev [Summer 1996], the identification of the yellow fibrous inclusions [often described as "horsetails," "tousled children's hairs," or "emanating from chromite grains"] was incorrectly attributed. These asbestiform inclusions—for many years believed to be byssolite—were identified as chrysotile, a variety of serpentine, by Dr. Edward J. Gübelin. He first reported the results of his analyses at the October 1992 International Gemmological Conference in Paris. The identification was made by means of SEM for the chemical composition and X-ray diffraction analysis for the crystal structure.

De Beers Natural versus Synthetic Diamond Verification Instruments

By Christopher M. Welbourn, Martin Cooper, and Paul M. Spear

Two instruments have been developed at De Beers DTC Research Centre, Maidenhead, to distinguish synthetic diamonds from natural diamonds. The DiamondSure™ enables the rapid examination of large numbers of polished diamonds, both loose and set in jewelry. Automatically and with high sensitivity, this instrument detects the presence of the 415 nm optical absorption line, which is found in the vast majority of natural diamonds but not in synthetic diamonds. Those stones in which this line is detected are "passed" by the instrument, and those in which it is not detected are "referred for further tests." The DiamondView™ produces a fluorescence image of the surface of a polished diamond, from which the growth structure of the stone may be determined. On the basis of this fluorescence pattern—which is quite different for natural as compared to synthetic diamonds—the trained operator can positively identify whether a diamond is natural or synthetic.

ABOUT THE AUTHORS

Dr. Welbourn is Principal Scientist and Dr. Spear is a Research Scientist in the Physics Department at De Beers DTC Research Centre, Belmont Road, Maidenhead, Berkshire, SL6 6JW, United Kingdom. Mr. Cooper is Research Director of De Beers DTC Research Centre.

Please see acknowledgments at the end of article.

Gems & Gemology, *Vol. 32, No. 3, pp. 156–169.*

The subject of cuttable-quality synthetic diamonds has been receiving much attention in the gem trade recently. Yellow to yellow-brown synthetic diamonds grown in Russia have been offered for sale at a number of recent gem and jewelry trade shows (Shor and Weldon, 1996; Reinitz, 1996; Johnson and Koivula, 1996), and a small number of synthetic diamonds have been submitted to gem grading laboratories for identification reports (Fryer, 1987; Reinitz, 1996; Moses et al., 1993a and b; Emms, 1994; Kammerling et al., 1993, 1995; Kammerling and McClure, 1995). Particular concern was expressed following recent announcements of the production and planned marketing of near-colorless synthetic diamonds (Koivula et al., 1994; "Upfront," 1995).

Synthetic diamonds of cuttable size and quality, and the technology to produce them, are not new. In 1971, researchers at the General Electric Company published the results of their production of synthetic diamond crystals up to 6 mm average diameter by the high-pressure temperature-gradient technique using "belt"-type presses (Wentorf, 1971; Strong and Chrenko, 1971; Strong and Wentorf, 1971). These included not only yellow-brown synthetic diamonds but also reduced-nitrogen near-colorless crystals and boron-doped blue crystals (Crowningshield, 1971). In 1985, Sumitomo Electric Industries Ltd., in Japan, started marketing their Sumicrystal™ range of yellow-brown synthetic diamonds; in 1993, they produced high-purity (i.e., near-colorless) synthetic diamond crystals fabricated into diamond "windows." De Beers Industrial Diamond Division (Pty) Ltd. has marketed its Monocrystal range of yellow-brown synthetic diamonds since 1987. None of these three manufacturers has marketed synthetic diamonds for other than industrial or technical applications.

Figure 1. Like their predecessors in many other gem materials, cuttable-quality synthetic diamonds pose a potential threat in the diamond marketplace. To protect the integrity of natural diamonds should significant numbers of synthetic diamonds ever enter the trade, De Beers DTC Research Centre has designed and built two types of instruments—the DiamondSure and the DiamondView—that, together, can successfully identify all synthetic diamonds produced by current synthesis equipment. This figure shows, bottom center and to the right, six De Beers experimental synthetic diamonds: two yellow-brown samples weighing 1.04 and 1.56 ct and four near-colorless synthetics ranging from 0.41 to 0.91 ct. At the top center and to the left are six natural diamonds, ranging from 1.10 ct to 2.59 ct. It is substantially more difficult and costly to grow near-colorless synthetic diamonds than to grow the more usual yellow-brown crystals. De Beers cuttable-quality synthetic diamonds are not available commercially; they have been produced solely for research and education. Natural diamonds courtesy of Louis P. Cvelbar and Vincent Kong, Vincent's Jewelry, Los Angeles. Photo © GIA and Tino Hammid.

In 1990, researchers from Novosibirsk, Russia, published their work on the temperature-gradient growth of synthetic diamonds in relatively small-scale, two-stage multi-anvil presses known as "split-sphere" or "BARS" systems (Pal'yanov et al., 1990). Since then, there have been a number of reports of various groups within Russia intending to set up BARS presses for the purpose of synthesizing diamond. Usually, only one crystal is grown in a BARS press at any one time, whereas many stones can be grown simultaneously in the larger "belt" presses.

Gemologists from GIA and other gemological laboratories have extensively examined synthetic diamonds from each of the above-mentioned manufacturers. Gemological characteristics of these synthetics have been published in a series of articles in *Gems & Gemology* (Crowningshield, 1971; Koivula and Fryer, 1984; Shigley et al., 1986, 1987, 1992; Rooney et al., 1993; Shigley et al., 1993a and b) and elsewhere (Sunagawa, 1995). The conclusion drawn from these studies is that all of the synthetic diamonds examined to date can be positively identified by the use of standard gemological techniques. These results have been summarized in "A Chart for the Separation of Natural and Synthetic Diamonds," published by GIA (Shigley et al., 1995).

The problem facing the gem trade should synthetic diamonds become widespread is that, in gen-

eral, most near-colorless diamonds are examined for grading purposes only, not for identification.

It is to be expected that, in the main, synthetic diamonds would be clearly identified and sold as such by an honest trade working within national laws and regulations. Nevertheless, a small number of synthetic diamonds have already entered the trade without being declared as synthetic. De Beers has long regarded this potential problem as a serious one. For the last 10 years, researchers at De Beers DTC Research Centre have been actively investigating the characteristic features of synthetic diamonds (see, e.g., Burns et al., 1990; Rooney, 1992). This work has been carried out in close collaboration with the De Beers Industrial Diamond Division's Diamond Research Laboratory in Johannesburg, South Africa, which has been developing high-pressure/high-temperature diamond synthesis techniques for industrial applications for over 40 years. One aspect of this work has been the production of experimental cuttable-quality synthetic diamonds (figure 1), with an extensive range of properties, both for research and for loan to the larger gemological laboratories throughout the world to give their staff members an opportunity to develop their own skills and identification techniques. (Note that these synthetic diamonds are not for sale by De Beers. The Monocrystal synthetic diamonds available commercially from De Beers Industrial Diamond Division (Pty) Ltd. are only sold in prepared forms and are not suitable for cutting as gems.) A second aspect has been the development of instruments that, should the need arise, could be made available to help rapidly identify synthetic diamonds. Such instrumentation would be important should near-colorless synthetic diamonds enter the market in significant numbers. If this were to happen, grading laboratories and others in the trade would need to screen substantial numbers of polished diamonds to eliminate the possibility of a synthetic diamond being sold as a natural stone and thus damage consumer confidence in gem diamonds.

Figure 2. The DiamondSure is based on the presence or absence of the 415 nm line in the stone being tested. Here it is shown with its fiber-optic probe mounted vertically for testing loose stones. On completion of a test, which takes about 4 seconds, the liquid-crystal display on the front panel will give a message of "PASS" or "REFER FOR FURTHER TESTS" (or sometimes "INSUFFICIENT LIGHT" if the stone is very dark or very strongly colored yellow or yellow-brown). Photo by M. J. Crowder.

Although such a circumstance would potentially have a profound impact on the conduct of the gem diamond trade, it is important to put the problem into context. The high-pressure apparatus required to grow synthetic diamonds is expensive, as are the maintenance and running costs. In addition, it is substantially more difficult and costly to grow near-colorless synthetic diamonds than it is to grow yellow-brown crystals. To reduce the amount of nitrogen (which gives rise to the yellow-brown color) that is incorporated into the growing crystal, chemicals that preferentially bond to nitrogen are introduced to the synthesis capsule. These chemicals, known as nitrogen "getters," act as impurities which have an adverse effect on the crystal growth process. To the best of our knowledge, the only near-colorless synthetic diamonds to appear on the gem market thus far were 100 Russian-grown crystals displayed at the May 1996 JCK Show in Las Vegas. The largest of these weighed about 0.7 ct, but two-thirds of the crystals weighed 0.25 ct or less. Most of these were not suitable for polishing because of inclusions, internal flaws, and distorted shapes.

Nevertheless, De Beers has considered it prudent to invest substantial resources to address this potential problem and thus ensure that the trade is prepared for this eventuality. This article describes two instruments, developed at De Beers DTC Research Centre, that are capable of screening large

numbers of diamonds and facilitating the rapid and unambiguous identification of synthetic diamonds.

Ideally, the trade would like to have a simple instrument that could positively identify a diamond as natural or synthetic with the same ease as a thermal pen distinguishes between diamonds and non-diamond simulants such as cubic zirconia. Unfortunately, our research has led us to conclude that it is not feasible at this time to produce such an ideal instrument, inasmuch as synthetic diamonds are still diamonds physically and chemically, and their distinguishing features are based on somewhat subtle characteristics involving the presence or absence of various forms of impurities and growth structures. The instruments developed at our Research Centre have been designed to be used in a two-stage procedure. The first instrument, called the *DiamondSure*™ allows the operator to screen large numbers of stones rapidly. This instrument will successfully detect all synthetic diamonds produced by current equipment (including experimental synthetics grown at the Diamond Research Laboratory at extremes of conditions and with non-standard solvent/catalysts). However, a small proportion of natural diamonds will also produce the same response from the instrument. A second stage of examination is therefore required. This could be by standard gemological examination. However, a second instrument has been developed, called the *DiamondView*™, which enables a positive identification to be made quickly and easily[1]. Certain aspects of the design of these instruments are proprietary and so cannot be described in this article. However, we have endeavored to give sufficient information on their operation to show clearly how they may be used to identify synthetic diamonds.

THE DIAMONDSURE™ SCREENING INSTRUMENT

Description. The DiamondSure (figure 2) has been designed for the rapid examination of large numbers of polished diamonds, whether loose or set in jewelry. It is 268 mm long by 195 mm deep by 107 mm high (10.6 × 7.7 × 4.2 ins.), and it weighs 2.8 kg (6.2 lbs.). Measurements are made by placing the table of a polished diamond on the tip of a fiber-optic probe, the diameter of which is 4 mm. For loose stones, the fiber-optic probe is mounted in a vertical position, and a collar is placed around the end of the probe so that stones can easily be positioned over the probe tip (again, see figure 2). The instrument can be used on diamonds mounted in jewelry provided that the table is sufficiently accessible for the probe tip to lie flat against it (see figure 3). When the probe tip is in contact with the table of the diamond being examined, the operator presses the TEST button on the front panel of the instrument or, alternatively, presses the button mounted on the side of the probe. The time required for the instrument to complete a measurement is approximately 4 seconds. It is designed to work with diamonds in the 0.05–10 ct range. This size range is determined by the diameter of the fiber tip, because the instrument responds to the light that is retro-reflected by the cut diamond and re-enters the probe tip. Should the need arise, fibers with larger or smaller diameters could be manufactured to accommodate larger or smaller stones. The instrument is powered by a universal-input-voltage power supply, and so is suitable for use in any country.

Figure 3. The DiamondSure probe can be removed from its mounting to test a diamond in a ring or other setting. Photo by M. J. Crowder.

The instrument automatically measures the intensity of retro-reflected light in a small region of the spectrum centered on 415 nm. Using proprietary software, it compares the intensity data, as a function of wavelength, to the 415 nm optical absorption line typically seen in natural diamond. The measurement is highly sensitive; values of 0.03 absorbance units at the peak of the 415 nm line, relative to a baseline through the absorption-line shoulders, are

[1] *The* DiamondSure *and* DiamondView *instruments are covered worldwide by granted or pending patent applications.*

easily detected. We detected the 415 nm line in over 95% of all natural diamonds tested by the DiamondSure instrument (see Test Samples and Results section, below), but not in any of the synthetic diamonds. If this feature is detected in a stone, the instrument displays the message "PASS." If this feature is not detected, the message "REFER FOR FURTHER TESTS" is displayed. If very dark or very strongly colored yellow or yellow-brown stones are measured, the message "INSUFFICIENT LIGHT" may be displayed. With such stones, the optical absorption in the wavelength range used by the instrument is so strong that practically no light is being returned to the detector. However, in the tests reported in detail in the Test Samples and Results section below, all the yellow-brown synthetic diamonds used—including the largest (2.53 ct) sample—tested successfully. If the "INSUFFICIENT LIGHT" message is obtained with a particularly large stone, repositioning the stone on the probe will often produce a valid measurement. If the probe tip does not lie flat against the table, the light detected may be composed mostly of light reflected from the table without entering the diamond. In this case, the instrument would "fail safe" by "referring" the sample.

Although the 415 nm defect is not present in as-grown synthetic diamonds, it can be formed in nitrogen-containing synthetics by very high-temperature heat treatment in a high-pressure press (Brozel et al., 1978). Temperatures in the region of 2350°C are required, together with a stabilizing pressure of about 85 kbars to prevent graphitization. At these extreme conditions, the lifetime of the expensive tungsten carbide press anvils becomes very short, the diamond surfaces are severely etched, and the likelihood that the diamond will fracture is significant. Given the present technology, it would not, therefore, be commercially practical to heat-treat synthetic diamonds to form sufficient 415 nm defects.

A small proportion of natural diamonds, less than 5% from our tests, do not exhibit the 415 nm feature strongly enough to be detected by the DiamondSure. These include D-color and possibly some E-color diamonds, as well as some brown diamonds. As for diamonds of "fancy" color, the 415 nm line is absent from natural-color blue (type IIb) diamonds, as well as from some fancy yellow and some pink diamonds. When these stones are tested, the DiamondSure displays the message "REFER FOR FURTHER TESTS." It is important to recognize that the fact that these stones were not "passed" by the instrument does not necessarily mean that they are synthetic or in any way less desirable than stones that have been passed. The message simply means that additional testing is required for an identification to be made.

Test Samples and Results. During the development of the DiamondSure, approximately 18,000 polished natural diamonds were tested. In the final phase of testing, which we report here, two instruments from an initial batch of 10 were each used to test a total of 1,808 randomly chosen known natural diamonds. Most of these 1,808 stones weighed between 0.25 and 1.00 ct, although we included some as small as 0.05 ct and some over 10 ct. The largest stone was 15.06 ct, and it tested successfully. Colors were in the D to R range, as well as some browns and some fancy yellows. In these particular tests, all except six stones were round brilliants; in an earlier experiment, though, more than a hundred fancy-shaped stones tested successfully.

The tests were carried out at the London offices of the De Beers Central Selling Organisation. The instruments were used by a number of operators. In general, a combination of daylight and fluorescent lighting was used, but no special care with respect to lighting conditions was necessary. The average figure for "referrals" for these 1,808 diamonds was 4.3%.

In a separate evaluation, we used a third DiamondSure to test 20 D-color stones, of various shapes, ranging from 0.52 to 11.59 ct. Eight of the stones were passed, and 12 were referred. This indicates that, because of its sensitivity, the instrument can detect a very weak 415 nm line even in some D-color stones.

The first two instruments were also tested on a range of De Beers experimental synthetic diamonds. A total of 98 samples were used: 23 in the yellow-brown range, 0.78–2.53 ct; 45 near-colorless, 0.20–1.04 ct; 15 pale-to-vivid yellow, 0.19–0.63 ct; and 15 medium-to-vivid blue, 0.24–0.72 ct. (See figure 1 for examples of the near-colorless and yellow De Beers synthetic diamonds tested.) All of these synthetic diamonds were round brilliants except for one fancy yellow sample, which was an emerald cut. Each was tested 10 times on each instrument. In addition, some yellow and near-colorless Russian BARS-grown synthetic diamonds were tested several times on one of the instruments. In all cases, the synthetic diamonds were "referred for further tests."

THE DIAMONDVIEW™ LUMINESCENCE IMAGING INSTRUMENT

Background: Growth Structure in Synthetic and Natural Diamonds. In the articles cited above on the gemological characteristics of synthetic diamonds, it was noted that the patterns of ultraviolet-excited fluorescence exhibited by synthetic diamonds are quite distinctive and so can be used to positively identify them. The DiamondView rapidly generates these fluorescence patterns—which are produced by differential impurity concentrations between growth sectors and growth bands—and provides clear images of them. With a little experience, it is relatively easy to recognize patterns that are characteristic of natural or synthetic diamonds. With practice, one can obtain and identify the fluorescence images of two or three diamonds per minute.

The reason that fluorescence patterns can be used to identify synthetic diamonds is that the basic growth structure of synthetic diamonds is quite distinct from that of all natural diamonds, and details of these growth structures can be inferred from the fluorescence pattern. Synthetic diamonds grow essentially as cubo-octahedra. The degree of development of cube {100} or octahedral {111} faces depends on a number of parameters, but most notably on the growth temperature. At relatively low growth temperatures, cube growth predominates; whereas at relatively high growth temperatures, the diamond morphology approaches that of an octahedron, although small cube faces are still present (Sunagawa, 1984; see figure 4). For synthetic diamonds grown using pure nickel as the solvent/catalyst, pure cubo-octahedra are produced. However, if other metals are used with or instead of nickel, then minor faces of dodecahedral {110} and trapezohedral {113} orientation also tend to be present (Kanda et al., 1989; see figure 5a). In certain circumstances (e.g., when cobalt is a constituent of the solvent/catalyst, and getters have been used to reduce the nitrogen content), additional trapezohedral {115} faces may be present (Rooney, 1992; Burns et al., 1996). For large synthetic diamonds grown by the temperature-gradient method, growth starts on a seed crystal of synthetic or natural diamond and develops outward and upward, as illustrated in figure 5b. If the crystal shown in figure 5a were to be sectioned along the planes A and B, the growth patterns exposed by these planes would be as shown in figures 5c and d, respectively. (For a comprehensive but easy-to-understand description of the numbers, or Miller indices, used to describe the orientation and position of faces on a crystal, see J. Sinkankas' *Mineralogy*, 1986, pp. 119–127.)

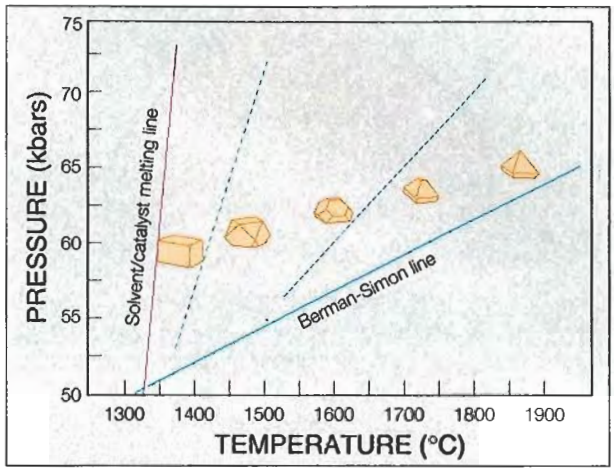

Figure 4. This schematic diagram shows the dependence of synthetic-diamond morphology on growth temperature (after Sunagawa, 1984). The Berman-Simon line separates the region in which diamond is the thermodynamically stable phase and graphite is metastable (above the line) from that where graphite is stable and diamond metastable (below the line). Diamond growth can only occur to the right of the solvent/catalyst melting line. The dashed lines approximately represent regions where similar morphologies are produced, indicating that pressure is also a factor in determining crystal shape.

Those regions of a crystal that have a common growth plane are referred to as growth sectors. As the crystal grows, different growth sectors tend to take up impurities in differing amounts. For instance, nitrogen, the impurity responsible for the yellow to yellow-brown color in synthetic diamonds, is generally incorporated at highest concentrations in {111} growth sectors, with the concentration in {100} sectors being about half that of {111} (Burns et al., 1990). (However, at low growth temperatures, the nitrogen concentration in {100} sectors exceeds that of {111} [Satoh et al., 1990].) Nitrogen levels are substantially lower in the {113} growth sectors and very much lower in the {110} sectors. The polished slice of synthetic diamond shown in figure 6 was cut parallel to the {110} plane, with the seed crystal at the bottom and the {001} face at the top. The variation in nitrogen concentration between growth sectors results in the zonation of the yellow color.

Nickel and cobalt impurities can also be taken up by the growing crystal to form optically active

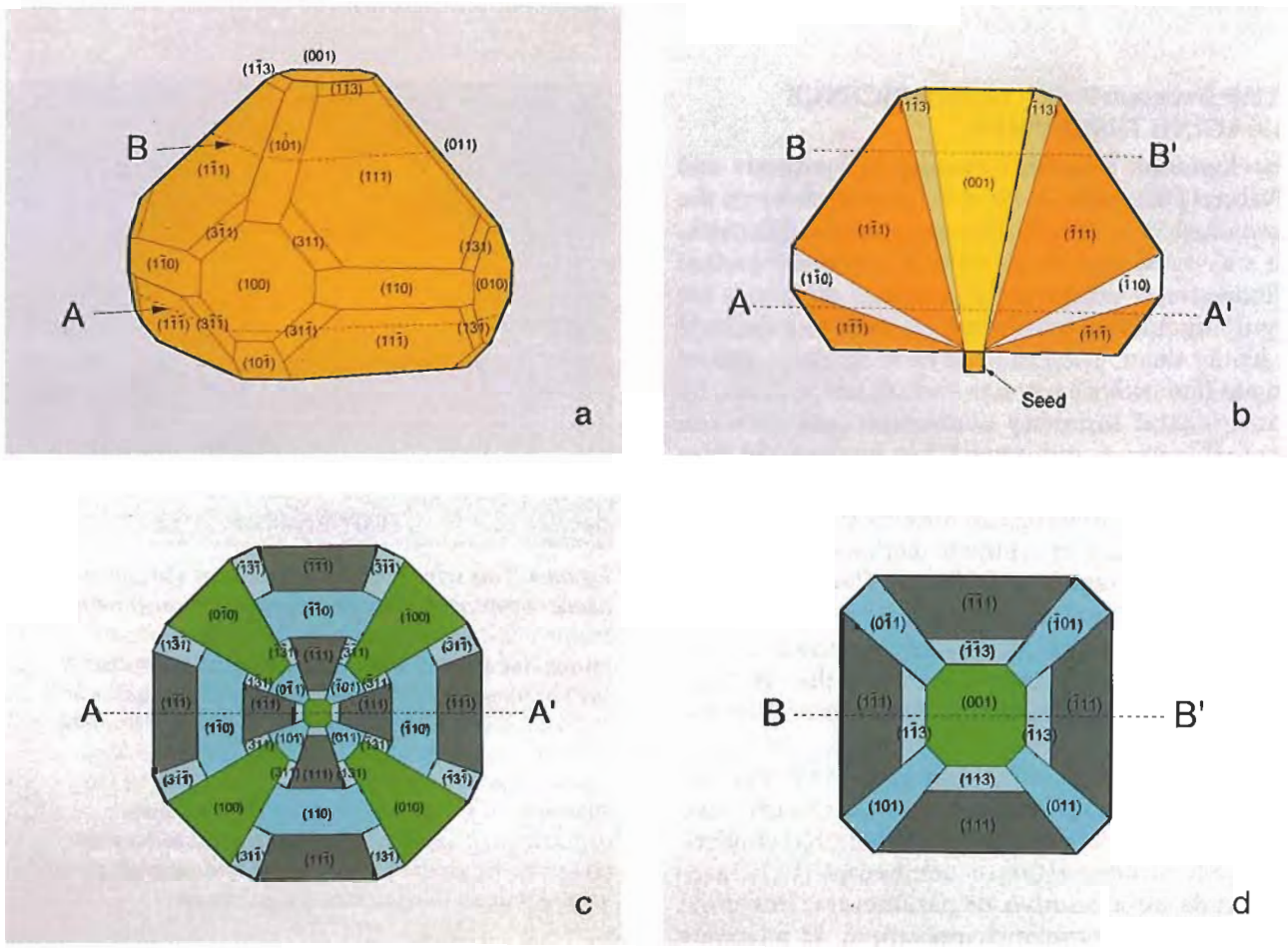

Figure 5. The idealized synthetic diamond crystal, seed-grown by the temperature-gradient method, exhibits major octahedral {111} and cube {100} growth faces, and minor dodecahedral {110} and trapezohedral {113} growth faces (a). A view of the central section parallel to the (110) dodecahedral plane of this same crystal shows the position of the seed at the base of the crystal, from which growth develops outward and upward (b). The variation in color saturation reflects the variation in nitrogen concentration between growth sectors in yellow-brown synthetic diamonds. The fluorescence pattern shown in (c) is that of a section from this synthetic diamond crystal, parallel to the (001) cube plane, indicated by the plane A in (a) and the line A-A′ in (b). In yellow-brown synthetics, {100} sectors tend to fluoresce green, {110} and {113} tend to fluoresce blue. and {111} sectors are usually largely inert. The fluorescence pattern shown in (d) is that of a (001) section indicated by the plane B in (a) and the line B-B′ in (b).

defects, but they are incorporated exclusively in {111} sectors (Collins et al., 1990; Lawson et al., 1996). In low-nitrogen synthetic diamonds, nickel gives rise to a green color; heat-treated cobalt-grown diamonds show a yellow fluorescence. Boron is another impurity that is readily taken up by a growing synthetic diamond. Blue, semi-conducting synthetic diamonds are produced by using chemical getters to reduce nitrogen levels and deliberately introducing boron into the synthesis capsule. Boron concentrations are highest for {111} sectors, next highest in {110} sectors, and substantially lower in other sectors. Even when these impurities are not present in concentrations high enough to influence the color of the crystal, they still can cause fluorescence behavior that varies between growth sectors.

For natural diamonds, the basic form of growth is octahedral. Small natural cubo-octahedral diamonds have been found, but these are very rare (J. W. Harris, pers. comm., 1990). Dodecahedral and trapezohedral flat-faced growth has never been observed in natural diamonds. Rounded dodecahedral diamonds are very common, but these shapes are formed by the dissolution of octahedral diamonds (Moore and Lang, 1974). Figure 7a is a schematic diagram of a natural diamond in which

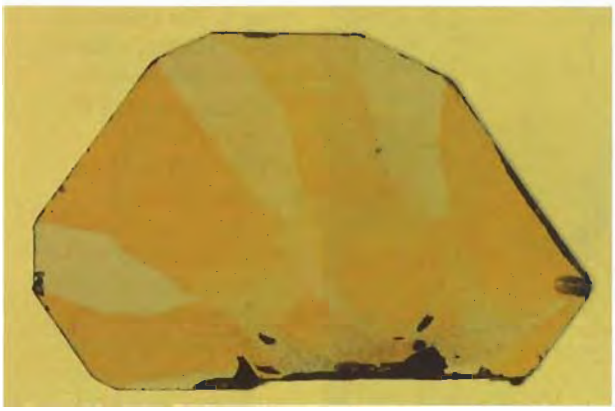

Figure 6. This optical micrograph of a slice cut parallel to the {110} dodecahedral plane from a De Beers yellow-brown synthetic diamond shows the greater concentration of nitrogen (and thus greater saturation of yellow) in the {111} growth sectors than in the {100}, {113}, or {110} growth sectors (again, refer to figure 5b for a diagram of the different growth structures in such a crystal at this orientation). The slice is 5.01 mm across × 3.20 mm high × 0.71 mm thick.

the octahedral faces have undergone partial dissolution so that rounded dodecahedral faces are beginning to form. A schematic diagram of a section through a central cube plane of this idealized crystal is shown in figure 7b.

Dodecahedral faces that appear flat may be found on "coated" diamonds, but here the growth is fibrous and quite distinct from flat-faced {110} growth (Machada et al., 1985).

A form of nonoctahedral growth that is relatively common in natural diamonds is so-called cuboid growth. The mean orientation of cuboid growth is approximately along cube planes, but the growth is hummocky and distinct from flat-faced cube growth. On the rare occasions that cuboid growth is well developed compared to octahedral growth, diamonds with quite spectacular shapes are produced, as is the case with the "cubes" found in the Jwaneng mine (Welbourn et al., 1989). It is not uncommon for otherwise octahedrally grown diamonds to have experienced a limited amount of cuboid growth, particularly on re-entrant octahedral faces. This is shown schematically in figure 7b.

For most natural diamonds, the conditions in which they grew fluctuated over time, so different types and levels of impurities were incorporated at different stages of growth. This resulted in differences in fluorescence behavior between growth bands within the crystal.

Uncut synthetic diamonds can be readily identified by visual inspection because of their crystal morphology and the remnants of the seed crystal present. However, these external features are lost when the stone is polished.

For many years, cathodoluminescence topography has been used to image growth-dependent pat-

Figure 7. In this schematic diagram of (a) the morphology of a typical natural diamond, the octahedral faces, decorated with trigon etch pits, have undergone partial dissolution so that rounded dodecahedral faces are beginning to form. The schematic diagram of the fluorescence pattern from a section through a central cube plane of this idealized crystal (b) shows concentric rectangular bands of octahedral growth and regions where re-entrant features have been overgrown by cuboid growth.

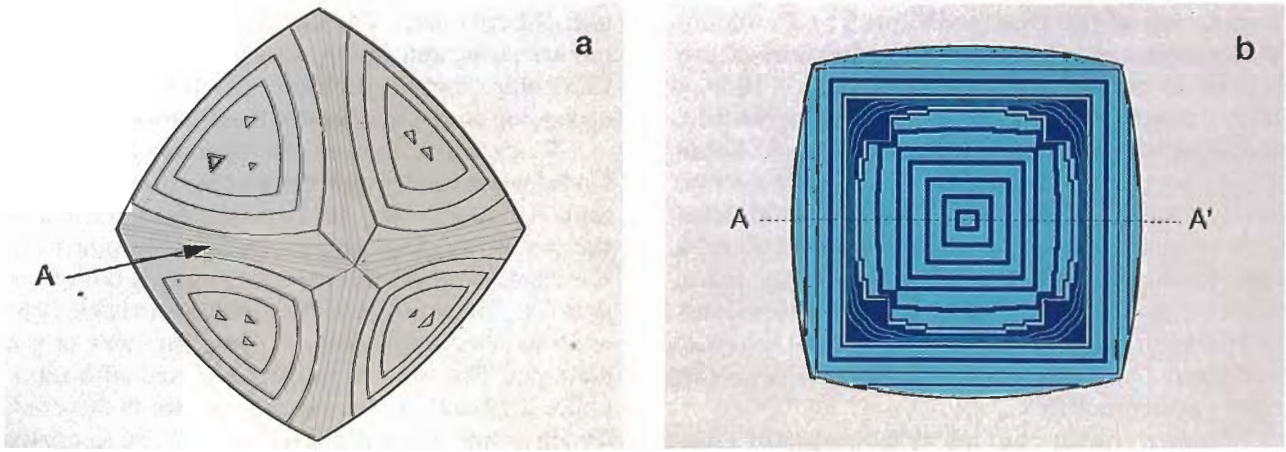

Figure 8. The DiamondView consists of a fluorescence imaging unit (left) in which the TV camera is located between two lamp housings (upper left), with special stone holders for loose (foreground and figure 9a) and ringset (foreground and figure 9b) diamonds, and a specially configured computer. Photo by M. J. Crowder.

terns in minerals, including diamond (Woods and Lang, 1975; Hanley et al., 1977; Marshall, 1988; Ponahlo, 1992). In cathodoluminescence (CL), an electron beam, rather than ultraviolet radiation, is used to excite luminescence. Commercial CL instruments use a cold cathode discharge tube operating in a relatively low vacuum to produce the electron beam. Although CL is invaluable in the study of minerals, the fact that it requires a vacuum can be a disadvantage when large numbers of stones must be surveyed rapidly, as it may take several minutes to pump down to the required pressure. Also, the surfaces of samples may become contaminated by deposits of products from the pump oil. It was to avoid these practical problems associated with CL that our Research Centre developed an ultraviolet-excited fluorescence imaging technique.

Description of the DiamondView. The DiamondView consists of a fluorescence imaging unit (60 cm high by 25 cm wide by 25 cm deep (24 in. × 10 in. × 10 in.), which weighs approximately 20 kg (44 lbs.), and a specially configured computer (figure 8). Loose stones are mounted between the jaws of a stone holder that allows the stone being examined (from 0.05 to approximately 10 ct) to be rotated about a horizontal axis while it is being viewed (see figure 9a). Ring-mounted stones can also be examined, provided that the total height of the ring is not too great (see figure 9b). Other simple jewelry mounts can also be accommodated.

The instrument illuminates the surface of a diamond with intense ultraviolet light, specially filtered such that almost all of the light reaching the sample is of wavelengths shorter than 230 nm. The energy of this ultraviolet light is equal to or greater than the intrinsic energy band-gap of diamonds. This has two important consequences. First, radiation of this energy will excite fluorescence in practically all types of diamond irrespective of whether they fluoresce to the standard long- and short-wave UV radiation (365 and 254 nm, respectively) routinely used by gemologists. Second, at wavelengths shorter than 230 nm, all types of diamond absorb light very strongly. This means that fluorescence is generated very close to the surface of the diamond, so that a clear two-dimensional pattern can be observed. The fluorescence emitted is viewed by a solid-state CCD (charge-coupled device) video camera that has been fitted with a variable-magnification objective lens. The camera has a built-in video picture store, and images can be integrated on the CCD chip from 40 milliseconds up to 10 seconds, depending on the intensity of the fluoresecence.

To examine a stone, the operator inserts the loaded stone holder into the port at the front of the unit. An interlocking safety mechanism eliminates the possibility of any ultraviolet light escaping from the instrument when the stone holder is out of the port. The stone is first illuminated with visible light and the camera is focused on, say, the table of the diamond. The stone is then illuminated with ultraviolet light and the fluorescence image is recorded. The instrument is controlled by an IBM PC-compati-

Figure 9. The loose-stone holder is inserted into the measurement port of the DiamondView (left). The gear mechanism allows the stone to be rotated about a horizontal axis while located within the instrument, for alignment and observation of surface fluorescence patterns characteristic of its internal growth structures. The ring holder (right) can accommodate a ring-set stone that has a total height no greater than 30 mm (1.2 in). Rings mounted in this holder can be rotated about the axis of the holder and moved forward and backward along this axis. Photo by M. J. Crowder.

ble computer running Microsoft® Windows™ 3.1–compatible proprietary software. The computer has a 120 MHz Pentium processor, 32 Mb of RAM (random access memory), and PCI (peripheral component interconnect) video input and graphics display cards. The fluorescence image is displayed on a high-resolution, 1024 × 768 pixel, computer monitor. If additional views of the stone are required, the stone holder can be rotated, without removing it from the chamber, to bring other parts of the stone's surface into view. Fluorescence images that are required for future reference can be stored on the PC's hard drive. The number of images that can be stored is limited only by the size of the hard drive. In this model, the 800Mb drive could hold over 500 images. Images can be archived using, for instance, a tape drive or writable compact disk. The display screen produced by the DiamondView software can be seen in figure 8. The mouse-operated buttons that control the instrument are located beneath the main window, in which the current image is displayed. This image may be compared with up to 16 previously recorded images. These can be recalled on four pages, each of which has four "thumb-nail" windows, displayed on the right of the main window. Tutorial files consisting of 16 "thumb-nail" images, complete with text notes, are provided in the software to help the operator identify fluorescence patterns. The user can also produce "customized" tutorial files.

Figure 10. This fluorescence image of a 0.3 ct near-colorless natural diamond shows concentric bands of octahedral growth with a re-entrant feature below the center of the image and several regions of hummocky cuboid growth. The blue color is typical of most natural diamonds and results from so-called band A emission together with some fluorescence from the 415 nm system.

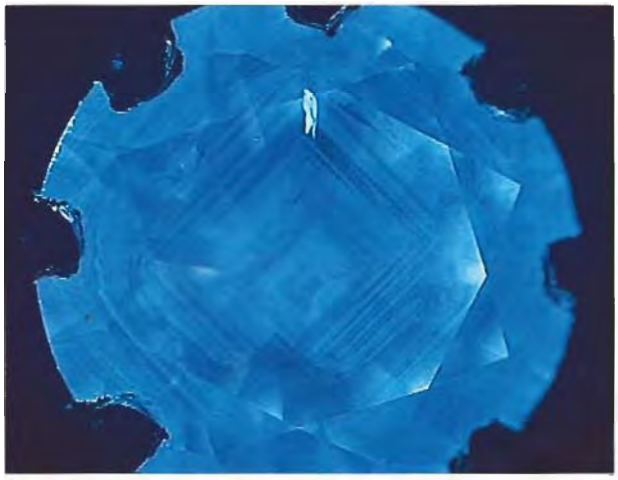

Sample Images. The DiamondView was tested with the same synthetic diamonds described above for the DiamondSure tests, together with about 150 randomly chosen natural diamonds. Following are some examples of the images obtained. Figure 10 shows the fluorescence image of a near-colorless natural 0.3 ct diamond mounted in an eight-claw ring setting. The fluorescence in this sample ranges from bright blue to dark blue; it is typical for natural diamonds and results from so-called blue band A emission together with some fluorescence from the 415 nm system (see, e.g., Clark et al., 1992). The stone was polished such that the table is close to a cube plane, and the striae visible in the image result

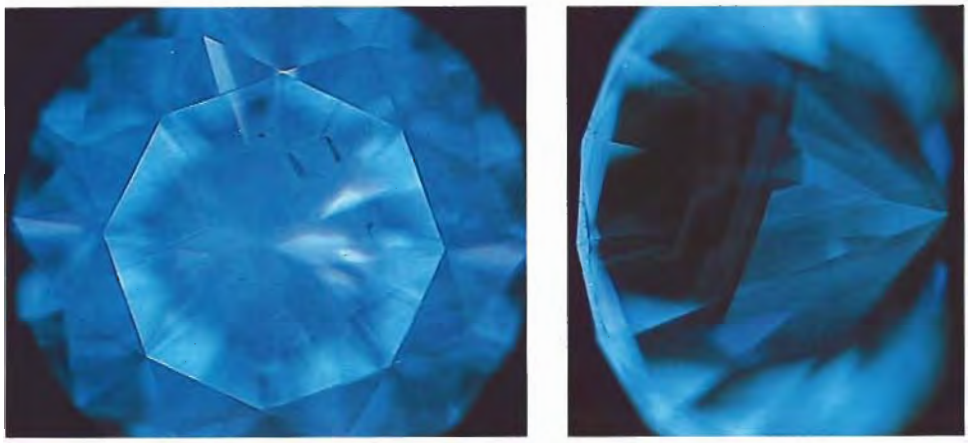

Figure 11. The fluorescence image of the table (left) of this 1.5 ct natural diamond shows concentric bands of octahedral growth and a number of re-entrant features. The pavilion of this stone (right) shows some narrow bright blue octahedral bands, with some re-entrant features, in an otherwise weakly fluorescing region.

from bands of octahedral growth intersecting the table. Re-entrant features are evident in the lower part of the image, and cuboid growth horizons can be seen in various places, particularly toward the left in the image. The concentric rectangular bands, the re-entrant feature below the center of the image, and the hummocky cuboid growth bands are all similar to those shown in idealized form in figure 7b.

Figure 12. In this yellow-brown plastically deformed natural diamond, approximately 0.1 ct, the fluorescence image shows green H3 (503 nm) emission from two sets of parallel slip bands. This type of plastic deformation, covering the entire stone, is not uncommon in natural diamonds, but it has not been found in synthetic diamonds.

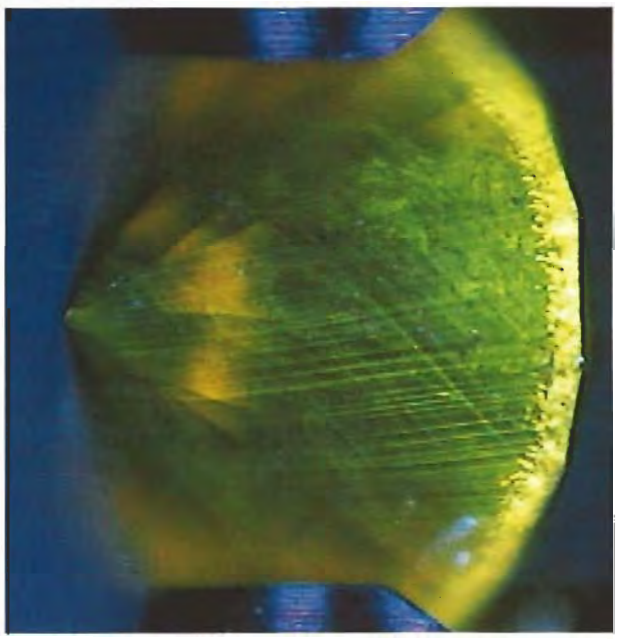

The fluorescence image of a 1.5 ct near-colorless natural diamond is shown in figure 11 (left). The banding is less pronounced in this stone than in the one shown in figure 10, but it is still apparent. However, the image of part of the pavilion of this stone shows greater contrast, as is evident in figure 11 (right).

The fluorescence image of an approximately 0.1 ct yellow-brown natural diamond is shown in figure 12. This diamond is plastically deformed, and the green lines are produced by slip bands (planes along which part of the crystal has undergone a shearing displacement) decorated by nitrogen-related H3 (503 nm) defects. Two sets of parallel slip bands may be seen. This type of plastic deformation, which covers the entire stone, is not uncommon in natural diamonds but has not been found in synthetic diamonds.

The DiamondView image of a 2.19 ct yellow-brown De Beers experimental synthetic diamond is shown in figure 13. From the symmetry of the pattern, it is clear that the table has been cut close to a cube plane. This image may be compared with the schematic diagram shown in figure 5c. The central (001) sector is surrounded by four other cube sectors, which fluoresce yellowish green, and by four inert octahedral sectors. The yellowish green color is due to the H3 (503 nm) system together with some green band A emission (again, see Clark et al., 1992). Narrow, blue-emitting dodecahedral sectors lie between pairs of cube and pairs of octahedral sectors.

The fluorescence image of a 0.33 ct near-colorless De Beers experimental synthetic diamond is shown in figure 14 (left). Although the fluorescence is blue, it is a less saturated, more grayish blue than is typical of natural diamonds (again, see Shigley et al., 1995). A brief examination of this image reveals

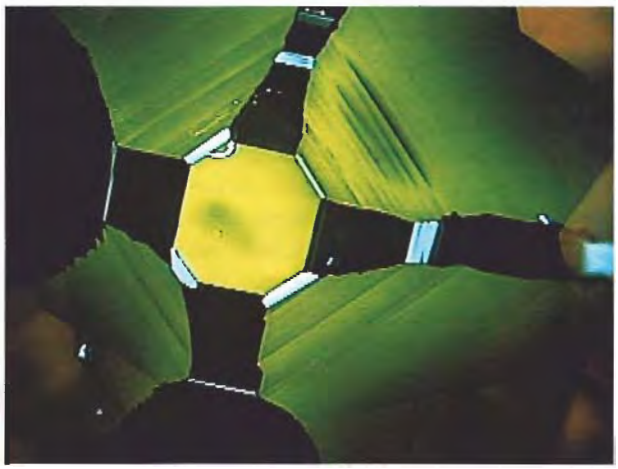

Figure 13. The fluorescence image of the table and some of the surrounding crown facets of this 2.19 ct yellow-brown De Beers experimental synthetic diamond shows yellowish green emission from the central (001) sector and four other cube sectors. The color is due to the nitrogen-related H3 (503 nm) system together with some green band A emission. The inert regions between the yellowish green cube sectors are octahedral sectors. Narrow, blue-emitting dodecahedral sectors lie between pairs of cube sectors and pairs of octahedral sectors. Trapezohedral {113} sectors had not developed significantly in this sample.

a central (001) sector surrounded by four somewhat brighter octahedral sectors. Pairs of octahedral sectors are separated by narrow, less intensely emitting dodecahedral sectors. The view of the pavilion of this stone (figure 14, center) shows the growth-sector pattern even more clearly. A weakly emitting (001) sector may be seen in the region of the culet. This is surrounded by pale blue {111} sectors lying between narrow, less strongly emitting {110} sectors.

The DiamondView has also been used to examine a complete range of synthetic diamonds, including both yellow and near-colorless Russian BARS stones. In all cases, the stones could be positively identified as synthetic from their fluorescence patterns.

Another feature of near-colorless and blue synthetic diamonds is that they tend to exhibit long-lived phosphorescence after excitation by ultraviolet light. Many natural diamonds do phosphoresce, but phosphorescence is relatively uncommon in near-colorless stones and is generally much weaker and for a shorter period than in near-colorless and blue synthetic diamonds. The DiamondView instrument has been designed to exploit this phenomenon in order to assist further in the identification process. Phosphorescence images can be captured at times from 0.1 to 10 seconds after the ultraviolet excitation has been switched off. An example of a phosphorescence image from the 0.33 ct near-colorless synthetic diamond is shown in figure 14 (right). The exposure time was 0.4 second, commencing after a delay of 0.1 second. Phosphorescence is strongest from octahedral growth sectors.

Figure 14. The fluorescence image of the crown (left) of this 0.33 ct near-colorless De Beers experimental synthetic diamond shows a near-central (001) sector surrounded by four somewhat brighter octahedral sectors, which are separated by narrow dodecahedral sectors. The blue color is less saturated than is typical of natural diamonds. The view of the pavilion (center) shows a weakly emitting (001) sector in the region of the culet surrounded by pale blue octahedral sectors lying between narrow, less strongly emitting dodecahedral sectors. A phosphorescence image (right), recorded with an exposure time of 0.4 second and a delay of 0.1 second after the ultraviolet excitation had been switched off, shows strongest phosphorescence from octahedral sectors. Strong, long-lived phosphorescence is a characteristic feature of near-colorless and blue synthetic diamonds.

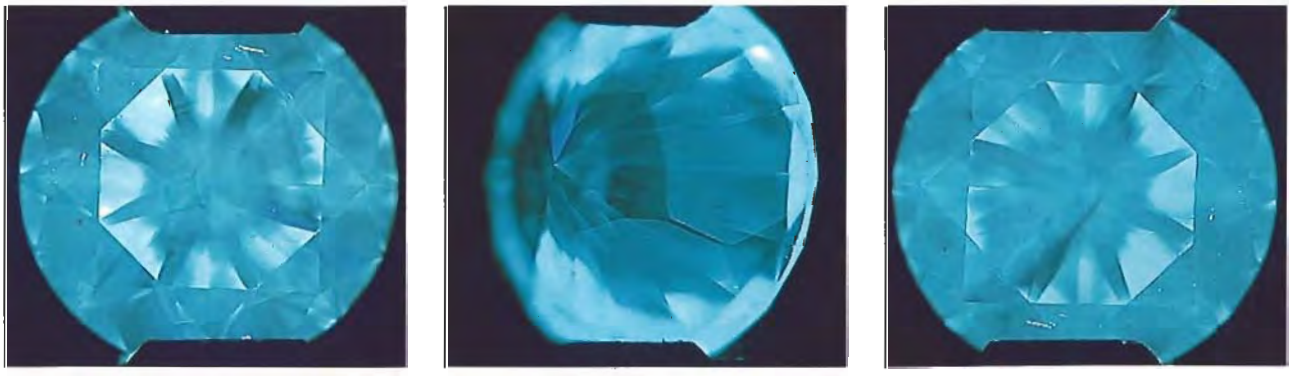

We have loaned the GIA Gem Trade Laboratory DiamondView and DiamondSure instruments, which they are evaluating for use as part of GIA GTL's standard diamond testing procedures. In this evaluation, the DiamondSure is the first test for all diamonds that the laboratory takes in (T. Moses, pers. comm., 1996). Using the DiamondView, GIA Research in Carlsbad, California, recorded fluorescence patterns on eight Russian and three Sumitomo Electric synthetic diamonds (all yellow). From these patterns, all of these diamonds were quickly and easily recognized as synthetic (J. E. Shigley, pers. comm., 1996).

CONCLUSION

The DiamondSure is a relatively inexpensive instrument capable of screening 10 to 15 stones per minute and automatically producing a "PASS" or "REFER FOR FURTHER TESTS" result. It is based on the presence or absence of the 415 nm line, which was found in more than 95% of natural diamonds tested but has not been found in any synthetic diamonds. Because a small proportion of natural diamonds would be referred by this instrument, additional testing may be required. The DiamondView is a more complex and significantly more expensive instrument. It enables the operator to determine whether a diamond is natural or synthetic on the basis of a far-ultraviolet-excited fluorescence image. Synthetic diamonds are identified by their distinctive growth-sector structure, whereas natural diamonds show either purely octahedral growth or a combination of octahedral and hummocky "cuboid" growth. Because only two or three stones can be examined per minute, and an operator must interpret the fluorescence image, it would not be practical to use the DiamondView alone for screening large numbers of stones. It would therefore be appropriate for both instruments to be used together or for operators of a DiamondSure to have ready access to a laboratory with a DiamondView.

At present, DiamondSure and DiamondView instruments are being loaned to a number of major gem testing laboratories throughout the world. Both instruments have been designed so that they can be manufactured in volume should near-colorless cuttable synthetic diamonds enter the gem market in significant numbers. Although it has yet to be shown that this will be the case, these instruments could be made commercially available quickly, should a real need arise. The price of the instruments will depend very much on the numbers to be produced, but it is estimated that a DiamondSure instrument might cost in the region of a few thousand dollars, whereas the more complex DiamondView might be 10 times as much.

The development of these instruments ensures that synthetic diamonds of cuttable quality can be easily identified. With such tools available to members of the gem trade, the existence of such synthetics should not be a cause of major concern.

Acknowledgments: The authors wish to thank all the members of the staff at De Beers DTC Research Centre, Maidenhead, who have been involved with the development of the instruments described in this article. Particular recognition is due to P. S. Rose and G. M. Brown, for the development of the DiamondSure™ *instrument, and to T. M. Payman and R. M. Caddens, for the development of the* DiamondView™ *instrument. S. J. Quinn was responsible for most of the instrument testing. The authors are also grateful to the synthesis team under Dr. R. C. Burns at the Diamond Research Laboratory, Johannesburg, for the supply of the De Beers experimental synthetic diamonds used to test these instruments.*

REFERENCES

Brozel M.R., Evans T., Stephenson R.F. (1978) Partial dissociation of nitrogen aggregates in diamond by high temperature–high pressure treatments. *Proceedings of the Royal Society of London, A*, Vol. 361, pp. 109–127.

Burns R.C., Cvetkovic V., Dodge C.N., Evans, D.J.F., Rooney M.-L.T., Spear P.M., Welbourn C.M. (1990) Growth-sector dependence of optical features in large synthetic diamonds. *Journal of Crystal Growth*, Vol. 104, pp. 257–279.

Burns R.C., Kessler S., Sibanda M., Welbourn C.M., Welch D.L. (1996) Large synthetic diamonds. In *Advanced Materials '96: Proceedings of the 3rd NIRIM International Symposium on Advanced Materials*, National Institute for Research in Inorganic Materials, Tsukuba, Japan, pp. 105–111.

Clark C.D., Collins A.T., Woods G.S. (1992) Absorption and luminescence spectroscopy. In J. E. Field Ed. *The Properties of Natural and Synthetic Diamond*, Academic Press, London, pp. 35–79.

Collins A.T., Kanda H., Burns R.C. (1990) The segregation of nickel-related optical centres in the octahedral sectors of synthetic diamond. *Philosophical Magazine B*, Vol. 61, No. 5, pp. 797–810.

Crowningshield R. (1971) General Electric's cuttable synthetic

diamonds. *Gems & Gemology*, Vol. 13, No. 10, pp. 302–314.
Emms E.C. (1994) Large gem-quality synthetic diamond identified by laboratory. *Gem and Jewellery News*, Vol. 4, No. 1, p. 4.
Fryer C.W. (1987) Gem trade lab notes: Synthetic diamond. *Gems & Gemology*, Vol. 23, No. 1, p. 44.
Hanley P.L., Kiflawi I., Lang A.R. (1977) On topographically identifiable sources of cathodoluminescénce in natural diamonds. *Philosophical Transactions of the Royal Society of London, A*, Vol. 284, No. 1324, pp. 329–368.
Johnson M.L., Koivula J.I., Eds. (1996) Gem news: Synthetic diamonds are in the marketplace. *Gems & Gemology*, Vol. 32, No. 1, p. 52.
Kammerling R.C., Moses T., Fritsch E. (1993) Gem trade lab notes: Faceted yellow synthetic diamond. *Gems & Gemology*, Vol. 29, No. 4, p. 280.
Kammerling R.C., McClure S.F. (1995) Gem trade lab notes: Synthetic diamond, treated-color red. *Gems & Gemology*, Vol. 31, No. 1, pp. 53–54.
Kammerling R.C., Reinitz I., Fritsch E. (1995) Gem trade lab notes: Synthetic diamond suite. *Gems & Gemology*, Vol. 31, No. 2, pp. 122–123.
Kanda H., Ohsawa T., Fukunaga O. (1989) Effect of solvent metals upon the morphology of synthetic diamonds. *Journal of Crystal Growth*, Vol. 94, pp. 115–124.
Koivula J.I., Fryer C.W. (1984) Identifying gem-quality synthetic diamonds: An update. *Gems & Gemology*, Vol. 20, No. 3, pp. 146–158.
Koivula J.I., Kammerling R.C., Fritsch E., Eds. (1994) Gem news: Near-colorless Russian synthetic diamond examined. *Gems & Gemology* Vol. 30, No. 2, pp. 123–124.
Lawson S.C., Kanda H., Watanabe K., Kiflawi I., Sato Y. (1996) Spectroscopic study of cobalt-related optical centers in synthetic diamond. *Journal of Applied Physics*, Vol. 79, No. 8, pp. 1–10.
Machada W.G., Moore M., Woods G.S. (1985) On the dodecahedral growth of coated diamonds. *Journal of Crystal Growth*, Vol. 71, pp. 718–727.
Marshall D.J. (1988) *Cathodoluminescence of Geological Materials*, Unwin Hyman Ltd., London.
Moore M., Lang A.R. (1974) On the origin of the rounded dodecahedral habit of natural diamond. *Journal of Crystal Growth*, Vol. 26, pp. 133–139.
Moses T., Kammerling R.C., Fritsch E. (1993a) Gem trade lab notes: Synthetic yellow diamond crystal. *Gems & Gemology*, Vol. 29, No. 3, p. 200.
Moses T., Reinitz I., Fritsch E., Shigley J.E. (1993b) Two treated-color synthetic red diamonds seen in the trade. *Gems & Gemology* Vol. 29, No. 3, pp. 182–190.
Pal'yanov Yu.N., Malinovsky I.Yu., Borzdov Yu.M., Khokhryakov A.F., Chepurov A.I., Godovikov A.A., Sobolev N.V. (1990) Use of the "split sphere" apparatus for growing large diamond crystals without the use of a hydraulic press. *Doklady Akademii Nauk SSSR, Earth Science Section*, Vol. 315, No. 5, pp. 1221–1224.
Ponahlo J. (1992) Cathodoluminescence (CL) and CL spectra of De Beers' experimental synthetic diamonds. *Journal of Gemmology*, Vol. 23, No. 1, pp. 3–17.
Reinitz I. (1996) Gem trade lab notes: A notable yellow synthetic diamond from Russia. *Gems & Gemology*, Vol. 32, No. 1, pp 44–45.
Rooney M.-L.T. (1992) (115) Growth in boron-doped synthetic diamonds. *Journal of Crystal Growth*, Vol. 116, pp. 15–21.
Rooney M.-L.T., Welbourn C.M., Shigley J.E., Fritsch E., Reinitz I. (1993) De Beers near colorless-to-blue experimental gem-quality synthetic diamonds. *Gems & Gemology*, Vol. 29, No. 1, pp. 38–45.
Satoh S., Sumiya H., Tsuji K., Yazu S. (1990) Differences in nitrogen concentration and aggregation among (111) and (100) growth sectors of large synthetic diamonds. In S. Saito, O. Fukunaga, and M. Yoshikawa, Eds., *Science and Technology of New Diamond*, KTK Scientific Publishers/Terra Scientific Publishing Co., Tokyo, pp. 351–355.
Shigley J.E., Fritsch E., Stockton C.M., Koivula J.I., Fryer C.W., Kane R.E. (1986) The gemological properties of Sumitomo gem-quality yellow synthetic diamonds. *Gems & Gemology*, Vol. 22, No. 4, pp. 192–208.
Shigley J.E., Fritsch E., Stockton C.M., Koivula J.I., Fryer C.W., Kane R.E., Hargett D.R., Welch C.W. (1987) The gemological properties of the De Beers gem-quality synthetic diamonds. *Gems & Gemology*, Vol. 23, No. 4, pp. 187–206.
Shigley J.E., Fritsch E., Reinitz I., Moon M. (1992) An update on Sumitomo gem-quality synthetic diamonds. *Gems & Gemology*, Vol. 28, No. 2, pp. 116–122.
Shigley J.E., Fritsch E., Reinitz I. (1993a) Two near-colorless General Electric type IIa synthetic diamond crystals. *Gems & Gemology*, Vol. 29, No. 3, pp. 191–197.
Shigley J.E., Fritsch E. Koivula J.I., Sobolev N.V., Malinovsky I.Yu., Pal'yanov Yu.N. (1993b) Gemological properties of Russian gem-quality synthetic yellow diamonds. *Gems & Gemology*, Vol. 29, No. 4, pp. 228–248.
Shigley J.E., Fritsch E., Reinitz I., Moses T.M. (1995) A chart for the separation of natural and synthetic diamonds. *Gems & Gemology*, Vol. 31, No. 4, pp. 256–264.
Shor R., Weldon R., Eds. (1996) Gem notes: Superings to market Russian synthetics. *Jewelers' Circular-Keystone*, May, pp. 62–63.
Sinkankas J. (1986) *Mineralogy*. Van Nostrand Reinhold Co., New York.
Strong H.M., Chrenko R.M. (1971) Further studies on diamond growth rate and physical properties of laboratory-made diamond. *Journal of Physical Chemistry*, Vol. 75, No. 12, pp. 1838–1843.
Strong H.M., Wentorf R.H. Jr. (1971) The growth of large diamond crystals. *Die Naturwissenschaften*, Vol. 59, No. 1, pp. 1–7.
Sunagawa I. (1984) Morphology of natural and synthetic diamond crystals. In I. Sunagawa, Ed., *Materials Science of the Earth's Interior*, Terra Scientific Publishing Co., Tokyo, pp. 303–330.
Sunagawa I. (1995) The distinction of natural from synthetic diamonds. *Journal of Gemmology*, Vol. 24, No. 7, pp. 485–499.
Upfront: Chatham bombarded with calls after broadcast (1995). *Jewelers' Circular-Keystone*, May, p. 26.
Welbourn C.M., Rooney M.-L.T., Evans D.J.F. (1989) A study of diamonds of cube and cube-related shape from the Jwaneng mine. *Journal of Crystal Growth*, Vol. 94, pp. 229–252.
Wentorf R.H. Jr. (1971) Some studies of diamond growth rates. *Journal of Physical Chemistry*, Vol. 75, No. 12, pp. 1833–1837.
Woods G.S., Lang A.R. (1975) Cathodoluminescence, optical absorption and X-ray topographic studies of synthetic diamonds. *Journal of Crystal Growth*, Vol. 28, pp. 215–226.

INTRODUCTION TO ANALYZING INTERNAL GROWTH STRUCTURES:

Identification of the Negative d *Plane in Natural Ruby*

By Christopher P. Smith

Growth-structure analysis has become increasingly important as a gemological tool for locality classification and distinguishing between natural and synthetic gemstones. This article presents the methods and instruments needed to analyze the internal growth structures of corundum. As an application of this testing procedure, the negative rhombohedral d *(01$\bar{1}$2) plane is documented as part of the crystal habit in a small number of natural rubies—both as a subordinate form and, for the first time in natural rubies, as a dominant crystal form. Until recently, this crystal face was primarily associated with flux-grown synthetic rubies and sapphires.*

ABOUT THE AUTHOR

Mr. Smith is manager of Laboratory Services, Gübelin Gemmological Laboratory, Maihofstrasse 102, 6000 Lucerne 9, Switzerland.

Acknowledgments: The author thanks Dr. E. J. Gübelin, S. Repetto, and various clients of the Gübelin Gemmological Laboratory for loaning samples; Dr. A. Peretti for introducing him to this testing procedure; and Dr. K. Schmetzer for his continuing work on the application of internal growth-structure analysis in gem identification, as well as his thoughtful review of earlier drafts. U. Gottscheu manufactured the stone holder modification, and the staff of the Gübelin Gemmological Laboratory provided useful comments. Readers interested in more information on the instrumentation and techniques presented here should contact the author. All photos are by the author unless otherwise indicated. All growth-structure photomicrographs are in transmitted light.

Gems & Gemology, Vol. 32, No. 3, pp. 170–184.

Over the past several years, the analysis of crystal habits and internal growth features observed in gemstones has gone beyond the realm of purely academic crystallography to applications in gem identification. The wealth of information learned through the determination of external habits and internal growth structures, which reflect the conditions in which the gem grew, can aid in (1) the separation of natural and synthetic gem materials, as well as (2) the identification and characterization of gemstones from different deposits around the world (figure 1).

For example, the type of twinning is an important factor in separating natural from synthetic amethyst (see, e.g., Crowningshield et al., 1986; Koivula and Fritsch, 1989; Kiefert and Schmetzer, 1991c). In diamond, internal growth structures (commonly referred to as graining) can affect the clarity of the stone (see, e.g., Kane, 1980) and be responsible for certain color manifestations (see, e.g., Kane, 1980; Hofer, 1985; Kane, 1987). These and other growth structures also aid in the separation of natural and synthetic diamonds (see, e.g., Shigley et al., 1992, 1993; Sunagawa, 1992; Rooney et al., 1993; and the Welbourn et al., 1996, article elsewhere in this issue on the new De Beers DiamondView instrument). Beryl classification from various sources, in addition to the separation of natural from synthetic emeralds, has also benefited from the study of internal and external growth features (see, e.g., Lind et al., 1986; Kiefert and Schmetzer, 1991b; Schmetzer et al., 1991).

In corundum in particular, growth-structure analysis has become a standard procedure in many laboratories for both source determination and natural versus synthetic distinctions (see, e.g., Schmetzer, 1986a and b; Schmetzer, 1987; Kiefert, 1987; Kiefert and Schmetzer, 1987, 1988, 1991c; Hänni and Schmetzer, 1991; Peretti and Smith, 1993; Hänni

Figure 1. A wealth of information can be learned through the analysis of internal growth structures, including the distinction of natural from synthetic gem materials and the probable locality of origin of natural stones. With a relatively simple equipment set-up, some study, and practice, the professional gemologist can make determinations that otherwise might require sophisticated instrumentation available to only the most advanced laboratories. Some of the most intense investigation has been done on rubies, so that fine natural rubies such as those shown here (63 ct total weight in the bracelet, 40 ct in the earrings) can be properly identified. Bracelet and earrings courtesy of Harry Winston Inc.; photo © Harold & Erica Van Pelt.

et al., 1994; Schmetzer et al., 1994; Smith and Surdez, 1994; Peretti et al., 1995; Smith et al., 1995).

To make this new tool more accessible to gemologists in all areas of the industry, this article describes the basic techniques and instrumentation that can be used to perform growth-structure analysis of gems. It also provides an example of how this procedure was recently applied to identify in natural rubies a rare crystallographic feature that had previously been considered an indicator of flux-grown synthetic rubies.

GROWTH-STRUCTURE ANALYSIS

Background. Understanding of the methods and applications that will be presented here requires, first, an explanation of some fundamentals of the analysis of internal growth structures. The external form of a crystal consists of a combination of individual crystal faces. The relative size and number of these faces dictate the overall external shape, or *habit*, of the crystal (figure 2). Which crystal faces form and their relative prominence are heavily influenced by the conditions of formation (e.g., pressure/temperature relationships, chemical fluctuations of the fluids from which the crystals precipitated, etc.). Consequently, analysis of these habits can provide important information concerning the way a particular gemstone grew. However, since the external habit of a stone is removed during the fashioning process, internal growth features are the only means to identify the original habit and crystal-growth characteristics in a faceted or polished gem.

The internal growth structures represent the succession of crystal "habits" that formed while the crystal was growing (figure 3). (That is, internal

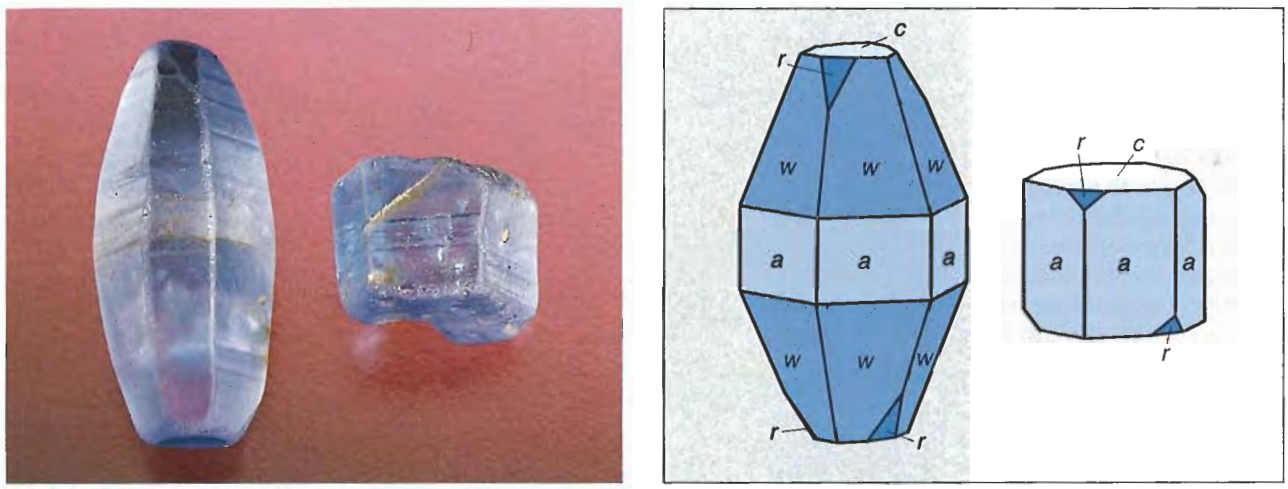

Figure 2. The external form, or habit, of a crystal is made up of a collection of various crystal faces. The number and relative prominence of these crystal faces can have a significant influence on the overall shape of the crystal. Shown here are bipyramidal (left) and tabular (right) blue sapphire crystals from Sri Lanka. The line diagrams illustrate which crystal faces comprise the habits of these two crystals: the basal pinacoid c *(0001), the positive rhombohedron* r *(10$\bar{1}$1), the hexagonal dipyramid* w *(11$\bar{2}$1), and the second-order prism* a *(11$\bar{2}$0). Photo by Shane F. McClure.*

growth planes were at one point external crystal faces. For consistency, the word *plane* will be used to refer to internal crystal forms, and the word *faces* will be reserved for describing external crystal forms.) Minerals form over a long period of time—sometimes continuously and sometimes discontinuously—until the conditions of the formation environment can no longer sustain that mineral's growth. This change in conditions can happen for a variety of reasons. For example, the crystal may be removed from the growth environment by geologic forces, or the growth environment no longer has the chemical/physical requirements (composition of fluids, temperature, pressure) to support the continued formation of that mineral, or there may be no more space for expansion because of competition from other minerals.

The internal structures that indicate the growth of a crystal can be compared to the "rings" of a tree. Just as each "ring" represents one year's growth of tree bark, the internal growth structures illustrate various stages in the history of a crystal's formation. Internal growth features can be observed in transparent gem materials in a variety of ways: as color zoning (which can fluctuate between the different stages of growth); by inclusions that form and concentrate along crystal faces, or coat the crystal's entire surface at one growth stage and then are enclosed by later phases (the latter is how "phantoms" are formed); or by the presence of "lines" that represent the interface or contact plane between consecutive stages of growth. These lines generally are visible with a microscope only when the interior of the gemstone is viewed in a direction parallel, or nearly parallel, to the traces of a specific plane, particularly if the stone is immersed in a liquid of similar refractive index (to reduce the reflection of light).

The appearance of these lines can be visualized by imagining a common type of window in which two sheets of glass have been vacuum sealed together. When you look perpendicular to the glass plane (i.e., as you would normally look through a window), the objects on the other side are not obstructed. However, if you examine the glass parallel to its main surface (i.e., along the edge), a "line" is visible where the two sheets of glass meet.

In 1985, Dr. Karl Schmetzer published his first paper dealing with the methods for determining internal growth structures in some uniaxial gemstones, with specific focus on corundum, beryl, and quartz (see also Schmetzer, 1986a). For a more in-depth discussion on methods and applications of determining growth structures in some uniaxial gemstones, the reader is referred to these papers and others by Schmetzer (1985, 1986a and b), Kiefert and Schmetzer (1991a–c), and Peretti et al. (1995). Following is a brief, step-by-step description of how to use this technique; it has been written specifically for those gemologists, like the author, who do not have a formal background in crystallography.

The Technique. The manner in which specific crystal planes can be identified relates to: (1) the position, or the angle, that the planes form relative to the optic-axis direction of the uniaxial gemstone; and (2) the angle created by the joining of two planes. In the technique used by the author to iden-

tify crystal planes, the equipment includes: a stone holder, modified by the author, which allows for rotation about both the vertical and horizontal axes (Box A); a horizontal microscope; an immersion cell containing methylene iodide; and a light source located behind the gemstone so light is transmitted through it (figure 4). Note that growth structures, color zoning, and the like, can also be seen, but not measured, with a standard binocular microscope using darkfield and various other illumination techniques. However, immersing the gemstone in a liquid will reduce the distortion of light and other detrimental effects, thereby significantly improving the visibility (and measurability) of the growth structures. The recommended procedure is as follows:

First examine each specimen with magnification in the immersion liquid to locate any color banding or other structural features that might be present. Then position the stone in the stone holder so that the direction of the growth planes selected for identification is oriented vertically, that is, perpendicular to the platform base that holds the immersion cell, thus allowing for the most accurate measurement of the angle between the optic-axis direction and the growth plane to be identified. The author has added this first step to the methods described by Schmetzer (1985, 1986a and b) and Kiefert and Schmetzer (1991a–c), in order to guarantee the most accurate measurement for those just beginning to use this testing method. When the growth planes are not in a vertical direction, but rather are at an angle, the angles measured may be off by a couple of degrees, thereby decreasing the accuracy of the technique.

Next, center the optic axis (c-axis) of the gemstone both horizontally and vertically, parallel to the observer's field of view. This is accomplished by using a pair of crossed polarizing filters and the dual-axis stone holder, which allows for a pivotal tilting both forward and backward, as well as a 360° rotation. By pivoting and rotating the stone holder (and the gemstone), look for the interference rings to converge toward the center of the stone (figure 5). At a certain point, you will notice the interference rings shift from converging to diverging. This indicates that the optic axis of the stone has just been "passed over." Here, make smaller adjustments to center the stone in that small area between where the interference rings converge and diverge.

During the final centering of the optic axis, very subtle movements left to right and backward to forward will cause the gemstone to go from white to dark to white again (whereas more exaggerated movements will again display the interference rings). When the optic axis is centered, the gemstone should appear essentially black. It may take some practice to become familiar with this procedure. Nevertheless, the accurate centering of the optic axis is essential to the correct identification of the growth planes to be measured.

Figure 3. Internal growth structures reveal the history of a gem's formation. Each internal growth plane seen in a stone was once a face on the original crystal as it grew. Changes in the formation environment can change the presence and prominence of the various faces, providing clues to the origin of the stone. Often one can see the succession of crystal habits that formed over time. In this idealized example of a ruby from Mong Hsu (Myanmar), the optic axis is located parallel to the length of the stone, and the small, horizontal, basal growth planes are positioned down the middle. An equal amount of growth-structure information is present to the left and right, revealing a habit of c, n, *and* ω. *Note that most gemstones do not reveal such a well-centered sequence of growth structures; typically, one side is either less complete than the other or absent. Immersion, magnified 10×.*

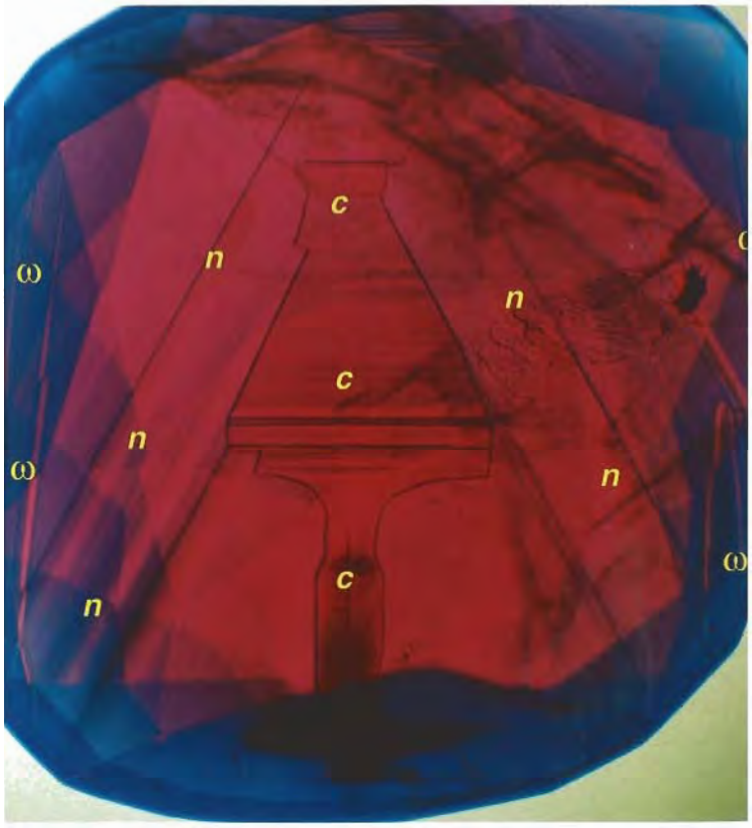

BOX A: THE MODIFIED STONE HOLDER AND ITS BENEFITS

Under optimal measuring conditions, the "optic axis" method has an accuracy of approximately ± 1° (Schmetzer, 1985, 1986a; Kiefert and Schmetzer, 1991a). These optimal conditions are present when the stone holder can be maintained in an essentially vertical position, so that the centered optic axis remains parallel to the observer's field of view (along a horizontal rotation plane), even after a 180° turn of the stone and stone holder. However, because the axial orientation of a faceted gemstone is usually random, the observer commonly must tilt the stone holder either forward or backward to center the optic axis. It has been proposed that the observer can tilt the stone holder up to approximately 40° and still get accurate readings (Kiefert and Schmetzer, 1991a). In the author's experience, however, centering the optic axis frequently requires that the stone holder be tilted to this degree or even further. Yet, on a 180° rotation or even a portion thereof, the optic-axis direction does not remain parallel along the horizontal rotation plane (figure A-1a). This increases the error factor and makes the determination of individual crystal planes more difficult.

The author's modification to the basic stone holder consists of two independently rotating, slightly curved, grooved channels (figure A-2). These channels allow for an additional rotation axis about the vertical plane. Therefore, the observer does not have to tilt the stone holder to large degrees, or reposition the gemstone in the stone holder, to center the optic axis of certain gemstones. Instead, he or she can rotate the gemstone itself by means of the channels, so that the c-axis maintains a parallel rotation about the horizontal plane and the field of view (figure A-1b). With this new rotation capability, the operator can correct major deviations, leaving the "fine tuning" adjustments to the tilting movement. It should not be necessary for the tilting movement to deviate more than approximately 5° either forward or backward from the vertical position, thereby always maintaining optimal measurement conditions. In addition, after locating the optic axis, the operator can now turn the gemstone 90° along the vertical rotation axis, to view the growth structures perpendicular to the c-axis (again refer to figure 3) without removing the gemstone and repositioning it in the stone holder.

Figure A-1. (a) When the stone holder and gemstone are tilted to large degrees, the optic axis is no longer parallel to the observer's field of view, thereby increasing the potential error factor in the measurement of the angles and making it more difficult to separate the different crystal planes. (b) With the modified stone holder, major corrections can be made by rotating the gemstone itself, so that the stone holder remains vertical and the optic axis stays parallel to the observer's field of view, even after a 180° turn. This permits optimal measuring conditions and accuracy. The arrow shows the optic-axis direction.

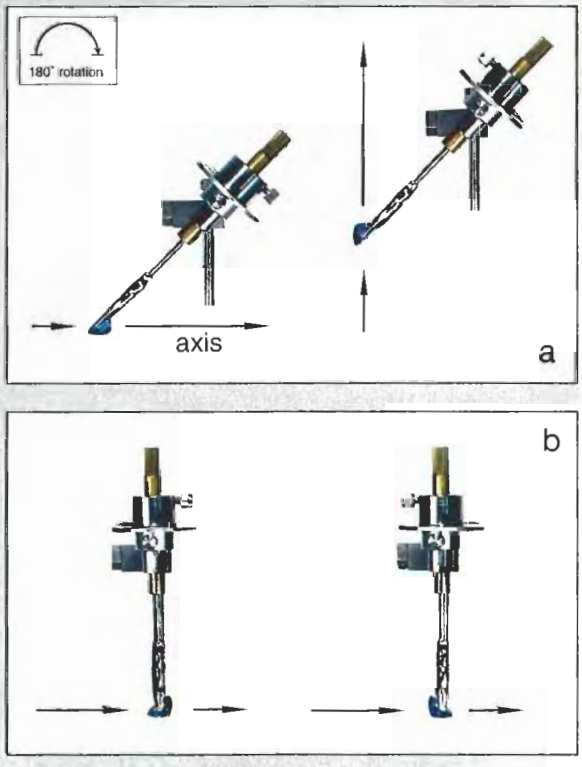

Figure A-2. The author's modification to the basic stone holder consists of two independently rotating grooved channels, which allow for an additional rotation capability so that the c-axis remains in a vertical position. Photo by Shane F. McClure.

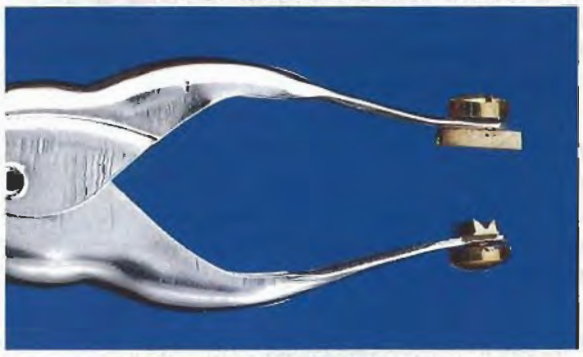

A simple method to check whether the optic axis is centered involves holding a jeweler's loupe between the microscope and the immersion cell. If the gemstone is centered properly, the loupe will act as a coniscope lens (similar to the glass sphere used with a polariscope), revealing the uniaxial optic figure.

Once the optic axis is centered, remove the polarizing filters and use the *set screw* to position the *pointer* of the stone holder at the 0° mark on the *indicator dial* (figure 6). Then rotate the stone and stone holder (left or right) until a vertical series of growth features is sharply delineated, often by color zoning (figure 7); the position of the pointer on the dial will show how many degrees these growth features are located from the optic-axis direction (figure 8). This number defines which crystal plane is represented by the growth features being examined (see table 1 for the crystal planes seen in corundum and their corresponding angles from the c-axis). The prism planes *a* $(11\bar{2}0)$ are seen at 0° (because they are parallel to the optic axis); whereas the basal pinacoid c (0001), which is perpendicular to the optic axis, has the largest potential reading, 90° (again, see table 1). All other crystal planes are located at angles between these two. Typically, a gemstone contains more than one series of growth planes. When complex growth structures are encountered, it may be helpful to center the optic axis first, and then rotate the stone holder as previously described to identify which growth planes are present.

Connecting growth planes can also be identified using a specially designed eyepiece that attaches to one of the microscope oculars. This eyepiece acts as a mini-goniometer, an instrument used by crystallographers to measure angles between crystal faces, enabling measurement of the angles created by connecting crystal planes within a stone (see, e.g., Kiefert and Schmetzer, 1991a). Contained within the eyepiece are two independently rotating disks, one with two lines intersecting at 90° (creating a cross) and the other consisting of small numbered marks around the periphery, indicating 360° in a complete circle. By lining up the longer "cross hair" parallel to one series of crystal planes and then rotating it so that it is parallel to the other series of crystal planes, one can use the scale around the periphery to determine the number of degrees in the angle created by the meeting of two or more crystal planes. (Author's note: The eyepiece described here is no longer commercially available from the Leica Corp. The reader is therefore referred to Kiefert and Schmetzer, 1991a, for a description of commercially available microscope oculars with "cross hairs" and an additional scale to measure the angles, which is

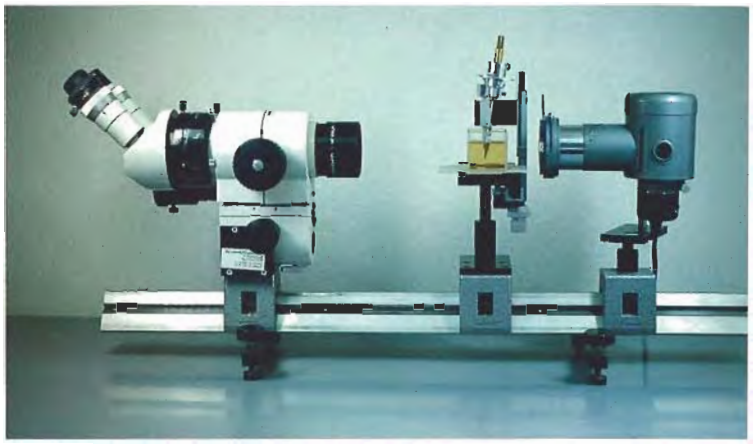

Figure 4. Internal growth structures are analyzed most readily with a horizontal microscope set-up such as this one, with the gemstone immersed in a container filled with methylene iodide and a light source positioned opposite the microscope head so as to transmit light through the sample. A horizontal microscope has the additional advantage of distancing the operator from the methylene iodide fumes.

Figure 5. Centering the optic axis of a uniaxial gemstone requires rotating the stone holder left to right as well as tilting it forward and backward. The interference rings should converge toward the center of the gemstone as the optic axis becomes centered. At the point where the optic axis is centered, the stone should appear essentially black. Also note the faint vertical growth planes visible in this sample. Immersion, between crossed polarizers, magnified 10×.

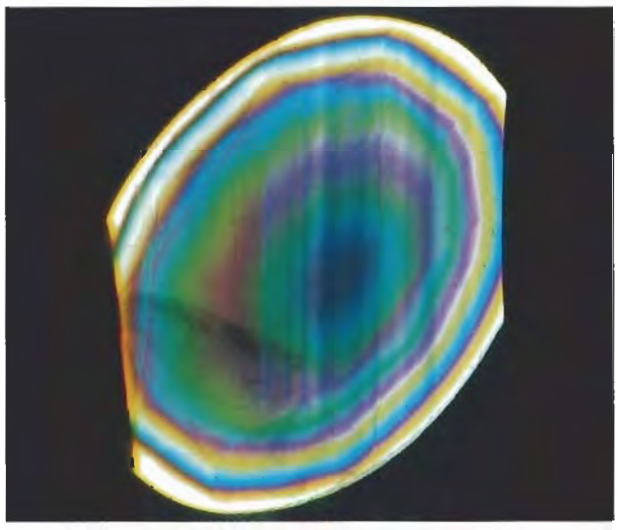

Figure 6. Once the optic axis has been successfully centered, before the stone is rotated to observe the growth features, the pointer must be positioned at the 0° mark on the indicator dial. Photo by Shane F. McClure.

added to the exterior of the eyepiece tube of the microscope.)

In contrast to the first ("optic axis") method, this second ("connecting planes") procedure does not depend on finding the optic-axis direction of the gemstone. (However, it is recommended that less

Figure 7. One of the most obvious ways to identify sharpened growth structures is through color zones, or bands, the thickness of which may fluctuate between consecutive periods of crystal growth. Shown here are broad blue color bands alternating with narrow colorless bands, parallel to dipyramidal v *(44$\bar{8}$3) planes, in a sapphire from Kashmir. The vertical growth planes are at 15.4° from the optic axis direction, and the angle created at the junction of the* v-v *planes is 123°. Immersion, magnified 15×.*

Figure 8. By rotating the stone holder until the growth features are sharply defined, the pointer will show the number of degrees, on the indicator dial, that the growth features are located from the optic-axis direction of the gemstone. The measurement of 20 shown here identifies a series of dipyramidal w *(11$\bar{2}$1) planes, which are located characteristically at 20.1° from the optic-axis direction. Photo by Shane F. McClure.*

experienced practitioners locate and identify at least one series of growth planes initially by the optic-axis method.) What is critical to the accurate measurement of the angles is that both series of growth planes and the points at which they meet are very sharp. With our knowledge of the exact angles formed by various connecting crystal planes (see table 2 for the "interfacial" crystal angles for corundum), once one set of crystal planes has been identified, connecting crystal planes can be identified without requiring reorientation of the stone to the

TABLE 1. The primary crystal planes and angles encountered in natural and synthetic corundum.[a]

Crystal plane	Designation	hkl indices	δ (angle from the c-axis)
Second-order hexagonal prism	a^b	(11$\bar{2}$0)	0°
Second-order hexagonal dipyramids	ω^b	(14 14 $\bar{2}$8 3)	4.5°
	v^b	(44$\bar{8}$1)	5.2°
	z^b	(22$\bar{4}$1)	10.4°
	v^b	(44$\bar{8}$3)	15.4°
	w^b	(11$\bar{2}$1)	20.1°
	n	(22$\bar{4}$3)	28.8°
Positive rhombohedron	r	(10$\bar{1}$1)	32.4°
Negative rhombohedron	d	(01$\bar{1}$2)	51.8°
Negative rhombohedron	γ^c	(01$\bar{1}$5)	72.5°
Basal pinacoid	c	(0001)	90°

[a] α- Al_2O_3, trigonal crystal class D_{3d} = 3 2/m. Adapted from Kiefert and Schmetzer, 1991a.
[b] More typically seen in natural corundum.
[c] More typically seen in synthetic corundum.

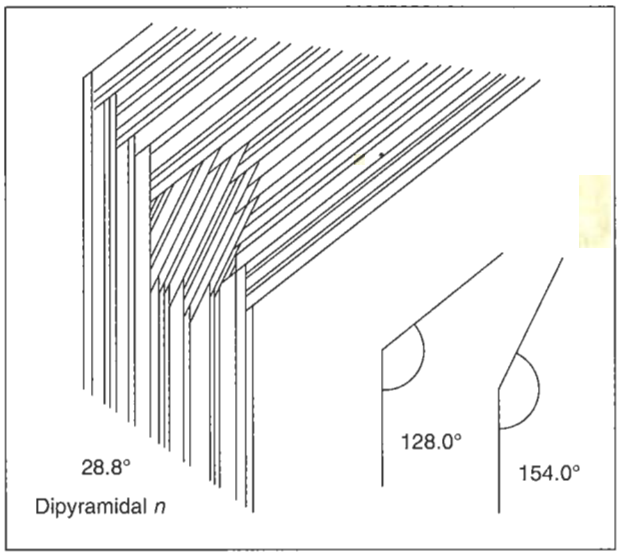

Figure 9. A second method of identifying internal growth structures uses a special eyepiece that is placed on one of the microscope oculars. It has a 360° scale around the periphery, and cross-hairs with which to measure the angle from one growth plane to a connecting plane—that is, the angle formed by the intersection of the two planes. In this illustration, the vertical lines have been identified, by the first (optic-axis) method described, as dipyramidal n *(22$\bar{4}$3) planes, with a measurement of 28.8° from the optic axis direction (see table 1). By determining the number of degrees between the* n *planes and the connecting planes, one can identify the remaining growth planes as positive rhombohedral* r *(10$\bar{1}$1) planes, with an angle of 154°, and a second series of dipyramidal* n *planes, with an angle of 128° (see table 2).*

optic axis (figure 9). When used in combination, the two methods provide a cross-check system.

During growth-structure analysis, a helpful method to study the crystal forms is to examine the gemstone perpendicular to the c-axis, that is, parallel to the basal growth structures (again, see figure 3). This is also the best way to determine changes in "habit" that took place during the growth of the original crystal. For a more complete description of this procedure, the reader is referred to Peretti et al. (1995, pp. 8–9).

THE NEGATIVE *d* PLANE IN NATURAL RUBY

Background. The study and determination of the crystal faces and habits for corundum is certainly not new to crystallography. For the most complete collection of corundum habits from various natural sources, the reader is referred to Victor Goldschmidt's *Atlas der Krystallformen*, published in 1918. Over the past decade, however, this analysis has taken the additional dimension of aiding in the separation of natural and synthetic corundums of various colors (Schmetzer, 1985, 1986a and b, 1987; Kiefert and Schmetzer, 1986, 1988, 1991c; Smith, 1992; Smith and Bosshart, 1993; Hänni et al., 1994; Schmetzer et al., 1994). Because consistent and reproducible crystal synthesis requires a controlled growth environment, most synthetic corundums display crystal habits that are typical of the specific methods (and uniform conditions) by which they are manufactured. In contrast, as a result of inconsistencies and fluctuations in the geologic conditions present during their formation, natural corundums display a much wider variety of crystal habits.

The structural differences between natural and synthetic corundums may be seen in a variety of attributes, including the presence or prominence of certain crystal planes, color-zoning characteristics, habit variations, combinations of crystal planes, and systems of twin lamellae. Of the crystal planes observed in flux-grown synthetic corundums produced by the various manufacturers (such as Chatham, Douros, Kashan, Knischka, and Ramaura), the negative rhombohedral *d* (01$\bar{1}$2) plane was found to be present with a frequency and prominence that has not been observed in natural corundums (Schmetzer, 1985, 1986a and b; Kiefert and Schmetzer, 1991a–c; Hänni et al., 1994). The negative *d* plane is positioned at 51.8° (again, see table 1) from the optic-axis direction. The negative *d* face is located at the terminations (or ends) of a

TABLE 2. The angles formed by the meeting of two crystal planes in natural and synthetic corundum.

Crystal planes	Angle	Crystal planes	Angle (90 + δ[a])	Crystal planes	Angle (180–δ[a])
a–a	120.0°	*c–a*	90.0°	*a–r*	147.6°
z–z	121.1°	*c–r*	122.4°	*a–n*	151.2°
v–v	123.0°	*c–d*	141.8°	*a–w*	159.9°
w–w	124.0°	*c–γ*	162.5°	*a–v*	164.6°
n–n	128.0°	*c–n*	118.8°	*a–z*	169.6°
r–r	86.1°	*c–w*	110.1°	*a–v*	174.8°
r–v	148.0°	*c–v*	105.4°	*a–ω*	175.5°
r–w	152.0°	*c–z*	100.4°		
r–n	154.0°	*c–v*	95.2°		
d–n	148.0°	*c–ω*	94.5°		
r–d	133.0°				

[a] *For the values of δ, see table 1.*

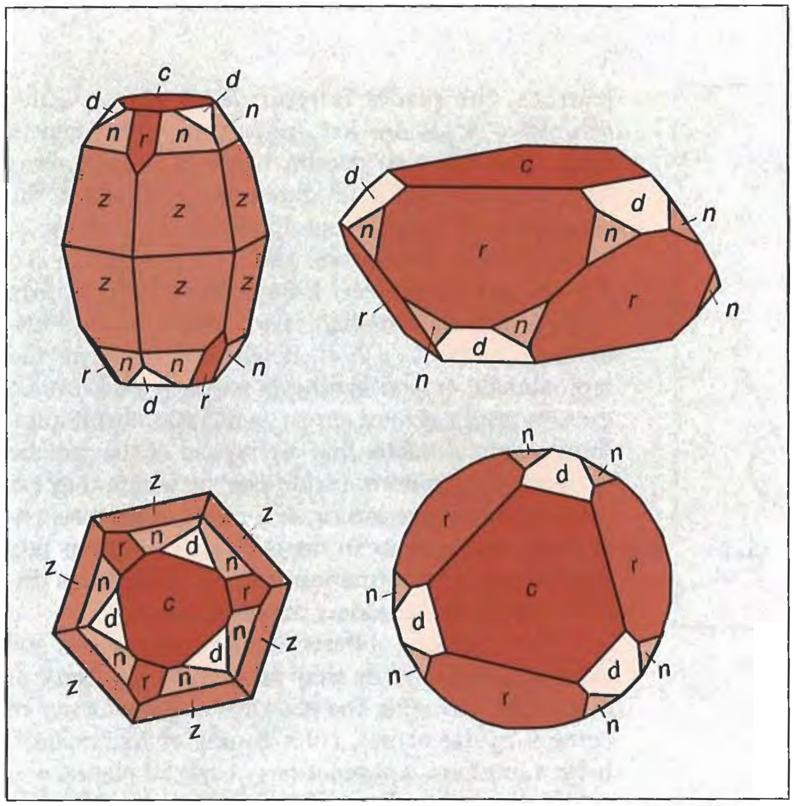

Figure 10. These diagrams illustrate the position of the negative rhombohedral d *$(01\bar{1}2)$ and other crystal faces in the morphology of natural and synthetic corundum. The drawing on the left recreates the probable original crystal habit for the 4.51 ct natural ruby described in this article, with the optic axis of the crystal inclined slightly from the vertical; the drawing below is of the same crystal viewed parallel to the optic axis (to illustrate how different crystal planes may look at different orientations in the three-dimensional crystal). Note the location of the negative* d *face from the terminations, or ends, of the crystal and between two* n *faces. On the Douros flux-grown synthetic ruby crystal shown on the right, the negative* d *face also connects to the positive* r *face, as well as to the* c *and* n *faces. Note how the relative prominence of the various crystal faces can dramatically affect the overall appearance of the crystal. The presence of faces other than* c, r, n, *and* d *suggests natural origin.*

corundum crystal, extending from the basal pinacoid *c* (0001), between two dipyramidal or prism faces, and opposite a positive rhombohedral *r* $(10\bar{1}1)$ face (figure 10). This crystal face has been reported historically in natural corundum (Bauer, 1896; Dana and Dana, 1904; Goldschmidt, 1918; Bauer and Schlossmacher, 1932). However, it appears that Max Bauer (1896) is the only source where a ruby crystal with a negative rhombohedral *d* $(01\bar{1}2)$ face was actually examined and illustrated. The other references appear to be citing Bauer (1896) as their source of the information. In the more modern literature, the negative *d* face has been described as representing a subordinate crystal form that, if present in natural corundum, would be very small (Schmetzer, 1986a). However, no references can be found in the modern literature to the observation of a negative rhombohedral *d* $(01\bar{1}2)$ plane on or in a natural ruby. This has led to the suggestion that the presence of a more dominant negative *d* plane, which is commonly found in synthetic ruby, can be used as an indication of synthetic origin (Schmetzer, 1985, 1986a and b; Kiefert and Schmetzer, 1991a–c).

As part of the gemological examination of several hundred rubies, the author used internal growth-structure analysis, incorporating the combination of both methods described previously. These analyses revealed the presence of subordinate and, in some cases, dominant negative rhombohedral *d* $(01\bar{1}2)$ planes in rubies that other tests proved were natural.

Materials and Methods. A total of eight natural rubies, between 0.15 ct and more than 25 ct, were identified with the negative rhombohedral *d* $(01\bar{1}2)$ crystal plane as part of their original habit (table 3). Two had been purchased in northern Vietnam by Dr. Eduard J. Gübelin (Lucerne, Switzerland) and Mr. Saverio Repetto (previously director of FINGEMS, Chiasso, Switzerland)—1.34 and 0.15 ct, respectively—and had been represented to them as originating from the Luc Yen mining region. Two others (7.03 and 25.55 ct) were reportedly from the Mogok Stone Tract in Myanmar, according to the clients who submitted them to the Gübelin Gemmological Laboratory for testing. The remaining four were also submitted to the Gübelin Gemmological Laboratory for examination, but without any indication as to their source.

A standard refractometer, desk-model spectroscope, and electronic scale equipped with the necessary attachments for hydrostatic specific gravity measurements were used to determine that the eight samples were ruby. As part of the routine examination, as well as once the negative *d* planes were identified, extensive tests were conducted to confirm that the stones were indeed natural. To

establish their natural origin by means of their internal features, a binocular microscope equipped with a darkfield light source was used in conjunction with fiber-optic lighting. Both of the methods described above were used to analyze the internal growth structures and twinning characteristics. Semi-quantitative chemical analysis was performed using a Spectrace TN5000 energy-dispersive X-ray fluorescence (EDXRF) spectrometer with a special measuring routine for corundum developed by Professor W. B. Stern of the University of Basel.

Results. The refractive indexes (n_ε = 1.760–1.764, n_o = 1.769–1.772; birefringence of 0.008–0.009), visible-range spectra (Cr^{3+} absorption bands), and specific gravity (3.98–3.99) were consistent with known properties for ruby. In addition, each of the stones had a combination of inclusion features, twinning, habit, and trace-element concentrations that provided proof of their natural origin (again, see table 3).

Among the natural inclusion features observed in these rubies were transparent, colorless, and whitish mineral inclusions; unaltered and thermally altered healed fractures; zones of dense, unaltered rutile needles (figure 11); and rutile needles that were broken as a result of heat treatment. Also noted were very fine-grained whitish clouds, "cross-hatch" or "flake-like" inclusion patterns, as well as "antennae-like" intersecting stringer formations (figure 12) and long, fine, needle-like tubules along the intersection of two or more systems of twin lamellae (commonly referred to as "boehmite needles").

When the internal growth structures provided enough information to recreate the crystal habit, typically two or more dipyramidal crystal and/or prism planes, combined with the basal and rhombohedral crystal planes, were present (figure 13; see also figure 10). The combinations of these inclusion features and internal growth structures alone provided sufficient evidence of the natural origin of the rubies described.

Observation of the Negative Rhombohedral *d* (01$\bar{1}$2) Plane. In the eight natural rubies described in this article, the negative *d* planes ranged from subordinate through dominant, sometimes within the same stone. The negative *d* plane in the 1.34 ct ruby varied slightly in prominence from subordinate to intermediate during the growth of the gem (figure 14). This ruby also had dipyramidal *w* planes, dipyramidal *z* planes (of varying size), positive rhombohedral *r*, and basal pinacoid *c* planes.

TABLE 3. Properties and internal characteristics of the eight natural rubies with the *d* (01$\bar{1}$2) plane.

Property/ Characteristic	Stone number							
	1	2	3	4	5	6	7	8
Carat weight	0.15	1.34	2.53	4.51	6.10	7.03	10.07	25.55
Inclusions	Transparent colorless crystals, very fine grained whitish clouds, short rutile needles	Rutile needles, healed fractures	Thermally altered healed fractures	Stringer patterns cloud patterns, rutile needles, transparent colorless crystals, "boehmite" needles	Flake-like and cross-hatch cloud patterns, thermally altered healed fractures	Transparent and whitish crystals, dissolved rutile needles, thermally altered healed fractures	Dissolved rutile needles, "boehmite" needles, thermally altered healed fractures	Clusters of small transparent colorless crystals, rutile needles, healed fractures
Evidence of heat treatment	No	No	Yes	No	Yes	Yes	Yes	No
Twinning parallel to *r*	None	1 system	None	2 systems	1 system	1 system	2 systems	None
Growth structures	*z* *r* and *d*	*c*–*w*–*z* *r* and *d*	*c*–*z*–ω or *v* *r* and *d*	*c*–*n*–*z* *r* and *d*	*c*–*n*–*z* *r* and *d*	*c*–*d*	*c*–*n*–*a* *r* and *d*	*c*–*n*–ω or *v* and *d*
d plane	Intermediate	Subordinate	Subordinate	Subordinate	Subordinate to dominant	Dominant	Dominant	Subordinate
Chemistry								
Al_2O_3	99.7	99.5	98.5	99.2	99.3	99.5	99.0	98.9
TiO_2	0.014	0.016	0.031	0.050	0.022	0.035	0.044	0.024
V_2O_5	0.032	0.051	0.027	0.016	0.016	0.016	0.034	0.108
Cr_2O_3	0.210	0.256	0.899	0.691	0.612	0.413	0.733	0.528
Fe_2O_3	0.038	0.093	0.018	0.023	0.012	0.003	0.006	0.009
Ga_2O_3	0.008	0.014	0.001	0.005	0.004	0.003	0.006	0.018

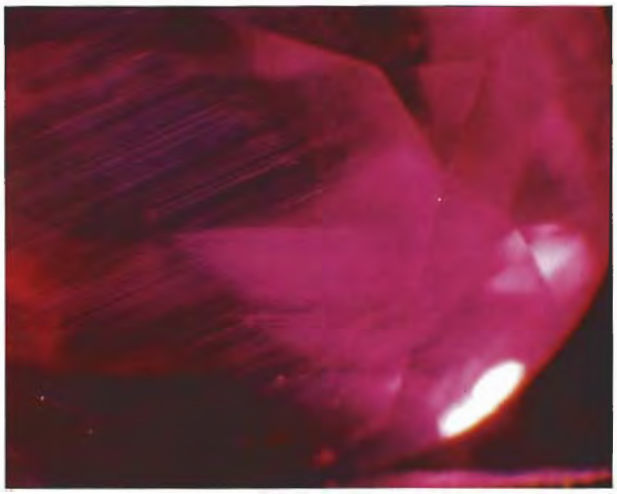

Figure 11. Unaltered rutile needles, concentrated more densely in bands parallel to subordinate negative d *planes, provided proof of natural origin in the 1.34 ct ruby obtained in Vietnam. Oblique fiber-optic illumination, magnified 20×.*

A subordinate negative *d* plane was present during most, but not all, of the growth observed in the 2.53 ct ruby. The dipyramidal planes ω or ν dominated the morphology of this gemstone, with subordinate *c*, *z*, and positive *r* planes also present. The 4.51 ct ruby had *c*, positive *r*, and two different dipyramidal—*n* and *z*—planes, with subordinate negative *d* planes having formed only during a brief period of crystal growth (refer again to figure 10).

Figure 12. "Antennae-like" stringer formations, a typical feature of Vietnamese rubies, helped confirm that the 4.51 ct stone was natural. Oblique fiber-optic illumination, magnified 22×.

The 25.55 ct ruby displayed dominant *c* planes and small negative *d* planes, which were present during the earlier stages of crystal growth (figure 15), as well as subordinate *n* planes and more dominant dipyramidal planes ω or ν.

Negative *d* planes and positive *r* planes of approximately equal, intermediate size were recorded in the 0.15 ct ruby (figure 16), along with subordinate *z* planes.

In the most striking examples, three rubies had dominant negative *d* planes. The 7.03 ct stone showed only dominant *c* planes along with the dominant negative *d* planes (figure 17). In addition to its dominant negative *d* planes (figure 18), the 10.07 ct ruby had dominant positive *r* planes and two systems of twin lamellae, along with dominant *c* and *a* planes, with more subordinate *n* planes. Yet another sample (6.10 ct), revealed negative *d* planes that ranged from subordinate to dominant (figures 19 and 20); it also displayed *c*, positive *r*, and two series of dipyramidal—*n* and *z*—planes (refer to figure 13).

Figure 13. Viewing the 6.10 ct ruby perpendicular to the optic axis, revealed a well-developed growth zoning, typical of natural rubies, that consisted of the basal pinacoid c *(horizontal growth planes), the hexagonal dipyramid* n *(the diagonal growth planes creating an angle of 118.8° with the basal planes), and the dipyramid* z *(the nearly vertical growth planes, with an angle of 100.4° from the basal growth planes). Immersion, magnified 10×.*

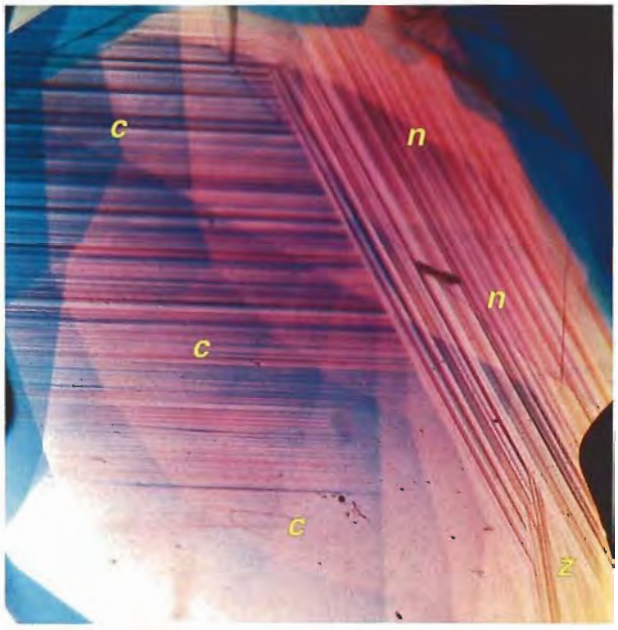

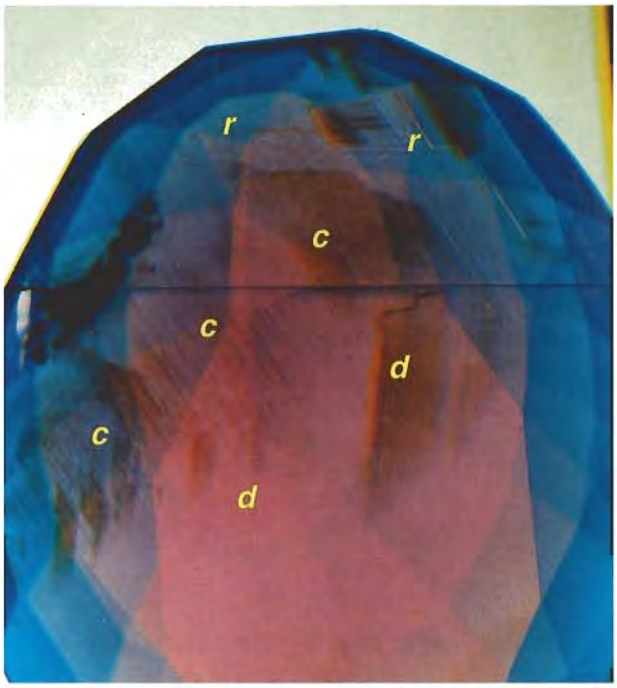

Figure 14. The negative d *planes in this 1.34 ct Vietnamese ruby varied in size slightly during the stages of growth that are visible in the faceted stone, but for the most part they were subordinate. The brownish bands following the growth structures are concentrations of short rutile needles. Also notice the sharp horizontal line, which is a twin plane parallel to a positive* r *plane. Immersion, magnified 15×.*

DISCUSSION

Since this author first identified the negative rhombohedral *d* (01$\bar{1}$2) plane in a natural ruby (Smith, 1992), he has identified this crystal plane in other samples. Statistically, however, this structural feature remains very rare, having been observed in less than 1% of the several hundred corundum samples (primarily ruby and blue sapphire) measured to date by the author. The term *corundum* is used in this context, because the author did identify the negative *d* plane in a natural blue sapphire loaned by Dr. H. A. Hänni, of the Swiss Gemmological Institute (SSEF), Basel; this stone also reportedly originated from northern Vietnam. Determining the conditions under which the negative *d* plane formed in these samples is beyond the scope of this research; we can only surmise that they must have been very special.

To use the presence of the negative *d* plane to separate natural and synthetic rubies, careful interpretation of the growth features present is paramount. The negative *d* plane (especially as a dominant feature) remains more common in flux-grown synthetic rubies than in natural rubies. However, the entire collection of structural features should always be used in combination with a careful analysis of the other inclusion features, as well as with the information learned from a chemical or possibly infrared spectral analysis. Whereas the basal pinacoid *c* and the positive rhombohedral *r* planes are typically seen in both natural and synthetic rubies, *n* is the only dipyramid seen in synthetic rubies. Natural rubies typically contain one or any combination of *a*, ω, ν , *z*, *v*, *w*, or *n*.

Aside from the various inclusion features present, it was possible to identify seven of the eight

Figure 15. Basal pinacoid c *planes dominated the growth structures seen in this 25.55 ct natural ruby, which was reportedly from Burma (Myanmar). The subordinate negative* d *planes were more prominent during the earlier stages of this gemstone's growth (creating an angle of 141.8°). The dark bands are concentrations of rutile needles oriented parallel to the growth planes. Immersion, magnified 15×.*

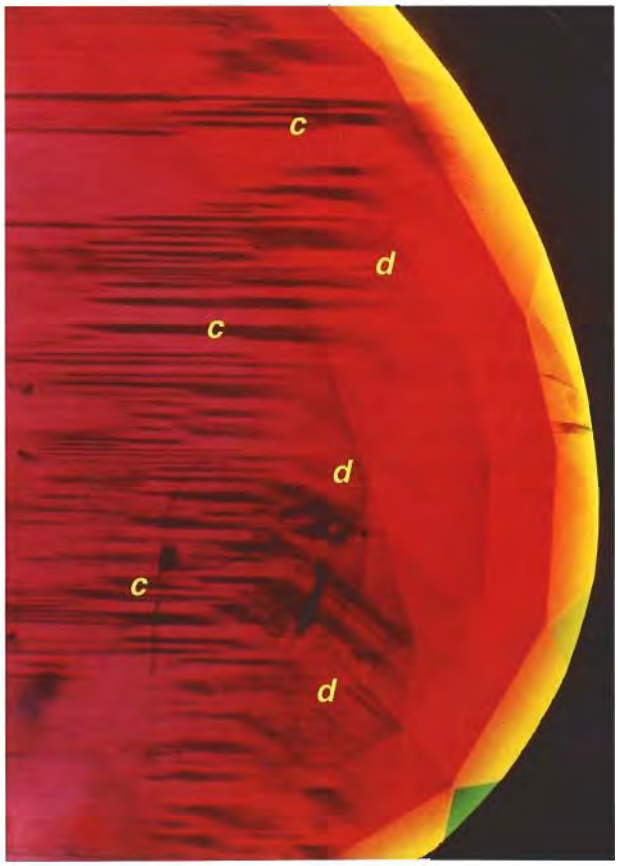

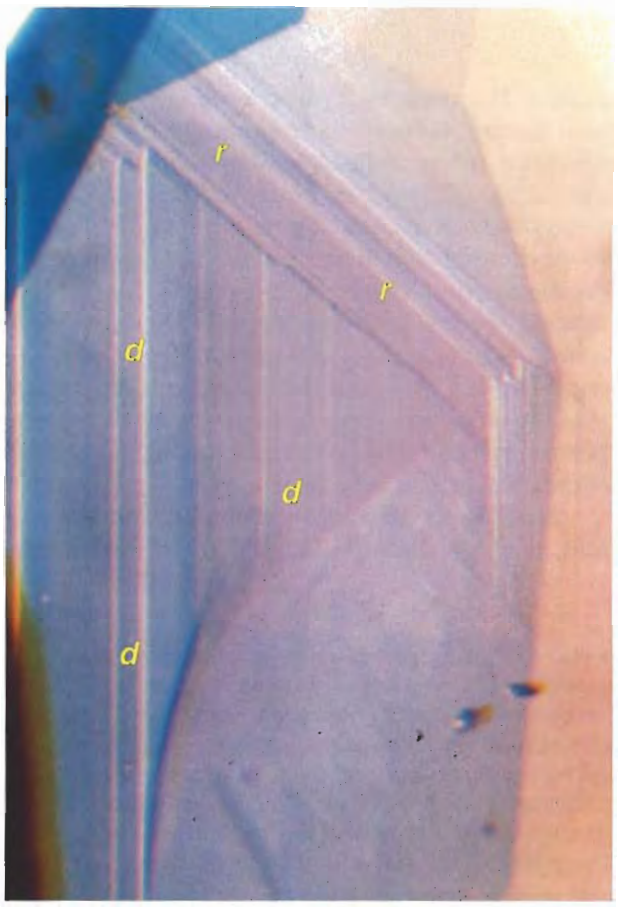

Figure 16. Intermediate negative d *planes are easily seen in this 0.15 ct Vietnamese ruby, connected to positive* r *planes. The angle created at the junction is 133.0°; however, the complimentary angle is also readily seen at 47.0° (180 – 133 = 47). Immersion, magnified 35×.*

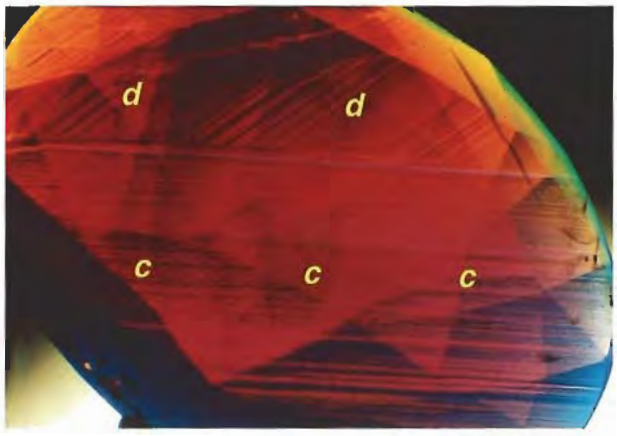

Figure 17. The most striking example comes from a 7.03 ct ruby, reportedly from Burma (Myanmar), in which the only growth structures present consisted of dominant c *planes and dominant negative* d *planes, which created an angle of 141.8°. Immersion, magnified 18×.*

rubies in the sample population (the exception was the 7.03 ct stone) as natural by the presence of internal growth structures (again, see table 3) that have not been seen in flux-grown synthetics. Consequently, if a negative *d* plane is seen in a ruby, then it is important to look also for the hexagonal dipyramid and prism crystal planes. If, in addition to the negative *d* plane, only *c*, positive *r*, and/or *n* are observed, care must be taken: Although this suite of features is typical for flux-grown synthetic rubies, it may also occur in natural rubies. If no characteristic inclusions are present, the use of analytical techniques such as EDXRF chemical analysis (see, e.g., Stern and Hänni, 1982) or infrared spectroscopy (see, e.g., Smith, 1995) is advised. If additional dipyramid or prism planes are present, then natural ruby is indicated. In addition, the negative rhombohedral γ $(01\bar{1}5)$ plane, located at 72.5° from the optic axis, is still considered indicative of a synthetic ruby in those very rare situations where it is present (Schmetzer, 1985, 1986a and b; Kiefert and Schmetzer, 1991a–c).

If a negative *d* plane is detected in a ruby of suspicious identity, then twinning characteristics can also provide important clues (Kiefert and Schmetzer,

Figure 18. Dominant negative d *planes are seen in this 10.07 ct natural ruby, creating an angle of 133.0° with dominant positive* r *planes. The "checkerboard" appearance of intersecting lines is the result of twinning parallel to two positive* r *planes, forming angles of nearly 90°. Immersion, magnified 9×.*

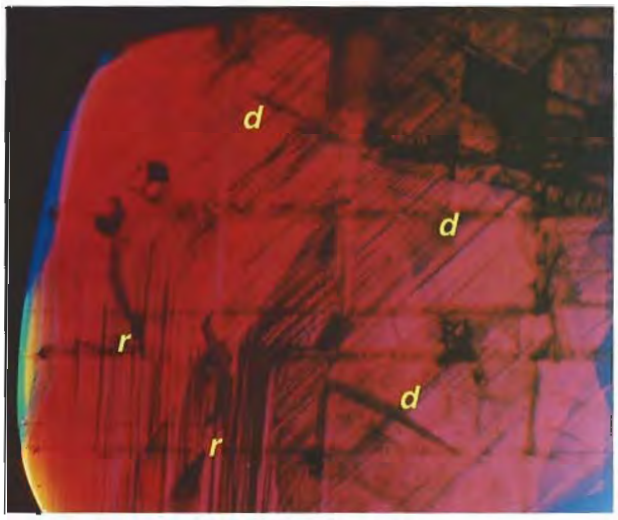

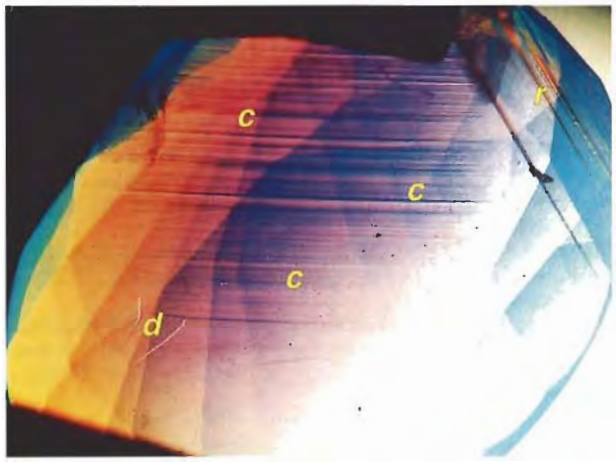

Figure 19. The negative d *planes in this 6.10 ct natural ruby ranged from subordinate to dominant. This view shows a subordinate form of negative* d *plane with dominant* c *planes. Immersion, magnified 10×.*

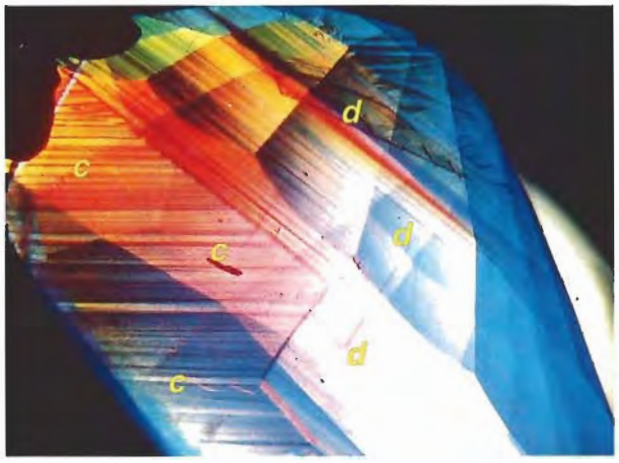

Figure 20. The 6.10 ct ruby also displayed dominant negative d *planes as the stone was rotated to view additional growth-structure characteristics. Immersion, magnified 8×.*

1986, 1988; Kiefert, 1987; Schmetzer, 1987, 1988). Twin planes parallel to the positive *r* planes (commonly referred to as "laminated twinning") are common in natural rubies, but they may also be present in flux-grown synthetic rubies produced by Kashan (and, less commonly, in those from Chatham or produced by the Verneuil method). In synthetic rubies, however, only rarely will the twin planes intersect one another. In contrast, twinning in natural rubies frequently has a "checkerboard" or "lattice work" appearance (again, see figure 18; Schmetzer, 1987). Other forms of twinning observed in natural and synthetic corundum can also aid in this separation (e.g., Kiefert, 1987; Schmetzer, 1988; Schmetzer et al., 1994; Hänni et al., 1994).

With regard to how the presence of the negative *d* plane may relate to source determinations, two of the rubies (1.34 and 0.15 ct) were purchased in Vietnam, and three others (2.53, 4.51, and 6.10 ct) revealed internal features typical of Vietnamese rubies. The suppliers of two of the remaining rubies (7.03 and 25.55 ct) indicated that they came from Myanmar. The author was unable to determine the probable source location of the 10.07 ct ruby. It is interesting that the negative *d* plane noted by Bauer (1896) also was reportedly in a natural ruby from Burma (now Myanmar). Therefore, it can be stated that to date the negative *d* plane has been observed in rubies from only two sources: Vietnam (Luc Yen) and Myanmar (Mogok Stone Tract). Whereas the author has examined five to 10 times as many Mogok as Vietnamese rubies, he has observed this plane more frequently in the Vietnamese stones.

CONCLUSION

The analysis of internal growth structures (internal indicators of crystal habit formation) in fashioned gemstones has been increasing in importance since it was first introduced to gemologists in 1985. The methods and principles involved can be learned and used by any gemologist with a minimum of specialized equipment. With experience, the study of growth structures—through the identification of individual and pairs of crystal planes—can help distinguish between fashioned natural and synthetic gems as well as help classify gemstones from various deposits. While this article focuses on the identification of growth planes, observations of color zoning and twinning characteristics can also provide key information relating to a natural/synthetic distinction or provenance determination (see, e.g., Schmetzer, 1987; Smith and Surdez, 1994; Peretti et al., 1995; Smith et al., 1995; Hänni et al., 1994).

According to earlier reports, the negative rhombohedral *d* (01$\bar{1}$2) plane was extremely rare in natural rubies and occurred only as a subordinate feature. However, this article has detailed for the first time in the professional literature the occurrence of negative *d* planes as intermediate to dominant crystal planes in natural rubies. It is potentially relevant to locality determination that to date the negative *d* plane has been observed only in rubies from Vietnam and Myanmar. These findings reinforce the importance of not relying on any single growth feature as conclusive proof of the natural or synthetic origin of a ruby or sapphire. Instead, identification and analysis of growth structures requires keen observation and interpretation of all the observed crystallographic features.

REFERENCES

Bauer M. (1896) Ueber das Vorkommen der Rubine in Birma. *Neues Jahrbuch für Mineralogie, Geologie und Palaeontologie*, Vol. 2, pp. 197–238.

Bauer M., Schlossmacher K. (1932) *Edelsteinkunde*, 3rd ed. Leipzig, Germany, Bernhard Tauchnitz.

Crowningshield R., Hurlbut C., Fryer C.W. (1986) A simple procedure to separate natural from synthetic amethyst on the basis of twinning. *Gems & Gemology*, Vol. 22, No. 3, pp. 130–139.

Dana J.D., Dana E.S. (1904) *The System of Mineralogy*, 6th ed. John Wiley and Sons, New York, London.

Goldschmidt V. (1918) *Atlas der Krystallformen*. Vol. 5. Carl Winters Universitätsbuchhandlung, Heidelberg, Germany.

Hänni H.A., Schmetzer K. (1991) New rubies from the Morogoro area, Tanzania. *Gems & Gemology*, Vol. 27, No. 3, pp. 156–167.

Hänni H.A., Schmetzer K., Bernhardt H-J. (1994) Synthetic rubies by Douros: A new challenge for gemologists. *Gems & Gemology*, Vol. 30, No. 2, pp. 72–86.

Hofer S.C. (1985) Pink diamonds from Australia. *Gems & Gemology*, Vol. 21, No. 3, pp. 147–155.

Kane R.E. (1980) The elusive nature of graining in gem-quality diamonds. *Gems & Gemology*, Vol. 16, No. 9, pp. 294–314.

Kane R.E. (1987) Three notable fancy-color diamonds: Purplish-red, purple-pink, and reddish-purple. *Gems & Gemology*, Vol. 23, No. 2, pp. 90–95.

Kiefert L., Schmetzer K. (1986) Morphologie und Zwillingsbildung bei synthetischen blauen Saphiren von Chatham. *Zeitschrift der Deutschen Gemmologischen Gesellschaft*, Vol. 35, No. 3/4, pp. 127–138.

Kiefert L. (1987) *Mineralogische Untersuchungen zur Charakterisierung und Unterscheidung Natürlicher und Synthetischer Saphire*. Diplomarbeit Universität Heidelberg, Germany, 203 pp.

Kiefert L., Schmetzer K. (1987) Blue and yellow sapphire from Kaduna Province, Nigeria. *Journal of Gemmology*, Vol. 20, No. 7-8, pp. 427–442.

Kiefert L., Schmetzer K. (1988) Morphology and twinning in Chatham synthetic blue sapphire. *Journal of Gemmology*, Vol. 21, No. 1, pp. 16–22.

Kiefert L., Schmetzer K. (1991a) The microscopic determination of structural properties for the characterization of optical uniaxial natural and synthetic gemstones, part 1: General considerations and description of the methods. *Journal of Gemmology*, Vol. 22, No. 6, pp. 344–354.

Kiefert L., Schmetzer K. (1991b) The microscopic determination of structural properties for the characterization of optical uniaxial natural and synthetic gemstones, part 2: Examples for the applicability of structural features for the distinction of natural emerald from flux-grown and hydrothermally-grown synthetic emerald. *Journal of Gemmology*, Vol. 22, No. 7, pp. 427–438.

Kiefert L., Schmetzer K. (1991c) The microscopic determination of structural properties for the characterization of optical uniaxial natural and synthetic gemstones, part 3: Examples for the applicability of structural features for the distinction of natural and synthetic sapphire, ruby, amethyst and citrine. *Journal of Gemmology*, Vol. 22, No. 8, pp. 471–482.

Koivula J.I., Fritsch E. (1989) The growth of Brazil-twinned synthetic quartz and the potential for synthetic amethyst twinned on the Brazil law. *Gems & Gemology*, Vol. 25, No. 3, pp. 159–164.

Lind T., Schmetzer K., Bank H. (1986) Blue and green beryls (aquamarines and emeralds) of gem quality from Nigeria. *Journal of Gemmology*, Vol. 20, No. 1, pp. 40–48.

Peretti A., Smith C.P. (1993) An in-depth look at Russia's hydrothermal synthetic rubies. *JewelSiam*, Vol. 4, No. 2, pp. 96–102.

Peretti A., Schmetzer K., Bernhardt H-J., Mouawad F. (1995) Rubies from Mong Hsu. *Gems & Gemology*, Vol. 31, No. 1, pp. 2–26.

Rooney M-L.T., Welbourn C.M., Shigley J.E., Fritsch E., Reinitz I. (1993) De Beers near colorless-to-blue experimental gem-quality synthetic diamonds. *Gems & Gemology*, Vol. 29, No. 1, pp. 38–45.

Schmetzer K. (1985) Ein verbesserter Probenhalter und seine Anwendung auf Probleme der Unterscheidung natürlicher und synthetischer Rubine sowie natürlicher und synthetischer Amethyste. *Zeitschrift der Deutschen Gemmologischen Gesellschaft*, Vol. 34, No. 1, pp. 30–47.

Schmetzer K. (1986a) An improved sample holder and its use in the distinction of natural and synthetic ruby as well as natural and synthetic amethyst. *Journal of Gemmology*, Vol. 20, No. 1, pp. 20–33.

Schmetzer K. (1986b) *Natürliche und synthetische Rubine-Eigenschaften und Bestimmung*. Schweizerbart, Stuttgart.

Schmetzer K. (1987) On twinning in natural and synthetic flux-grown ruby. *Journal of Gemmology*, Vol. 20, No. 5, pp. 294–305.

Schmetzer K. (1988) A new type of twinning in natural sapphire. *Journal of Gemmology*, Vol. 21, No. 4, pp. 218–220.

Schmetzer K., Bernhardt H-J., Biehler R. (1991) Emeralds from the Ural Mountains, USSR. *Gems & Gemology*, Vol. 27, No. 2, pp. 86–99.

Schmetzer K., Smith C.P., Bosshart G., Medenbach O. (1994) Twinning in Ramaura synthetic rubies. *Journal of Gemmology*, Vol. 24, No. 2, pp. 87–93.

Shigley J.E., Fritsch E., Reinitz I., Moon M. (1992) An update on Sumitomo gem-quality synthetic diamonds. *Gems & Gemology*, Vol. 28, No. 2, pp. 116–122.

Shigley J.E., Fritsch E., Koivula J.I., Sobolev N.V., Malinovsky I.Y., Pal'yanov Y.N. (1993) The gemological properties of Russian gem-quality synthetic yellow diamonds. *Gems & Gemology*, Vol. 29, No. 4, pp. 228–248.

Smith C.P. (1992) Contributions to the crystal growth analysis of natural and synthetic rubies: Identification of a dominant negative rhombohedral "*d*" plane (01$\bar{1}$2) in natural ruby. *60th Anniversary Proceedings, Zeitschrift der Deutschen Gemmologischen Gesellschaft*, Vol. 41, No. 4, pp. 182–183.

Smith C.P., Bosshart G. (1993) New flux-grown synthetic rubies from Greece. *JewelSiam*, Vol. 4, No. 4, pp. 106–114.

Smith C.P., Surdez N. (1994) The Mong Hsu ruby: A new type of Burmese ruby. *JewelSiam*, Vol. 4, No. 6, pp. 82–98.

Smith C.P. (1995) Contribution to the nature of the infrared spectrum for Mong Hsu rubies. *Journal of Gemmology*, Vol. 24, No. 5, pp. 321–335.

Smith C.P., Kammerling R.C., Keller A.S., Peretti A., Scarratt K.V., Khoa N.D., Repetto S. (1995) Sapphires from southern Vietnam. *Gems & Gemology*, Vol. 31, No. 3, pp. 168–186.

Stern W.B., Hänni H.A. (1982) Energy dispersive X-ray spectrometry: a non-destructive tool in gemmology. *Journal of Gemmology*, Vol. 18, No. 4, pp. 285–296.

Sunagawa I. (1992) Morphology aspects of diamonds, natural and synthetic, stable and metastable growth. *60th Anniversary Proceedings, Zeitschrift der Deutschen Gemmologischen Gesellschaft*, Vol. 41, No. 4, pp. 184–185.

GIA 97 TUCSON

EVERYTHING UNDER THE SUN IN GEMOLOGY AND JEWELRY MANUFACTURING ARTS EDUCATION

GIA ALUMNI & ASSOCIATES EVENTS

- GIA President's Award Reception on Jan. 31
- General Membership Breakfast Meeting on Feb. 1
- Alumni Gala & Awards Evening on Feb. 2

EXHIBITS

To find out what's new in GIA GEM Instruments, the GIA Bookstore, *Gems & Gemology*, GIA Education, GIA ARMS, and Alumni & Associates, stop by the GIA booths at the AGTA GemFair in the Convention Center Galleria and the GLDA Show in the Holiday Inn Broadway Lobby spaces 6 & 7.

For more information about GIA classes and seminars in Tucson,
Call Today Toll-Free:
(800) 421-7250 ext. 269
(Alumni Events ext. 724)
Outside the U.S., call:
(310) 829-2991 ext. 269
or FAX: (310) 453-7674

GIA TUCSON '97
CLASSES AND SEMINARS

January 27–February 4, 1997

Topics include:
Diamond Grading
Gem Identification
Colored Stone Grading
Detecting Synthetic Diamonds
Detecting Treated Gems
Identifying Challenging Synthetics
Gem ID Challenge with John Koivula
GIA ARMS: Your Roadmap to Greater Profitability
GIA Research: Year in Review
Introduction to Insurance Replacement Appraisals
Working with Wax
Wax Carving Techniques
Bench Tricks
Advanced Fabrication
Mass Finishing Techniques–Textures
Flush, Bezel, Gypsy Setting

Plus! NEW in '97:
Working with Platinum
Chain Making
Working with Precious Metal Clay
Casting Stones in Place
Channel Setting with the AllSet Tool
Scrap Preparation and Sampling

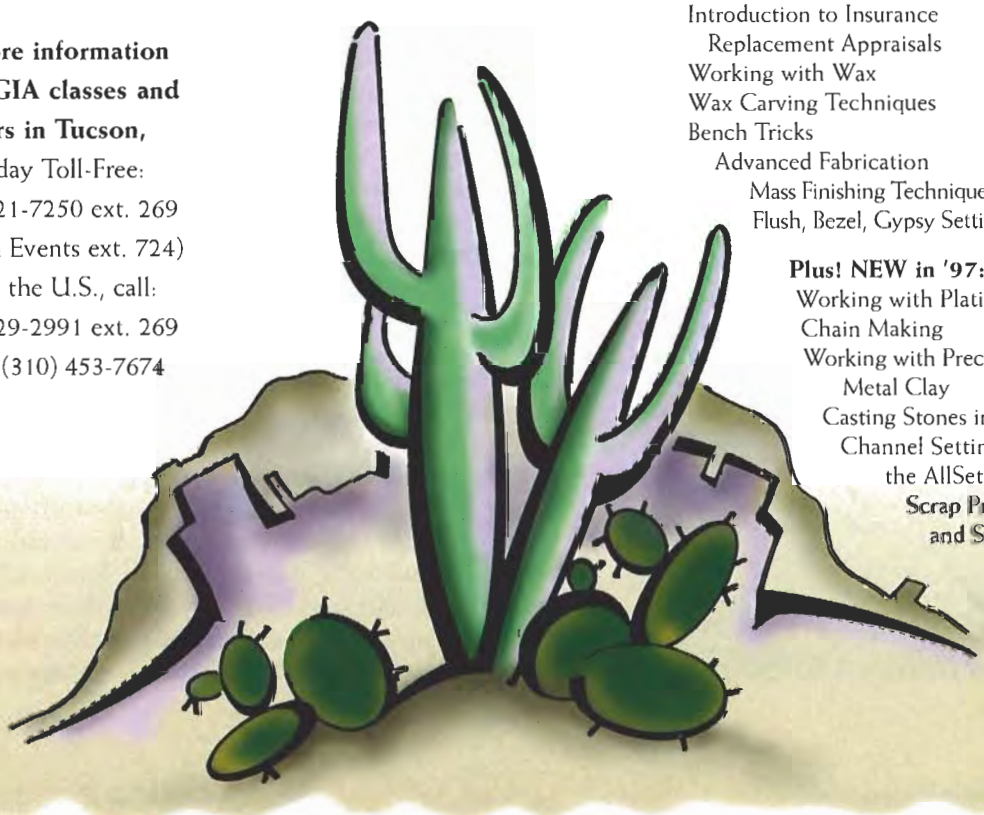

GGTu7

RUSSIAN FLUX-GROWN SYNTHETIC ALEXANDRITE

By Karl Schmetzer, Adolf Peretti, Olaf Medenbach, and Heinz-Jürgen Bernhardt

Synthetic alexandrite is being flux-grown in Russia in a molybdenum-, bismuth-, and germanium-bearing solvent by means of the reverse-temperature gradient method. Characteristic properties include habit, twinning, growth patterns, residual flux inclusions, trace-element contents, chemical zoning, color zoning, and spectroscopic features in the visible and infrared ranges. The relationship between production technique and characteristic properties is discussed, and diagnostic properties that can be used to distinguish these synthetics from natural alexandrite are disclosed.

ABOUT THE AUTHORS

Dr. Schmetzer is a research scientist residing in Petershausen, Germany. Dr. Peretti, former director of the Gübelin Gemmological Laboratory, is an independent gemological consultant residing in Adligenswil, Switzerland. Dr. Medenbach and Dr. Bernhardt are research scientists at the Institut für Mineralogie of Ruhr-Universität, Bochum, Germany.

Acknowledgments: The authors thank R. Goerlitz of Idar-Oberstein, Germany, for the loan of many of the synthetic alexandrites. Samples were also provided in 1988 and 1991 by Dr. A. Ya. Rodionov and the late Dr. A. S. Lebedev, then research scientists at the Institute of Geology and Geophysics, Novosibirsk, Russia. Infrared spectroscopy was performed by Dr. L. Kiefert of SSEF, Basel, Switzerland. Prof. Dr. W. Stern, Geochemical Laboratory, University of Basel, helped prepare the X-ray fluorescence spectra.

Photos are by the authors unless otherwise noted.

Gems & Gemology, Vol. 32, No. 3, pp. 186–202.

Fine alexandrites are even rarer than fine rubies, sapphires, and emeralds. The major factors determining price are size, clarity, brilliancy, color in daylight, color change in artificial light, and country of origin. The finest alexandrites are characterized by a lively and intense green color in daylight with a prominent color change to purplish red or reddish purple in incandescent light. The most prestigious source of natural alexandrites is Russia, specifically the Ural mountains, where they were first discovered. Fine alexandrites occasionally appear at international auctions. For example, a 31 ct alexandrite sold for almost US$185,000 at Christie's May 1992 auction in Geneva. Dealers in Idar-Oberstein report the sale of fine, large (over 5 ct) alexandrites for $10,000–$20,000 per carat, and even higher for exceptional stones (R. Guerlitz and A. Wild, pers. comm., 1996).

During the past 10 years, new deposits of natural alexandrite have been found in Minas Gerais, Brazil (Bank et al., 1987; Proctor, 1988; Cassedanne and Roditi, 1993; Karfunkel and Wegner, 1993); in Orissa and Madhya Pradesh, India (Patnaik and Nayak, 1993; Newlay and Pashine, 1993); and, most recently, near Songea in southern Tanzania (see "News on the Songea Deposit . . .", 1995; Kammerling et al., 1995). In addition, gem alexandrites are still being recovered from the historic emerald deposits of the Ural Mountains (Eliezri and Kremkow, 1994; Laskovenkov and Zhernakov, 1995).

As greater quantities of gem alexandrite enter the market, significant amounts of faceted alexandrites are being submitted to gemological laboratories for testing. Occasionally, distinguishing natural from synthetic has been difficult, notably for flux-grown synthetics, but especially when a specimen lacks diagnostic mineral inclusions (see Bank et al., 1988; Henn and Bank, 1992; Kammerling, 1995). These difficulties are caused by the similarity of growth structures and healing "feathers" in natural alexandrites from different localities to residual flux feathers in flux-grown synthetic alexandrites. In addition, hematite platelets in natural alexandrites sometimes resemble platinum inclusions in their flux-grown synthetic counterparts.

Figure 1. As the number of natural alexandrites in the marketplace increases, so does the quantity of synthetic alexandrites. One of the most convincing synthetic alexandrites is the material that is being flux grown in Russia. Shown here is a 1.08 ct (6.3 × 5.3 mm) faceted Russian flux-grown synthetic alexandrite in fluorescent light (left) and incandescent light. Photos © GIA and Tino Hammid.

The Russian-produced synthetic alexandrites (figure 1) can imitate the highest-quality natural alexandrites—such as those from the Ural mountains. Yet some natural alexandrites have sold for up to 300 times as much as their synthetic counterparts. Consequently, these synthetic alexandrites occasionally are misrepresented in the trade as Uralian alexandrites. One of the authors (A.P.) recently encountered two instances of synthetic alexandrites offered for sale as natural stones in Switzerland.

According to the voluminous scientific and patent literature available to the authors, synthetic alexandrite and synthetic chrysoberyl can be grown from the melt (Czochralski, Verneuil, Bridgman, and floating-zone techniques), hydrothermally, by the flux method, and by chemical vapor deposition (for a good description of most of these modern crystal-growth techniques, see Kimura and Kitamura, 1993). Because of such factors as production costs and the small crystals that result from some of these growth techniques, gem-quality synthetic alexandrites have been grown commercially and released to the market by just a few companies, which use the Czochralski, floating-zone, or flux method.

Two types of flux-grown synthetic alexandrite have been produced commercially for gem purposes. Since the 1970s, Creative Crystals Inc. of San Ramon, California, has produced synthetic alexandrite crystals by a method that uses a lithium polymolybdate flux, as described in the Cline and Patterson patent (1975).

The second type has been produced at various locations in the former USSR since the late 1970s or early 1980s, using a method originally developed at the Institute of Geology and Geophysics, Siberian Branch of the Academy of Sciences of USSR in Novosibirsk. A few crystals grown by this method were given to one of the authors (K.S.) by Drs. A. Ya. Rodionov and A. S. Lebedev in 1988 and 1991. Preliminary results from the examinations of these samples were never published because of the very small sample base. That situation has changed. Considerable quantities (many kilos) of rough

Russian synthetic alexandrite are now commercially available, either directly from Novosibirsk or indirectly from Bangkok, and large parcels of rough are being cut in Sri Lanka, especially for the American market (G. E. Zoysa, pers. comm., 1995). For the present study, the authors examined more than 200 synthetic alexandrites with properties that indicated that they were all produced by roughly the same method (i.e., using fluxes that were similar in composition). In addition, one commercial source of Russian flux-grown synthetic alexandrite is the Design Technological Institute of Monocrystals, also in Novosibirsk, which works in cooperation with the Institute of Geology and Geophysics. During a 1994 visit to Novosibirsk, one of the authors (A.P.) obtained information first hand at both institutes and saw demonstrations of part of the growth facilities, including the use of crucibles and furnaces.

The production technique used for Russian flux-grown synthetic alexandrite was briefly mentioned by Godovikov et al. (1982) and later described, in greater detail, by Rodionov and Novgorodtseva (1988) and Bukin (1993). The gemological properties of Russian flux-grown synthetic alexandrites were first described by Trossarelli (1986) and later by Henn et al. (1988), Henn (1992), and Hodgkinson (1995). The present article examines the relationship between production technique and typical properties, and identifies those characteristics that can be used to distinguish these synthetics from natural alexandrite.

TABLE 1. Modern techniques for the flux growth of chrysoberyl and alexandrite.

Authors	Inventors/ assigned to	Flux	Growth conditions[a]		Dopant (oxide)	Remarks
Farrell et al. (1963)		$PbO–PbF_2$	s, sn	sc	—	Chrysoberyl
		PbO	sn	fe	—	Chrysoberyl
Farrell and Fang (1964)		PbO	s, sn	sc	—	Chrysoberyl
		$PbO–PbF_2$	s, sn	sc	—	Chrysoberyl
		$Li_2MoO_4–MoO_3$	s, sn	sc	Cr	Alexandrite
	Bonner and Van Uitert (1968)/Bell Telephone Laboratories	$PbO–PbF_2–SiO_2 \pm B_2O_3$	sn	sc	Cr	Alexandrite
Tabata et al. (1974)		$PbO–PbF_2 \pm B_2O_3$	sn	sc	—	Chrysoberyl; B_2O_3 is used as habit modifier
	Cline and Patterson (1975)/ Creative Crystals Inc.	$Li_2MoO_4–MoO_3$ (also Li–niobate, tungstate and $PbO–PbF_2$)	s, sn	sc	Cr, Fe	Alexandrite
	Machida and Yoshihara (1980,1981) /Kyoto Ceramic Co.	Li_2MoO_4	s	sc	Cr, V	Alexandrite
Godovikov et al. (1982)		"Flux"		tg		Alexandrite
	Hirose (1984)/Suwa Seikosha K.K.	$V_2O_5 \pm$ Mo- or W–Oxides				Alexandrite
	Kasuga (1984)/Suwa Seikosha K.K.	Li_2MoO_4, MoO_3, V_2O_5, LiOH	s		Cr, Fe	Alexandrite
	Togawa (1985)/ Suwa Seikosha K.K.	V_2O_5	s	sc, tg	Cr	Alexandrite
	Isogami and Nakata (1985,1986)/Kyocera Corp.	Li_2MoO_4	s	sc	Fe, Ce, V, Co, W, Cr, Ni, Mn	Cat's-eye; TiO_2, SnO_2, ZrO_2, or GeO_2 causing asterism
Rodionov and Novgorodtseva (1988)		"Flux"	sn	sc, tg		Alexandrite; two habits according to experimental conditions: platy or equidimensional
Bukin (1993)		$Bi_2O_3–MoO_3$	s, sn	tg (sc, fe)	Cr,Ti	Alexandrite; laser applications

[a] *fe = flux evaporations, s = seeded growth, sc = slow cooling, sn = spontaneous nucleation, and tg = temperature gradient.*

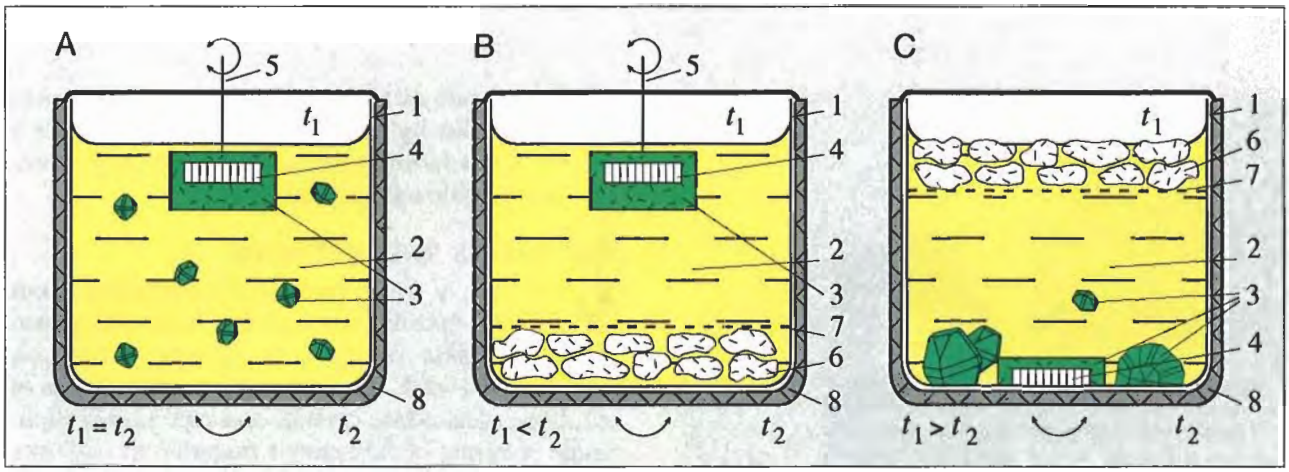

Figure 2. Three main processes have been described for the flux growth of beryllium-bearing oxides and silicates such as synthetic alexandrite and emerald: (A) slow cooling of a saturated melt, with seeded growth or growth by spontaneous nucleation; (B) seeded growth in a temperature gradient, with a growth zone above the dissolution zone; and (C) seeded growth or growth by spontaneous nucleation in a reverse temperature gradient, with a growth zone at the bottom of the crucible below the dissolution zone. Key: 1 = platinum crucible, 2 = flux melt, 3 = growing crystals, 4 = seed, 5 = platinum seed holder, 6 = nutrient, 7 = baffle, 8 = insulation, t_1 = temperature in the upper part of the crucible, t_2 = temperature in the lower part of the crucible. The circular arrows at the top of A and B indicate the possible rotation of the seed holder; arrows at the bottom of all three processes represent the possible crucible rotation. Adapted from Bukin (1993).

FLUX GROWTH OF SYNTHETIC ALEXANDRITE: HISTORY AND DEVELOPMENT

Early 19th-century experiments in the flux growth of synthetic chrysoberyl were summarized by Elwell and Scheel (1975). More modern flux techniques to grow synthetic chrysoberyl and/or alexandrite started in the 1960s (table 1). Most procedures use the slow-cooling technique (figure 2A). First, the solvent of flux and nutrient (Al_2O_3 + BeO + color-causing dopants) is heated above the point at which the flux liquefies and is then held at that temperature for a period sufficient to dissolve the nutrient oxides in the flux (Farrell and Fang, 1964). Next, the melt is cooled slowly at a constant rate until the flux solidifies. Last, the crystals that grew in the flux during cooling are removed from the crucible by dissolving the flux (e.g., in hot nitric acid). Common fluxes used for chrysoberyl and alexandrite are PbO-PbF_2, Li_2MoO_4-MoO_3, and V_2O_5 (see table 1). The temperatures at which the cooling process begins and ends vary according to the composition of the flux used. They generally range from 1350°C to 800°C. Cooling rates are usually between 0.125°C and 3°C per hour. Both seeded growth and growth by spontaneous nucleation are used (again, see figure 2A). Seed crystals may be natural or synthetic chrysoberyl or alexandrite. Cr_2O_3, Fe_2O_3, and/or V_2O_3 are used as dopants.

The morphology of synthetic chrysoberyl or alexandrite depends primarily on the composition of the flux and not on the temperatures or cooling gradients used. Tabata et al. (1974) demonstrated the influence of B_2O_3 on the habit of chrysoberyl grown from PbO-PbF_2 solvents: They observed a distinct modification of habit from platy (flux without B_2O_3) to prismatic or equidimensional (flux with B_2O_3).

Isolated attempts to grow synthetic chrysoberyl or alexandrite by the flux evaporation technique have had poor results (see Farrell et al., 1963). In this method, constant heating of the melt in open crucibles leads to supersaturation of the melt and the growth of crystals by spontaneous nucleation.

Godovikov et al. (1982) first mentioned the possible growth of alexandrite by the temperature-gradient method, which works by creating a convection current within the crucible. According to a Japanese patent application by Togawa (1985), the nutrient is placed at the bottom of the crucible, where a certain temperature is reached and then maintained. A seed crystal is placed into the melt in the upper part of the crucible, which is held at a temperature lower than that at the bottom of the crucible (figure 2B). As the nutrient dissolves into the solution, circulation begins between the warmer and cooler areas in the crucible (convection currents). When the solution with the nutrient reaches the cooler area, it becomes supersaturated and crystals begin to form. These different temperatures are

Figure 3. The Russian flux-grown synthetic alexandrite crystals examined were either single crystals (right, 9 × 7 mm) or cyclic pseudohexagonal twins (left, 12 × 11 mm), which are shown here in incandescent light. Photo © GIA and Tino Hammid.

maintained, with the growth zone *above* the dissolution zone, for weeks or even months.

Rodionov and Novgorodtseva (1988) described a reverse temperature-gradient technique—in which the growth zone is located *below* the dissolution zone—for the growth of synthetic alexandrite. In this method, the nutrient is placed in the upper part of the crucible, where a certain temperature is reached and then maintained, while the bottom of the crucible is held at a lower temperature (figure 2C; temperatures are in the same range as those noted above for the slow-cooling process). With this technique, synthetic alexandrite crystals grow by spontaneous nucleation, usually in contact with the bottom of the crucible (Rodionov and Novgorodtseva, 1988), although seeded growth (with a seed placed at the bottom of the crucible) is also possible (Bukin, 1993).

The solvent used in Russia is a complex bismuth-molybdenum flux, mainly composed of Bi_2O_3 and MoO_3 (A. Ya. Rodionov, pers. comm., 1988; Bukin 1993; confirmed during a visit by one of the authors [A.P.] to Novosibirsk in 1994).

The basic growth technique that was developed in Novosibirsk forms synthetic alexandrite crystals with two different habits—thin and platy or more isometric and equidimensional—depending on controlled change in the growth conditions (Rodionov and Novgorodtseva, 1988). Growth rates of 0.13 to 0.35 mm per day in different crystallographic directions have been obtained. For example, a 14 × 8 × 9 mm crystal was grown by spontaneous nucleation over three months with this technique (Rodionov and Novgorodtseva, 1988). According to Bukin (1993), crystals as large as 2–3 cm (over one inch) can be grown by spontaneous nucleation in a reverse-temperature gradient, and even larger samples are possible with seeded growth.

MATERIALS AND METHODS

In 1994, one of the authors (A.P.) purchased about 50 synthetic alexandrites that had been flux grown in Russia. These samples were selected in Bangkok from six lots, each of which contained hundreds of synthetic alexandrite crystals and represented thousands of carats of flux-grown material. In addition, R. Goerlitz of Idar-Oberstein, Germany, loaned the authors a lot of about 150 rough crystals that he had purchased in Novosibirsk in 1993. This sample of more than 200 Russian flux-grown synthetic alexandrites used for the present study also included material submitted by Novosibirsk scientists to one of the authors (K.S.) in 1988 and 1991. All of the original samples were rough crystals; the few faceted gems studied (see, e.g., figure 1) were fashioned from rough from the Bangkok and R. Goerlitz lots.

About half of the crystals were fully developed single crystals or cyclic twins with one irregular planar surface (figure 3). Compared to the smooth crystal faces, this irregular surface was somewhat rough and uneven; it probably represents the contact plane of the growing crystal with the bottom of the crucible (see the later discussion of growth conditions). Most of the balance of the samples had one irregular plane or surface that was obviously produced by sawing or breaking, probably to remove some impure, non-gem-quality material or to separate the single crystals or twins from larger clusters. Seven smaller crystals (sizes up to 4 mm) were fully developed without any irregular surface plane.

We performed standard gemological testing on about 40 of these crystals. To identify the internal growth planes and the external crystal faces, we studied about 50 crystals with a Schneider horizontal (immersion) microscope, which had a specially designed sample holder as well as specially designed (to measure angles) eyepieces (Schmetzer, 1986; Kiefert and Schmetzer, 1991; see also Peretti et al., 1995). In addition, we examined about 10 samples with an optical goniometer (an instrument used to measure crystal angles). By a combination of these methods, we identified all crystal faces and the most characteristic growth patterns. We studied and photographed the inclusions and internal structural features using the Schneider immersion microscope (with Zeiss optics) and an Eickhorst vertical microscope (with Nikon optics) and fiber-optic illumination.

Solid inclusions and solid phases on the surfaces of the crystals were characterized by X-ray powder diffraction analysis with a Gandolfi camera, by a Cambridge Instruments scanning electron microscope with an energy-dispersive X-ray detector (SEM-EDS), and by energy-dispersive X-ray fluorescence analysis (EDXRF) using a Tracor Northern Spectrace TN 5000 system.

We also performed qualitative chemical analysis of 22 samples using the same EDXRF instrumentation. For quantitative analysis of nine other samples, a CAMECA Camebax SX 50 electron microprobe was used. To evaluate nonhomogeneous chemical compositions of the alexandrite crystals, we measured 2–5 traverses (of 40 to 140 point analyses each) across the samples. For more detailed information, we also had one scan with 625 point analyses.

Polarized absorption spectra in the visible and ultraviolet range were recorded for nine microscopically untwinned single crystals with a Leitz-Unicam SP 800 double-beam spectrometer and a Zeiss multichannel spectrometer. Infrared spectroscopy was carried out on 11 samples using a Philips PU 9800 FTIR spectrometer.

RESULTS

Visual Appearance. The samples varied from slightly yellowish green to green and bluish green in daylight and from slightly orangy red to red and purplish red in incandescent light (again, see figures 1 and 3). No distinct color zoning was apparent in either the rough or faceted samples.

On the faces of some crystals, we observed a fine-grained white crust. In irregular cavities of other samples, we found a fine-grained gray or yellowish gray material.

Crystallography. All samples examined revealed an equidimensional habit, which was formed by three pinacoids *a*, *b*, and *c*; by four different rhombic prisms, designated *s*, *m*, *x*, and *k*; and by the rhombic dipyramid *o* (table 2). The seven small crystals that lacked rough or uneven faces were fully developed single crystals (see, e.g., figures 4 and 5).

All of the crystals with one uneven face—and those crystals that were sawn or broken—had three dominant faces: the pinacoid *a*, the rhombic prism *x*, and the rhombic dipyramid *o*. Frequently, the rhombic prism *k* was also present, and the pinacoid *c* was subordinate. About 90% of these crystals were cyclic twins (figures 6 and 7), which consisted of three individuals twinned by reflection across the rhombic prism (031) and forming a pseudohexagonal contact twin (figures 6 and 8). The remaining 10% of the samples were untwinned single crystals.

For those crystals that were not broken or sawn, the most frequently observed habit consisted of the *a*, *x*, *o*, and *k* faces (figures 6C and D). Also common was a habit formed by the three faces *a*, *x*, and *o* (figure 6A). Crystals with an additional *c* pinacoid were somewhat rarer (see table 2 and figures 6B and E).

Most of the cyclic twins were somewhat distorted; that is, identical crystal faces varied in their respective sizes between the three individuals of the cyclic twin. Examples are shown in figures 6C and D, in which varying sizes were drawn for the rhombic prism *x*. Consequently, a typical crystal of Russian flux-grown alexandrite is a combination of the two trillings drawn in figures 6C and D, with sizes of the *x* faces varying within the cyclic twin.

In a few single crystals with one irregular face, the pinacoid *b* and the rhombic prism *m* were also observed (see figure 5). In one of these single crystals, an additional rhombic prism *i* was also present (table 2).

Gemological Properties. Table 3 summarizes the gemological properties of the Russian flux-grown synthetic alexandrites examined. The values are more or less within the ranges published by others for crystals of this material (Trossarelli, 1986; Henn et al., 1988; Rodionov and Novgorodtseva, 1988; Henn, 1992; Bukin, 1993).

Specifically, these Russian synthetic alexandrites are distinctly pleochroic. Their color change is

TABLE 2. Morphological crystallography of Russian flux-grown synthetic alexandrites.

	Designation	hkl[c]	Type
Faces	*a*	(100)	pinacoid
	b[a]	(010)	pinacoid
	c	(001)	pinacoid
	s[a]	(120)	rhombic prism
	m[a]	(110)	rhombic prism
	x	(101)	rhombic prism
	k	(021)	rhombic prism
	i[b]	(011)	rhombic prism
	o	(111)	rhombic dipyramid
	Faces	**Number of crystals**	
Habit	*a x o*	21	
	a x o c	7	
	a x o k	49	
	a x o c k	10	
Characteristic angles formed by two faces	*ax* 141°	*xx'* 78°	
	ao 137°	*oo'* 86°	
	kk' 81.5°	*kk'* 141.5° (re-entrant)	

[a] *Observed only in single crystals.*
[b] *Observed only in one single crystal.*
[c] *Orientation of the unit cell for the Miller indices: a = 4.43, b = 9.40, c = 5.48.*

Figure 4. This 3 × 4 mm untwinned synthetic alexandrite single crystal was grown by spontaneous nucleation without crucible contact. (The darkish patches on some crystal faces are the result of carbon coating for microprobe analysis.) Photomicrograph by John I. Koivula.

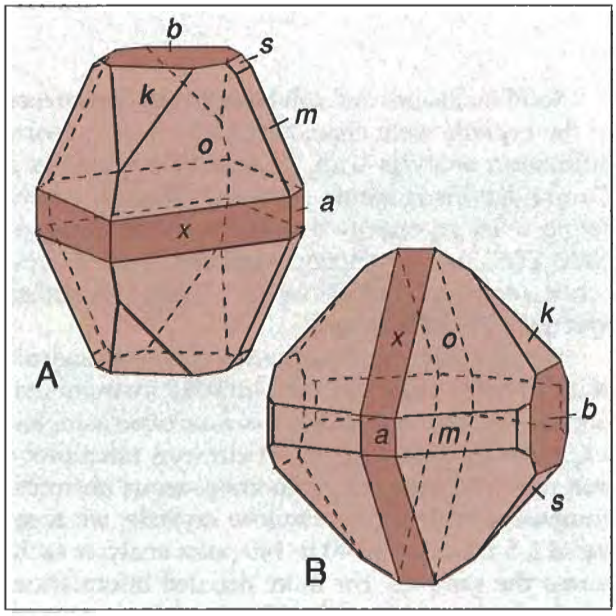

Figure 5. This illustration shows the untwinned synthetic alexandrite in figure 4 in two different orientations (A, B). The second orientation (B) is consistent with the orientation of the cyclic twins in figure 6.

caused by a change in two of the pleochroic colors—parallel to the a- and b-axes, with the latter making the greater contribution—when illumination is changed from day or fluorescent to incandescent light. The most intense color change was observed for those synthetic alexandrites that revealed a yellowish orange color in daylight and a reddish orange color in incandescent light parallel to the b-axis; a somewhat weaker color change was observed for samples that revealed a pleochroic color of greenish yellow or yellow in daylight and yellowish orange or orangy yellow color in incandescent light parallel to the b-axis (table 3; see also Schmetzer et al., 1980).

Microscopic Characteristics. *Structural Properties (Growth Features and Twinning).* As mentioned earlier, most of the sample Russian flux-grown synthetic alexandrites were twinned. When examined with polarized light, the three individuals of the trilling and their twin boundaries became clearly visible—especially when the polarizer was rotated (figure 8). The angle between twinned individuals is 59.88° (not quite 60°—Goldschmidt and Preiswerk, 1900; Goldschmidt, 1900), which is why the twin boundaries are not exactly planar faces (figure 9). In some samples, the twin boundary between two individuals of the cyclic twin revealed a microstructure of small inclusions of alexandrite crystals oriented parallel to the third individual of the trilling. Most of the twinned samples revealed a 141.5° re-entrant angle formed by two rhombic prism faces k and k^1 (figures 6 and 10).

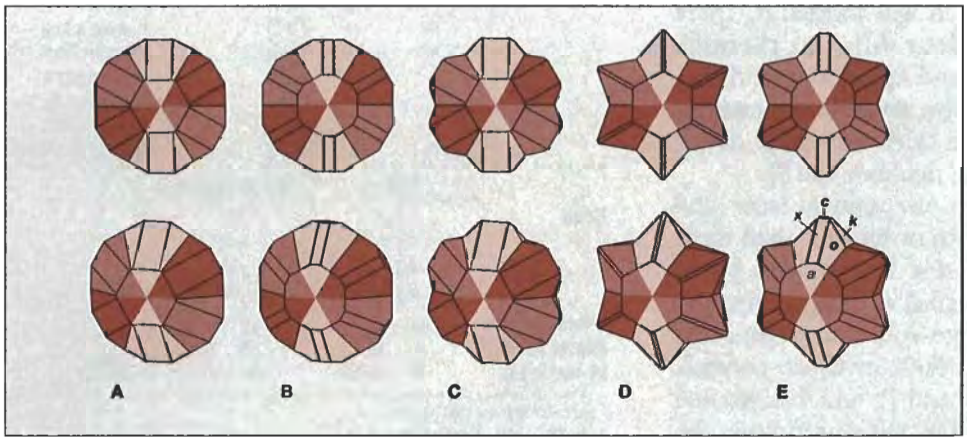

Figure 6. The crystal habits of cyclic-twin flux-grown synthetic alexandrites are shown here in these idealized drawings, as they appear looking down the a-axis (top row) and slightly oblique to the a-axis (bottom row). The habit of the crystals is formed by the pinacoid a, *the rhombic prisms* x *and* k, *and by the rhombic dipyramid* o; *the pinacoid* c *is a subordinate face.*

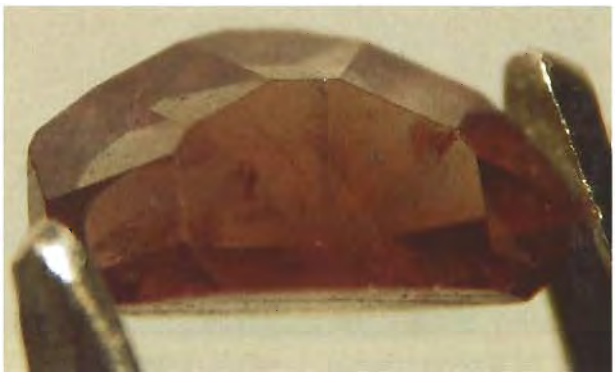

Figure 7. This approximately 3 × 5.5 mm cyclic twin of Russian synthetic alexandrite reveals an irregular contact plane (below) with the crucible; the habit of the crystal is formed by a, x, *and* o *faces (see figure 6A).*

The internal growth features of both the rough and faceted Russian synthetic alexandrites corresponded to the external morphology of the crystals. All single crystals or cyclic twins that showed one irregularly oriented uneven plane—that is, all samples that grew in contact with the crucible—revealed distinct internal growth planes parallel to the four dominant faces *a*, *x*, *k*, and *o*.

In a view parallel to the crystals' a-axis (i.e., perpendicular to the *a* pinacoid), growth planes parallel to different *k* prism faces were visible in most of the samples (about two out of three; again, see figures 6 and 10). Two characteristic angles were observed in this orientation: an angle of 81.5° formed by two *k* prism faces of one individual, and a re-entrant angle of 141.5° formed by two *k* faces of two individuals of the twin (see table 2). All of these *kk'* characteristic growth structures also were observed in the faceted synthetic alexandrites (figure 11).

Figure 8. The three individuals and the twin boundaries of this trilling are clearly visible when this cyclic twin of synthetic alexandrite is viewed parallel to the a-axis, using a polarizer and immersion. Magnified 10x.

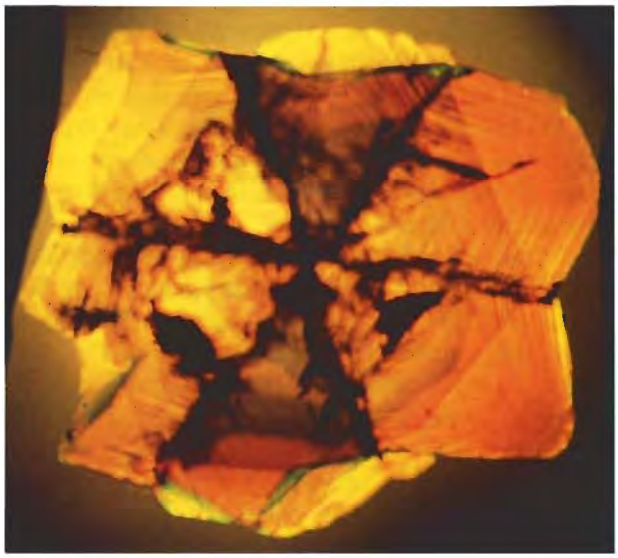

In a view parallel to the b-axis (figure 12A), a second characteristic growth pattern *ax* was observed in all samples. This consists of *a* pinacoids and *x* prism faces, which form a 78° angle (figure 13). By rotating the crystal approximately 29° about the a-axis (figure 12B), we saw a third characteristic growth pattern *ao*. Visible in all samples, it is formed by *a* pinacoids in combination with *o* dipyramids (figure 14). In this case, the characteristic angle (formed by the two rhombic dipyramids *o*) measures 86°. So, three characteristic patterns of growth structures were observed in single crystals and cyclic twins of Russian synthetic alexandrites: *ax* and *ao* in all samples, and *kk'* in approximately two-thirds of the samples.

In about 10% of the single crystals and twins examined, we saw a distinct color zoning—an intense red core (in incandescent light) and a lighter red rim—with the microscope. These areas are separated by a somewhat rounded, very intense red boundary (figure 15). This was the only color zoning seen in any of the samples.

In those small single crystals that were obviously grown without contact with the crucible (again,

TABLE 3. Gemological properties of Russian flux-grown synthetic alexandrites.

Property	Observations	
	Day (fluorescent) light	Incandescent light
Color	Yellowish green or green or bluish green	Orangy red or red or purplish red
Pleochroism		
X parallel to a-axis	Reddish purple	Purplish red
Y parallel to b-axis	Greenish yellow or yellow or yellowish orange	Orangy yellow or yellowish orange or reddish orange
Z parallel to c-axis	Blue-green	Blue-green
Refractive indices		
n_x	1.740 –1.746	
n_z	1.748 –1.755	
Density (g/cm^3)	3.67–3.74	
UV fluorescence		
Long-wave	Bright red	
Short-wave	Weak red or inert	

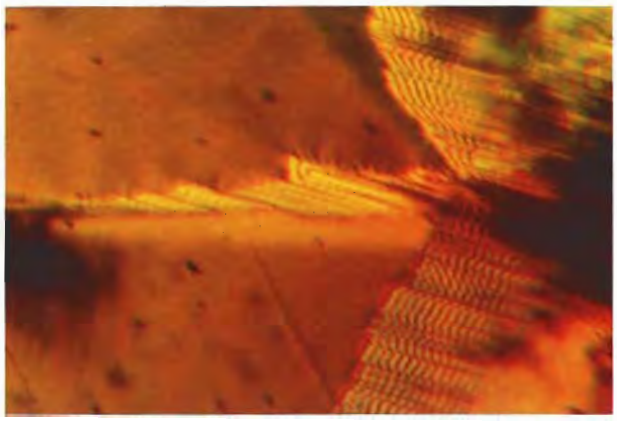

Figure 9. The twin boundaries in this cyclic twin of synthetic alexandrite show a distinct step-like structure. View almost parallel to the a-axis; immersion, crossed polarizers, magnified 60×.

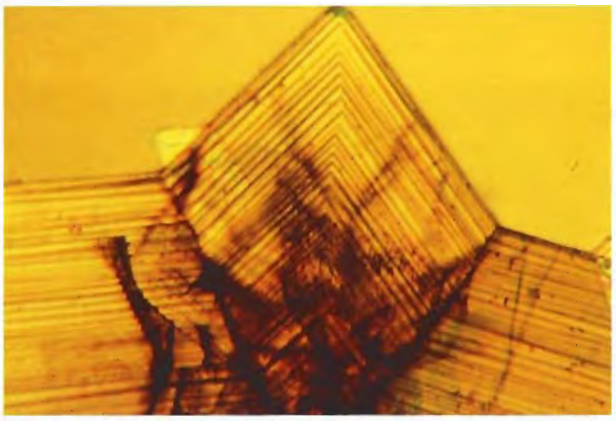

Figure 10. Growth structures parallel to different k *prism faces form a characteristic angle of 81.5°; re-entrant angles of 141.5° are formed by two different crystals of the cyclic twin. View parallel to the a-axis; immersion, magnified 35×.*

see figure 4), only very weak growth structures were found parallel to external crystal faces.

Inclusions. Various forms of residual flux were observed in many of the Russian synthetic alexandrites. These include "feathers" or "fingerprints" that consist mainly of isolated droplets or dots, which could be confused with healing features in natural alexandrites. Occasionally, we saw two-phase inclusions of residual flux and spherical bubbles, formed by shrinkage of the trapped flux as it cooled. Feathers of interconnecting tubes or channels (figure 16) also were frequently seen. In some crystals, planar, almost continuous, thin films within a net-like or web-like (i.e., emanating outward from a central point) pattern of flux were observed (figure 17). Occasionally, birefringent refractive components were also found in these flux "nets" (figure 18). In many cases, the flux inclusions took the form of wispy veils (figure 19).

In some of the samples, we observed metallic inclusions (particles or needles). On the basis of EDXRF analyses of similar-appearing solid phases on the surfaces of some of the crystals, we identified these inclusions as platinum.

Figure 11. The view parallel to the a-axis reveals characteristic growth structures parallel to the different k *prism faces of the cyclic twin in this faceted flux-grown synthetic alexandrite. Immersion, magnified 45×.*

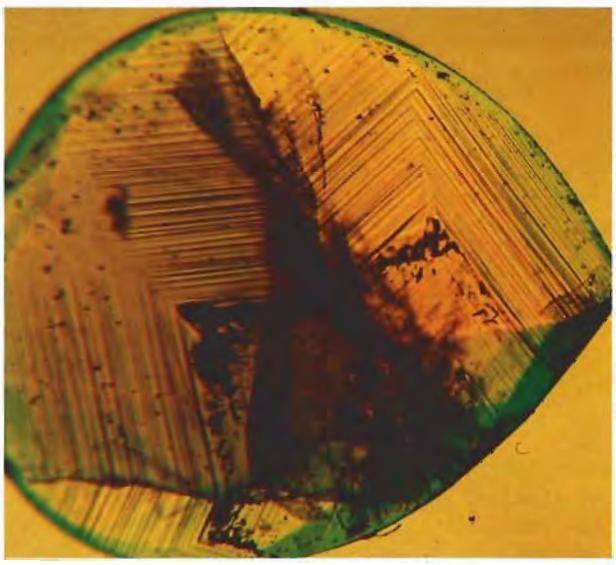

Chemistry. The EDXRF spectra of the faceted samples and rough crystals with clean faces—that is, without any flux residue on the surface or in open pits or cavities—indicated varying amounts of Cr, V, Fe, Ga, Ge, Bi, and Mo (figure 20), as well as the expected Al. On the basis of these EDXRF results, we added Ge to the list of elements that we measured with the electron microprobe. X-ray fluorescence analysis also confirmed the presence of Sn, traces of which were detected in the course of the microprobe analyses.

Initial scans by electron microprobe revealed zonal variations of all minor-to-trace elements, but zoning of Cr, Fe, and Ge—and sometimes V—was particularly evident. A detailed scan (about 3 mm in length, with 625 point analyses) across one sample (see table 4, sample 7) revealed a distinct zoning and correlation of Cr, Fe, and Ge. In this sample, Ge showed a positive correlation with Fe and a negative correlation with Cr. In other words, when Ge increased, Fe also increased, but Cr decreased as

growth conditions changed. In other samples, however, a negative correlation between Ge and Fe was observed; that is, when Ge increased, Fe decreased. Two synthetic alexandrites had a positive correlation between V and Fe, and one sample showed a positive correlation between Cr and Ge.

Table 4 summarizes the analytical results. In all samples, distinct amounts of Cr and Fe were present as chromophores (see Spectroscopic Features and Discussion sections below); in two alexandrites (samples 2 and 5), minor concentrations of V were also detected. In one single crystal (sample 9), the vanadium content was distinctly higher than the chromium; EDXRF revealed a similar condition of V > Cr in two other small single crystals.

An extreme variation in Cr_2O_3, FeO, and GeO_2 was observed in two samples (2 and 6). With the microscope, both revealed distinct color zoning: a somewhat irregular, very intensely colored boundary zone between a somewhat lighter core and a somewhat lighter rim (see figure 15). One of these synthetic alexandrites (figure 21) was sawn and polished to match the orientation in figure 12A, so that electron microprobe traverses could be made across

Figure 12. (A) This view parallel to the b-axis of a Russian synthetic alexandrite crystal reveals an orientation with a *pinacoids and* x *prism faces perpendicular to the projection plane. (B) After a rotation of the crystal through an angle of approximately 29°, the projection plane is perpendicular to* a *pinacoids and* o *dipyramids.*

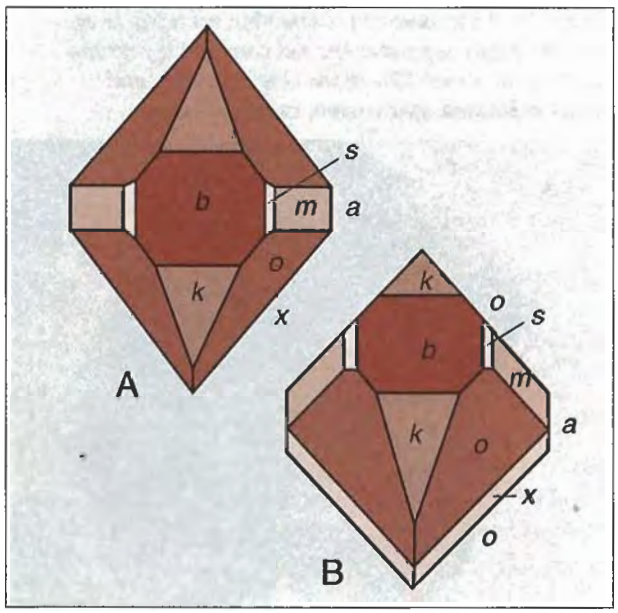

Figure 13. In this crystal, a *pinacoids and* x *prism faces (see figure 12A) form a growth pattern characteristic for synthetic alexandrite; the* x *prism faces form a characteristic angle of 78° (see inset). Immersion, magnified 30x and (inset) 50×.*

growth zones related to *x* (scan 1) or *a* (scans 2 and 3) faces. The distribution of Cr, Fe, and Ge is shown in figure 22, which represents the analytical data obtained in scan 2. This traverse reveals inner and outer cores, a boundary area, and a rim, similar to the zoning seen with the microscope (figure 21). The inner core had the most GeO_2 as well as distinct amounts of Cr_2O_3 and FeO. In the outer core, GeO_2 content was almost half that of the inner core, and the Cr_2O_3 and FeO contents were somewhat more than that of the inner core (table 5). The rim contained distinctly less Ge and Fe than the core, as well as slightly less Cr. In the boundary zone between core and rim, the Cr content jumped to an extremely high value and then dropped progressively in several steps toward the rim. Scans 1 and 3 (figure 21) revealed similar results (table 5). A scan across a second color-zoned alexandrite (sample 2) showed similar Cr zoning in the boundary area.

All samples had traces of Ga_2O_3 and trace-to-minor amounts of SnO_2 (table 4). MnO and TiO_2 were always close to the detection limit of the microprobe.

Solid Phases on the Surfaces of Rough Crystals. Several types of foreign matter were found on the surfaces of the rough synthetic alexandrites or in cavities, cracks, or pits in the surface.

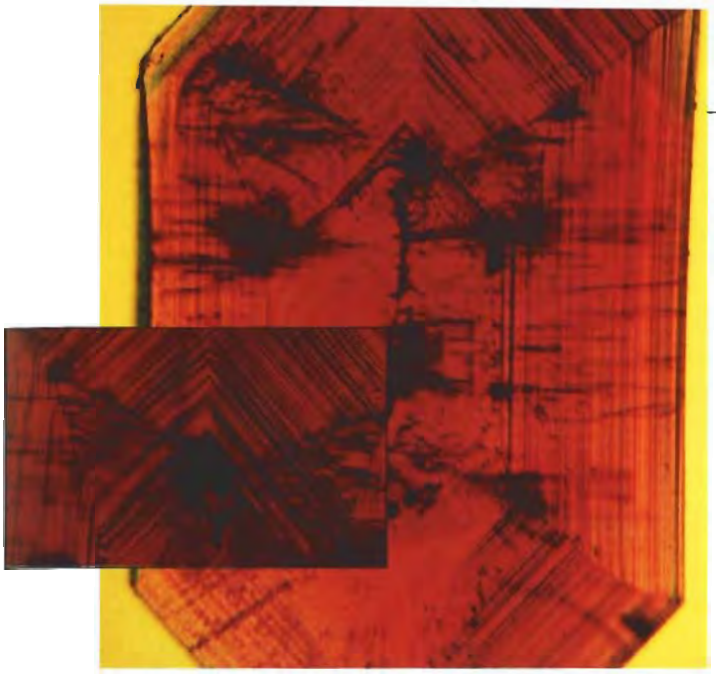

Figure 14. Here, a pinacoids and o dipyramids (see figure 12B) form a growth pattern that is also characteristic for synthetic alexandrite; the o dipyramids form a characteristic angle of 86° (see inset). Immersion, magnified 30x and (inset) 50×.

White polycrystalline crusts were removed from four samples and identified as anatase (TiO_2) by a combination of X-ray powder diffraction analysis, SEM-EDS, and EDXRF. Highly reflective particles on the surface of rough alexandrites (figure 23) were identified by EDXRF as platinum, most probably originating from the crucible. On the surface of a few samples, we also observed a pattern of platinum particles: a tetrahedral particle with a smaller skeleton-like crystal that is trailed by a thin needle. Similar platinum particles occasionally were found as inclusions.

Gray, fine-grained materials in cavities, pits, and cracks were identified in several cases as molybdenum- and bismuth-bearing compounds, that is, as residual flux. In one sample, the X-ray fluorescence spectrum of a crust of this gray, fine-grained material revealed characteristic lines for tungsten as well as for Mo and Bi. The morphology of this particular sample was typical of that described earlier for other samples (see figure 6).

Spectroscopic Features. *Ultraviolet-Visible Spectroscopy.* The polarized absorption spectra for the single crystals of flux-grown synthetic alexandrite were consistent with data reported in the literature for chromium, vanadium, and iron as chromophores in natural and synthetic alexandrites (Farrell and Newnham, 1965; Bukin et al., 1978, 1980; Schmetzer et al., 1980; Powell et al., 1985).

Infrared Spectroscopy. The infrared spectra of the rough and faceted samples showed some characteristic absorption bands in the 2800 to 3300 cm^{-1} range (figure 24). In samples obtained from Novosibirsk (1993), the following absorption maxima were found (in cm^{-1}): 2855, 2921, 2938 (shoulder), 3205 and 3224; samples originating from Bangkok (1994) revealed maxima at 2855, 2921, 2938 (shoulder), 3095, and 3196 cm^{-1}. Because water and/or hydroxyl absorption bands—especially in the 2500 to 3000 cm^{-1} range—are absent from the spectra of synthetic alexandrites, infrared spectroscopy is a powerful tool for separating natural and synthetic alexandrites (Leung et al., 1983, 1986; Stockton and Kane, 1988).

DISCUSSION

Growth Conditions of Russian Flux-Grown Synthetic Alexandrites. The experimental results of our study are consistent with the descriptions published by Rodionov and Novgorodtseva (1988) and Bukin (1993) of growth techniques for Russian flux-grown synthetic alexandrites. The uniform morphology and chemical properties of our samples indicate that these synthetic alexandrites were grown from a solvent consisting of molybdenum-, bismuth-, and germanium-bearing compounds, most probably oxides. The nutrient contained the main components of chrysoberyl (Al_2O_3, BeO), as well as color-causing dopants (chromium, vanadium [sometimes], and iron oxides). Cr, V, and Fe are known chro-

Figure 15. An intense red, somewhat rounded, irregular boundary separates the red core and lighter red rim seen in about 10% of the single crystals and twins examined. Immersion, magnified 20×.

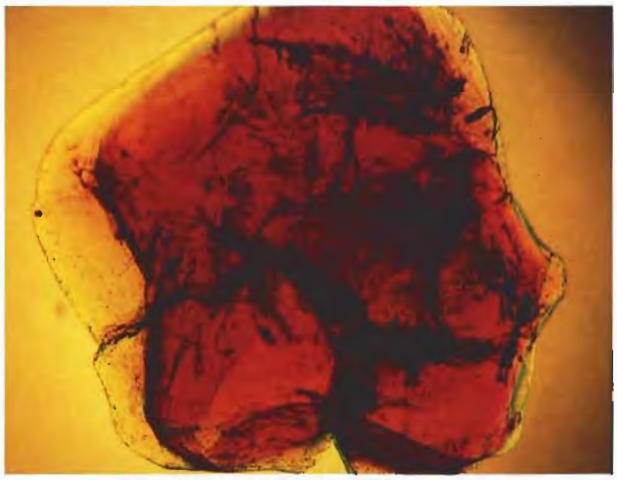

Figure 16. Interconnecting tubes of residual flux form characteristic "feathers" in this Russian flux-grown synthetic alexandrite. Immersion, magnified 40×.

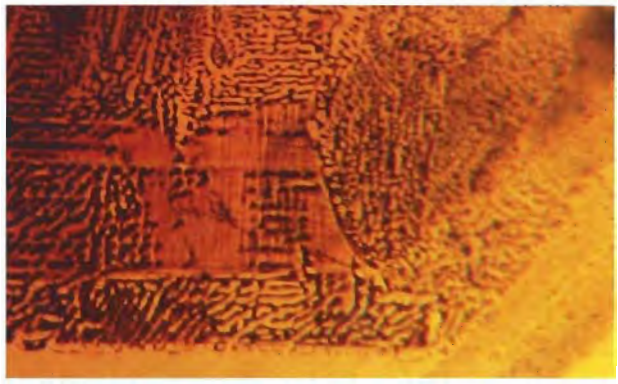

Figure 17. Some of the synthetic alexandrites revealed planar thin films in a net-like pattern of flux. Immersion, magnified 50×.

mophores of both natural and synthetic alexandrites (Farrell and Newnham, 1965; Bukin et al., 1980; see also table 1). A varying intensity of color change in different samples is caused by the absolute chromium and iron contents of the samples and by the chromium distribution between two different Al-sites of the chrysoberyl lattice (Solntsev et al., 1977; Bukin et al., 1980; Schmetzer et al., 1980).

We already knew that Mo and Bi were components of the fluxes used in Russia to grow synthetic alexandrite (A. Ya. Rodionov, pers. comm., 1988; Bukin, 1993). However, our chemical data do not agree with those given by Henn et al. (1988) and Henn (1992), who reported the presence of sulfur. It is possible that they mistook the characteristic L_α line of Mo (at 2.31 KeV) for the K_α line of sulfur (at 2.29 KeV).

Ge has not been mentioned before as a trace element in Russian flux-grown synthetic alexandrites. The only reference we found to Ge in synthetic alexandrite refers to patent applications by Isogami and Nakata (published in 1985 and 1986), who described a dopant of GeO_2 used to grow synthetic chrysoberyl and alexandrite cat's-eyes. Because Ge is normally found in tetrahedral coordination in oxide structures, the zoning of Ge identified by electron microprobe suggests an isomorphic substitution of beryllium by germanium in the lattice of our samples. This disproves our preliminary assumption that the Ge came from compounds in cavities or fissures ("feathers," "fingerprints") within the synthetic alexandrites. It is most likely that the incorporation of Ge into the chrysoberyl lattice is very sensitive to small temperature changes and/or to small variations in the composition of the flux, as is indicated by the extreme variation in Ge in the microprobe scans (see table 5 and figure 22). Because Ge was positively correlated to Fe in some of the samples, but others revealed a negative correlation between iron and germanium, we could not prove a coupled substitution of beryllium and aluminum by

Figure 18. Birefringence can be seen in some of the components of this net-like pattern of residual flux. Immersion, crossed polarizers, magnified 80×.

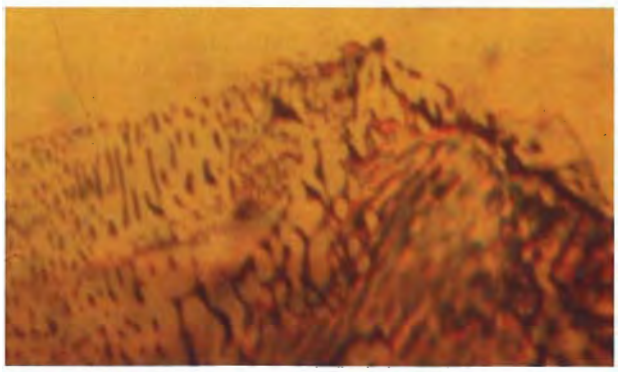

Figure 19. Residual flux takes the form of wispy veils in this Russian synthetic alexandrite. Fiber-optic illumination, magnified 70×.

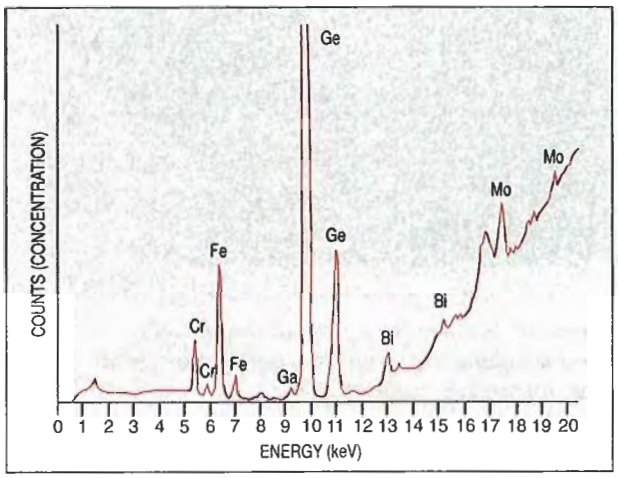

Figure 20. This EDXRF spectrum of a rough synthetic alexandrite was taken from an optically clean crystal face. The spectrum reveals distinct amounts of the chromophores (Cr, Fe), traces of Ga, distinct Ge concentrations, and residues of the flux (Bi, Mo).

germanium and iron (for charge compensation) in all samples. Thus, we do not presently know exactly how Ge is incorporated into the chrysoberyl lattice, but it is probably due to special growth conditions. It is very likely that one of the special growth conditions—mentioned by Rodionov and Novgorodtseva (1988) for the production of more-or-less equidimensional crystals (not thin platelets)—accounts for the presence of a germanium-bearing compound in the solvent, which was found in all samples obtained since 1988 (see table 4).

Our results also indicate that at least some Russian synthetic alexandrites were grown experimentally in a Mo-Bi-W-bearing flux. The use of a tungsten-bearing compound in the solvent was mentioned by Cline and Patterson (1975). Solid phases on the surfaces of the crystals we examined are representative of the major components of the flux (Mo and Bi, sometimes W) and the crucible material (Pt). At this time, however, no explanation is available for the presence of white crusts of anatase on some samples (G. Bukin, pers. comm., 1995), and our chemical analyses of the samples (table 4) do not indicate the presence of titanium in the solvent during growth.

Ga is known as a trace element in natural alexandrites (Ottemann, 1965; Ottemann et al., 1978), but small amounts of Ga recently have been observed in Czochralski- and flux-grown synthetic alexandrite (Schrader and Henn, 1986; Henn et al., 1988; Henn 1992). To the authors' knowledge, Sn

TABLE 4. Electron microprobe analyses of nine Russian flux-grown synthetic alexandrites.

Variable	Sample 1	Sample 2	Sample 3	Sample 4	Sample 5	Sample 6[a]	Sample 7	Sample 8	Sample 9
Origin	Novosibirsk 1988	Novosibirsk 1991	Novosibirsk 1993	Novosibirsk 1993	Novosibirsk 1993	Novosibirsk 1993	Bangkok 1994	Bangkok 1994	Bangkok 1994
Description	Cyclic twin	Cyclic twin	Cyclic twin	Cyclic twin	Single crystal	Cyclic twin	Cyclic twin	Cyclic twin	Single crystal
Growth zoning	Yes	Yes	Yes	Yes	Yes	Yes	Yes	Yes	No
Color zoning	No	Yes	No	No	No	Yes	No	No	No
Number of scans	4	2	1	1	1	5	1[b]	1	1
Number of analyses	160	85	66	50	71	560	100[b]	85	60
Approx. length of scans	3 mm	2 mm	10 mm	3.5 mm	6.5 mm	4–10 mm	2.5 mm	3.5 mm	3 mm
Analyses in wt.% (range)									
Ga_2O_3	0.01–0.07	0.01–0.05	0.01–0.06	0.02–0.07	0.01–0.07	0.01–0.06	0.00–0.13	0.01–0.11	0.01–0.06
Al_2O_3	78.20–79.87	74.03–78.31	76.80–78.08	77.21–79.55	77.59–79.47	74.86–78.65	77.92–79.83	78.05–80.17	76.92–78.52
V_2O_3	0.00–0.03	0.00–0.29	0.01–0.03	0.00–0.03	0.01–0.19	0.00–0.03	0.00–0.03	0.00–0.03	0.70–1.01
GeO_2	0.00–0.06	0.13–0.50	1.48–3.33	0.30–1.93	0.27–0.85	0.10–1.57	0.27–1.89	0.59–1.16	0.00–0.04
Cr_2O_3	0.17–0.32	0.28–4.64	0.29–0.36	0.33–0.74	0.21–0.27	0.44–4.55	0.28–0.96	0.34–0.43	0.43–0.49
MnO	0.00–0.02	0.00–0.01	0.00–0.02	0.00–0.02	0.00–0.02	0.00–0.02	0.00–0.02	0.00–0.02	0.00–0.03
FeO	0.43–0.62	0.33–1.37	0.50–0.56	0.43–0.56	0.73–0.91	0.33–1.42	0.22–0.46	0.51–0.60	1.27–1.42
TiO_2	0.00–0.02	0.00–0.02	0.00–0.02	0.00–0.02	0.00–0.03	0.00–0.02	0.00–0.02	0.00–0.03	0.02–0.04
SnO_2	0.00–0.04	0.00–0.04	0.32–0.45	0.10–0.36	0.00–0.05	0.00–0.06	0.01–0.15	0.19–0.29	0.03–0.08
Color	Cr, Fe	Cr > V, Fe	Cr, Fe	Cr, Fe	Cr > V, Fe	Cr, Fe	Cr, Fe	Cr, Fe	V > Cr, Fe

[a] *See also table 5.*
[b] *For this particular sample, an additional detailed scan for GeO_2, Cr_2O_3, and FeO with 625 point analyses was performed.*

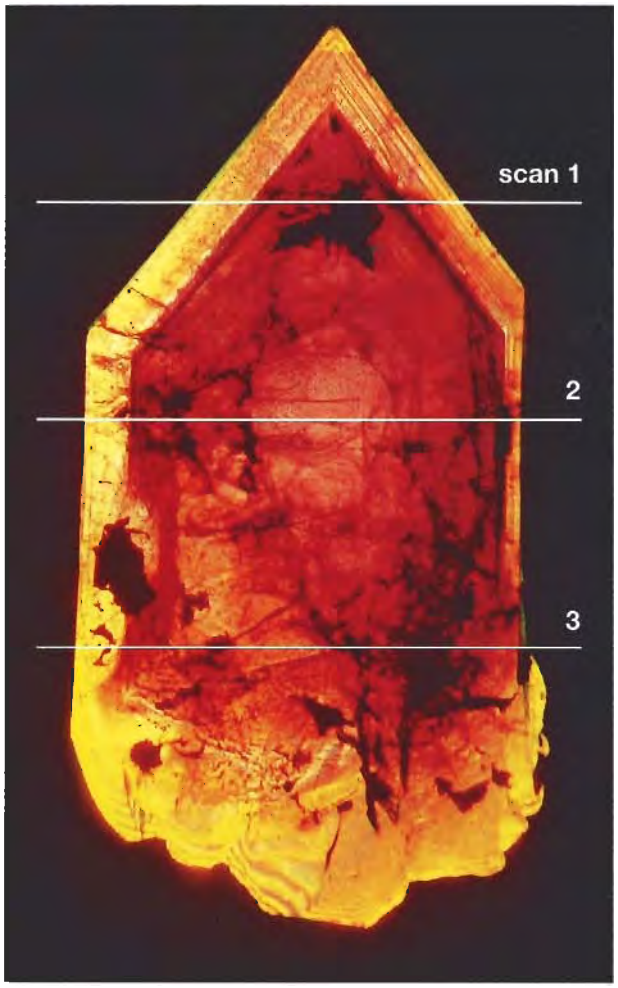

Figure 21. Visible in this color-zoned alexandrite are inner and outer red cores; a narrow, very intense, red boundary; and a light red rim (the yellow in this photo is a function of the immersion liquid and the illuminant). The three electron microprobe traverses across this section covered growth zones confined to x *(scan 1) and* a *(scans 2 and 3) faces. View parallel to the b-axis, immersion, crossed polarizers, magnified 15×.*

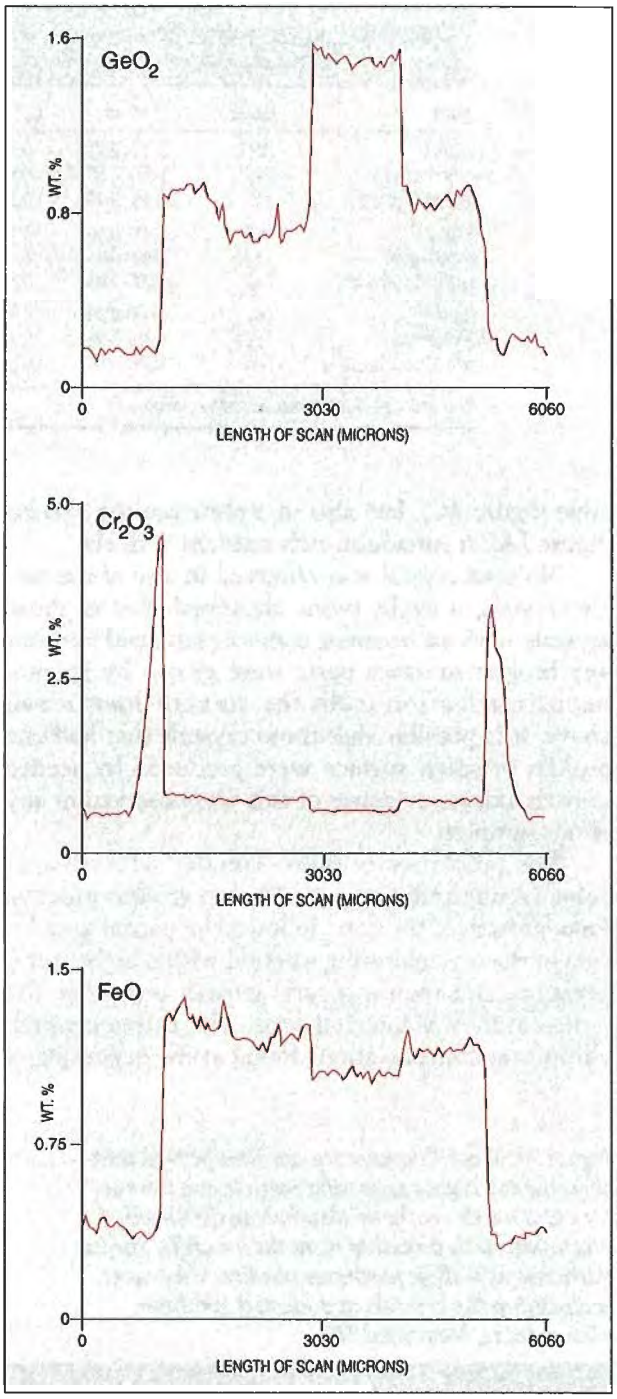

Figure 22. An electron microprobe traverse across the synthetic alexandrite shown in figure 21 (scan 2) revealed distinct zoning of the major trace elements—Ge, Cr, and Fe. The inner and outer cores, a narrow boundary, and a rim are recognizable in these plots (no. of analyses: 120; approx. length of scan: 6 mm).

previously was known as a trace element only in natural alexandrites (Ottemann, 1965; Ottemann et al., 1978; Kuhlmann, 1983). Its presence in some of our samples makes it less useful than before as an indicator of natural origin.

The traces of gallium and tin came from impure chemicals used in the nutrient, and were not intentionally added to the solvent system, according to Dr. G. V. Bukin (pers. comm., 1995).

Most of the alexandrites were grown in a negative temperature gradient in contact with the bottom of a platinum crucible, as described for beryllium-bearing oxides and silicates by Bukin (1993; figure 2C). The exception, the seven small single crystals that did not show an irregular surface plane, were grown by spontaneous nucleation without contact to the crucible. This is possible in a temperature-gradient system in the lower part of the cru-

TABLE 5. Electron microprobe analyses (in weight percent) of a Russian flux-grown alexandrite with pronounced color zoning[a].

Scans	Oxide	Left rim	Left boundary	Core	Right boundary	Right rim
Scan 1:	GeO_2	0.12–0.21	0.15–0.30	0.70–1.12	0.13–0.19	0.11–0.19
growth zone	Cr_2O_3	0.50–0.58	0.59–4.20	0.63–0.86	0.62–2.93	0.47–0.59
related to prism *x*	FeO	0.38–0.46	0.34–0.43	1.08–1.23	0.34–0.37	0.34–0.42
Scan 2:	GeO_2	0.12–0.18	0.14–0.21	0.66–1.57	0.15–0.31	0.15–0.24
growth zone	Cr_2O_3	0.46–0.61	0.69–4.55	0.57–0.84	0.66–3.58	0.48–0.54
related to pinacoid *a*	FeO	0.37–0.45	0.35–0.45	1.03–1.38	0.33–0.57	0.38–0.42
Scan 3:	GeO_2	0.18–0.24	0.14–0.25	0.42–1.46	0.12–0.23	0.10–0.13
growth zone	Cr_2O_3	0.48–0.58	0.71–2.98	0.62–0.82	0.81–3.91	0.44–0.50
related to pinacoid *a*	FeO	0.37–0.41	0.34–0.40	1.07–1.42	0.34–0.38	0.37–0.38

[a] *For other data on this sample, see table 4, sample 6.*

cible (figure 2C), but also in a slow-cooling system (figure 2A). A vanadium-rich nutrient is likely.

No seed crystal was observed in any of the single crystals or cyclic twins examined; that is, those crystals with an irregular contact plane and without any broken or sawn parts were grown by spontaneous nucleation from the solvent mentioned above. It is possible that those crystals that had one broken or sawn surface were produced by seeded growth, but no evidence of this was observed in any of our samples.

The properties of those samples with distinct color zoning indicate a multi-step growth process: First, growth of the core, followed by partial dissolution of the crystal during a period with a higher temperature; and then a second growth period, as the temperature was lowered again. The extremely high chromium concentrations found at the beginning of the second growth phase in these samples indicate an increase in the Cr concentration of the flux during the dissolution period.

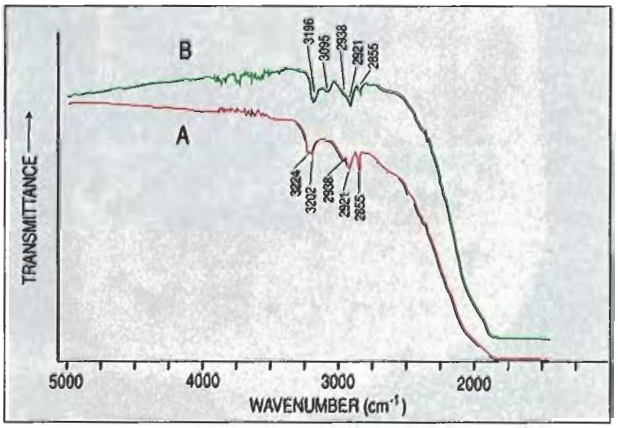

Figure 24. The infrared spectra of Russian flux-grown synthetic alexandrites show characteristic absorption bands in the 2800 to 3300 cm^{-1} range. Sample A was obtained from Novosibirsk in 1993; sample B was acquired in Bangkok in 1994.

Figure 23. X-ray fluorescence analysis proved that these white, highly reflecting particles on the surface of a rough synthetic alexandrite consisted of platinum, most probably from the crucible. Similar particles, as well as platinum needles, were seen included in the crystals and faceted synthetic alexandrites. Magnified 50×.

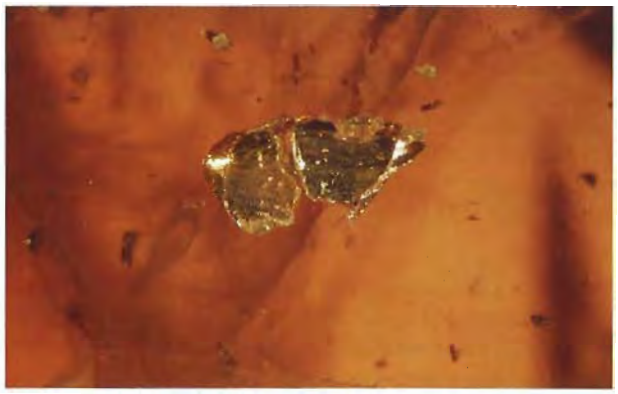

All samples with this distinct chromium zoning revealed an intense color and a good to very good color change, which is explained by the thin intermediate layer of alexandrite with an extremely high chromium content (which could remain, at least partly, after fashioning).

Diagnostic Properties. Faceted Russian flux-grown synthetic alexandrites may show a number of features that distinguish them from natural alexandrites.

Careful microscopic examination can detect characteristic forms of residual flux and platinum particles (see also Trossarelli, 1986; Henn et al., 1988; Henn, 1992; Hodgkinson, 1995). Although some patterns of residual flux resemble the healing

fractures seen in natural alexandrites (see, e.g., Bank et al., 1987; Henn, 1987; Bank et al., 1988), to date patterns with birefringent components and/or thin films of flux with a net- or web-like structure have been seen only in synthetic alexandrites.

Characteristic growth patterns—which are formed by four dominant crystal faces *a*, *x*, *k*, and *o* in the Russian synthetic alexandrites—can be observed with immersion microscopy. However, characteristic twin structures and growth patterns in natural gem-quality alexandrites from major localities have not yet been published. Consequently, we do not know how useful these features will be in an identification. Preliminary results indicate that the rhombic prism *k* (021), which is seen in most Russian flux-grown synthetic alexandrites, is extremely rare in natural samples (see, e.g., Goldschmidt, 1913). Characteristic color zoning—an intensely colored, somewhat rounded boundary between a lighter center and rim—is also diagnostic for some of the Russian samples.

Traces of germanium, molybdenum and/or bismuth, and sometimes tungsten, provide proof of synthesis. All can be readily determined by X-ray fluorescence analysis. Traces of gallium and tin can be found in natural alexandrites and in synthetic Russian samples, as can the chromophores chromium, iron, and sometimes vanadium. Therefore, these trace elements are of no diagnostic value.

Infrared spectroscopy of Russian synthetic flux-grown alexandrites shows some absorption bands in the 2800 to 3300 cm^{-1} range that are characteristic of this material. Like other synthetic alexandrites, this material lacks the water-related absorption bands that are typical of natural alexandrites.

Gemological properties—such as refractive indices, density, pleochroism, and UV-visible absorption spectra—are of no help in separating Russian flux-grown synthetic alexandrites from their natural counterparts.

CONCLUSIONS

The chemical, physical, and microscopic properties of the more than 200 Russian flux-grown synthetic alexandrites we tested are consistent with known details of the production techniques developed in Russia for this material. Platinum crucibles—with a flux containing molybdenum-, bismuth-, and germanium-bearing components—are placed in a reverse temperature gradient, in which the growth zone is located below the dissolution zone. Almost equidimensional alexandrite crystals grow in this system by spontaneous nucleation in contact with the bottom of the crucible. The nutrients—which consist of Al_2O_3, BeO, and the chromophores (chromium, iron, and sometimes vanadium oxides)—are placed in the upper parts of the crucibles. The morphology of the crystals, and their chemical and physical properties, are related to the exact compositions of the fluxes and the nutrients, as well as to the temperatures in the upper and lower parts of the crucibles. The manufacturers will not reveal the specific growth conditions, and the details of these conditions cannot be deduced from study of the synthetic alexandrites that result.

A careful microscopic examination of inclusions and structural characteristics (growth patterns and twinning) may be helpful—but is often not conclusive—in separating natural from synthetic alexandrite. However, modern gemological laboratories, especially those with X-ray fluorescence and infrared spectroscopy, should have no problem identifying the synthetic Russian alexandrite material currently available in the trade.

REFERENCES

Bank F.H., Bank H., Gübelin E., Henn U. (1987) Alexandrite von einem neuen Vorkommen bei Hematita in Minas Gerais, Brasilien. *Zeitschrift der Deutschen Gemmologischen Gesellschaft*, Vol. 36, No. 3/4, pp. 121–131.

Bank H., Gübelin E., Henn U., Malley J. (1988) Alexandrite: Natural or synthetic? *Journal of Gemmology*, Vol. 21, No. 4, pp. 215–217.

Bonner W.A., Van Uitert L.G.G. (1968) Growth of divalent metal aluminates. United States Patent No. 3,370,963; February 27.

Bukin G.V. (1993) Growth of crystals of beryllium oxides and silicates using fluxes. *Growth of Crystals*, Vol. 19, pp. 95–110.

Bukin G.V., Eliseev A.V., Matrosov V.N., Solntsev V.P., Kharchenko E.I., Tsvetkov E.G. (1980) The growth and examination of optical properties of gem alexandrite (in Russian). In *Inhomogenity of Minerals and Crystal Growth, Proceedings of the XI General Meeting of the International Mineralogical Association, Novosibirsk, 1978*, Moscow, pp. 317–328.

Bukin G.V., Volkov S.Yu., Matrosov V.N., Sevastyanov B.K., Timoshechkin M.I. (1978) Optical generation in alexandrite ($BeAl_2O_4$: Cr^{3+}) (in Russian). *Kvantovaya Elektronika*, Vol. 5, No. 5, pp. 1168–1169.

Cassedanne J., Roditi M. (1993) The location, geology, mineralogy and gem deposits of alexandrite, cat's-eye and chrysoberyl in Brazil. *Journal of Gemmology*, Vol. 23, No. 6, pp. 333–354.

Cline C.F., Patterson D.A. (1975) Synthetic crystal and method of making same. United States Patent No. 3,912,521; October 14.

Eliezri I.Z., Kremkow C. (1994) The 1995 ICA World Gemstone Mining Report. *ICA Gazette*, December 1994, pp. 1, 12–19.

Elwell D., Scheel H.J. (1975) *Crystal Growth from High-Temperature Solutions*. Academic Press, London, New York, San Francisco, 634 pp.

Farrell E.F., Fang J.H. (1964) Flux growth of chrysoberyl and

alexandrite. *Journal of the American Ceramic Society*, Vol. 47, No. 6, pp. 274–276.
Farrell E.F., Fang J.H., Newnham R.E. (1963) Refinement of the chrysoberyl structure. *American Mineralogist*, Vol. 48, pp. 804–810.
Farrell E.F., Newnham R.E. (1965) Crystal-field spectra of chrysoberyl, alexandrite, peridot, and sinhalite. *American Mineralogist*, Vol. 50, pp. 1972–1981.
Godovikov A.A., Bukin G.V., Vinokurov V.A., Kalinin D.V., Klyakhin V.A., Matrosov V.N., Nenashev B.G., Serbulenko M.G. (1982) Development of synthesis techniques for minerals of economic importance in the USSR (in Russian). *Geol. Geofiz.*, Vol. 1982, No. 12, pp. 42–54.
Goldschmidt V. (1900) Zur Theorie der Zwillings- und Viellingsbildung, illustrirt am Chrysoberyll. *Zeitschrift für Krystallographie und Mineralogie*, Vol. 33, pp. 468–476.
Goldschimdt V. (1913) *Atlas der Krystallformen, Band II, Calaverit-Cyanchroit*. Carl Winters Universitätsbuchhandlung, Heidelberg.
Goldschmidt V., Preiswerk H. (1900) Chrysoberyllzwilling von Ceylon. *Zeitschrift für Krystallographie und Mineralogie*, Vol. 33, pp. 455–467.
Henn U. (1987) Inclusions in yellow chrysoberyl, natural and synthetic alexandrite. *Australian Gemmologist*, Vol. 16, No. 6, pp. 217–220.
Henn U. (1992) Über die diagnostischen Merkmale von synthetischen Alexandriten aus der Gemeinschaft Unabhängiger Staaten (GUS). *Zeitschrift der Deutschen Gemmologischen Gesellschaft*, Vol. 41, No. 2/3, pp. 85–93.
Henn U., Bank H. (1992) Examination of an unusual alexandrite. *Australian Gemmologist*, Vol. 18, No. 1, pp. 13–15.
Henn U., Malley J., Bank H. (1988) Untersuchung eines synthetischen Alexandrits aus der UdSSR. *Zeitschrift der Deutschen Gemmologischen Gesellschaft*, Vol. 37, No. 3/4, pp. 85–88.
Hirose T. (1984) Method for washing flux (in Japanese). Japanese Patent Application, Laid-Open No. 5-39796; March 5.
Hodgkinson A. (1995) Alexandrite chrysoberyl surprises. *Australian Gemmologist*, Vol. 19, No. 1, pp. 25–28.
Isogami M., Nakata R. (1985) Katzenauge aus synthetischem Chrysoberyll-Einkristall. German Patent Application, Laid-Open No. 3434595, April 18.
Isogami M., Nakata R. (1986) Chrysoberyl cat's-eye synthetic single crystal. United States Patent No. 4,621,065; November 4.
Kammerling R.C. (1995) Gem trade lab notes: Synthetic alexandrite flux grown without diagnostic inclusions. *Gems & Gemology*, Vol. 31, No. 3, p. 196.
Kammerling R.C., Koivula J.I., Fritsch E., Eds. (1995) Gem News: Sapphires and other gems from Tanzania. *Gems & Gemology*, Vol. 31, No. 2, pp. 133–134.
Karfunkel J., Wegner R. (1993) Das Alexandritvorkommen von Esmeraldas de Ferros, Minas Gerais, Brasilien. *Zeitschrift der Deutschen Gemmologischen Gesellschaft*, Vol. 42, No. 1, pp. 7–15.
Kasuga K. (1984) Synthesizing method of artificial alexandrite single crystal (in Japanese). Japanese Patent Application, Laid-Open No. 59-107995; June 22.
Kiefert L., Schmetzer K. (1991) The microscopic determination of structural properties for the characterization of optical uniaxial natural and synthetic gemstones, part 1: General considerations and description of the methods. *Journal of Gemmology*, Vol. 22, No. 6, pp. 344–354.
Kimura S., Kitamura K. (1993) Growth of oxide crystals for optical applications. *Journal of the Ceramic Society of Japan*, Vol. 101, No. 1, pp. 22–37.
Kuhlmann H. (1983) Emissionsspektralanalyse von natürlichen Rubinen, Sapphiren, Smaragden und Alexandriten. *Zeitschrift der Deutschen Gemmologischen Gesellschaft*, Vol. 32, No. 4, pp. 179–195.
Laskovenkov A.F., Zhernakov V.I. (1995) An update on the Ural emerald mines. *Gems & Gemmology*, Vol. 31, No. 2, pp. 106–113.
Leung C.S., Merigoux H., Poirot J.P., Zecchini P. (1983) Sur l'identification des pierres fines et de synthèse par spectroscopie infrarouge. *Revue de Gemmologie a.f.g.*, No. 75, pp. 14–15.
Leung C.S., Merigoux H., Poirot J.P., Zecchini P. (1986) Infrared spectrometry in gemmology. In *Morphology and Phase Equilibria of Minerals, Proceedings of the 13th General Meeting of the International Mineralogical Association, Varna 1982*, Sofia, Bulgaria, pp. 441–448.
Machida H., Yoshihara Y. (1980) Synthetic single crystal for alexandrite gem. United States Patent No. 4,420,834; December 23.
Machida H., Yoshihara Y. (1981) Synthetischer Einkristall für einen Alexandrit Edelstein. German Patent Application, Laid-Open No. 2925330; April 2.
Newlay S.K., Pashine J.K. (1993) A note on the finding of rare gemstone alexandrite in Madhya Pradesh. *National Seminar on Gemstones, December 11–12*, Bhubaneswar, India, pp. 88–90.
News on the Songea deposit from SSEF (1995) *ICA Gazette*, June, p. 6.
Ottemann J. (1965) Gallium und Zinn im Alexandrit. *Neues Jahrbuch für Mineralogie Monatshefte*, Vol. 1965, No. 2, pp. 31–42.
Ottemann J., Schmetzer K., Bank H. (1978) Neue Daten zur Anreicherung des Elements Gallium in Alexandriten. *Neues Jahrbuch für Mineralogie Monatshefte*, Vol. 1978, No. 4, pp. 172–175.
Patnaik B.C., Nayak B.K. (1993) Alexandrite occurrence in Orissa. *National Seminar on Gemstones, December 11–12*, Bhubaneswar, India, p. 87.
Peretti A., Schmetzer K., Bernhardt H.-J., Mouawad F. (1995) Rubies from Mong Hsu. *Gems & Gemology*, Vol. 31, No. 1, pp. 2–26.
Powell R.C., Xi L., Gang X., Quarles G.J., Walling J.C. (1985) Spectroscopic properties of alexandrite crystals. *Physical Review B*, Vol. 32, No. 5, pp. 2788–2797.
Proctor K. (1988) Chrysoberyl and alexandrite from the pegmatite districts of Minas Gerais, Brazil. *Gems & Gemology*, Vol. 24, No. 1, pp. 16–32.
Rodionov A.Ya., Novgorodtseva N.A. (1988) Crystallization of colored varieties of chrysoberyl by solution-melt and gas transport methods (in Russian). *Tr. In-Ta Geol. i Geofiz. SO AN SSSR*, Vol. 708, pp. 182–187.
Schmetzer K. (1986) An improved sample holder and its use in the distinction of natural and synthetic ruby as well as natural and synthetic amethyst. *Journal of Gemmology*, Vol. 20, No. 1, pp. 20–33.
Schmetzer K., Bank H., Gübelin E. (1980) The alexandrite effect in minerals: Chrysoberyl, garnet, corundum, fluorite. *Neues Jahrbuch für Mineralogie Abhandlungen*, Vol. 138, No. 2, pp. 147–164.
Schrader H.-W., Henn U. (1986) On the problems of using gallium content as a means of distinction between natural and synthetic gemstones. *Journal of Gemmology*, Vol. 20, No. 2, pp. 108–113.
Solntsev V.P., Kharchenko E.J., Matrosov V.N., Bukin G.V. (1977) Distribution of chromium ions in the chrysoberyl structure. *Vses. Mineral. Obs. Akad. Nauk SSSR, Trudy IV. Vses. Sympos. Isomorphismu*, Part 2, pp. 52–59.
Stockton C.M., Kane R.E. (1988) The distinction of natural from synthetic alexandrite by infrared spectroscopy. *Gems & Gemology*, Vol. 24, No. 1, pp. 44–46.
Tabata H., Ishii E., Okuda H. (1974) Growth and morphology of chrysoberyl single crystals. *Journal of Crystal Growth*, Vol. 24/25, pp. 656–660.
Togawa E. (1985) Method for synthesizing single crystal by flux method (in Japanese). Japanese Patent Application, Laid-Open No. 60-81083; May 9.
Trossarelli C. (1986) Synthetic alexandrite from USSR. *La Gemmologia*, Vol. 11, No. 4, pp. 6–22.

GIA GEM TRADE LAB NOTES

ARAGONITE

A 55.10 × 37.80 × 9.04 mm white translucent carved pendant (figure 1) was recently submitted to the West Coast laboratory for identification. It had been represented to the client as nephrite jade.

The piece was similar in appearance to nephrite and had a comparable specific gravity of 2.84. Magnification revealed an aggregate structure. No absorption spectrum was seen with a desk-model spectroscope. The refractive index measurements, which were vague and difficult to determine because of the poor polish, gave values of 1.50 and 1.65. There was a decided "blink" effect when the Polaroid plate was rotated.

Other gemological properties were: moderate yellowish white fluorescence to long-wave ultraviolet radiation (with yellow fluorescence in fractures), moderate light yellow fluorescence to short-wave UV, and effervescence when touched in an inconspicuous spot with a minute droplet of a 10% hydrochloric acid solution. Although these properties were not sufficient to identify the material, they proved that it was not nephrite. The effervescence, together with the R.I. "blink" effect, indicated that it was a carbonate. X-ray powder diffraction analysis identified the carving as aragonite.

Aragonite is not often used as a gem material because of its low hardness (about 4 on the Mohs scale). A blue massive aragonite from Peru, with gemological properties slightly different from those of this specimen, was described in the Winter 1992 Gem News section (pp. 269–270).

SFM and MLJ

Figure 1. This carved pendant resembled nephrite, but advanced testing techniques proved that it was aragonite.

DIAMOND

Different Colors from the Same Rough

Yellow to brown colors in diamond are usually caused by nitrogen impurities found in various states of aggregation (see "Colour Centres in Diamonds," by A. T. Collins, *Journal of Gemmology*, 1982, Vol. 18, No. 1, pp. 37–75). It has been shown that nitrogen is often distributed unevenly in the diamond crystal (see, e.g., "Fractionation of Nitrogen Isotopes in a Synthetic Diamond of Mixed Crystal Habit," by S. R. Boyd et al., *Nature*, Vol. 331, February 18, 1988, pp. 604–607). Consequently, it is common that two near-colorless diamonds cut from the same piece of rough will differ by a few color grades. Hydrogen impurities may also cause an uneven distribution of gray or brown color in diamond (see "Gemmological Properties of Type Ia Diamonds with an Unusually High Hydrogen Content," by E. Fritsch and K. Scarratt, *Journal of Gemmology*, Vol. 23, No. 8, 1993, pp. 451–460).

Last fall, a diamond dealer shared a particularly vivid example of the consequences of such variability with staff members in the East Coast lab. Although he had noticed some unevenness to the color before sawing the rough diamond into the two pieces shown in figure 2, he had expected that the rough would produce two fancy-color stones. However, the larger of the two pieces yielded a 3.79 ct "radiant" cut with a color grade of Fancy Brownish Yellow, whereas the smaller piece finished out as a 0.78 ct pear shape of G color.

Although the two pieces had some similar gemological proper-

Editor's note: The initials at the end of each item identify the contributing editor(s) who provided that item.

Gems & Gemology, *Vol. 32, No. 3, pp. 204–212*

Figure 2. These two pieces are from the same brownish yellow rough diamond. Nearly all the color ended up in the 7.32 ct portion, whereas the 1.35 ct piece is near-colorless.

ties—such as inclusions in both of small brown crystals (probably garnet, judging from their partly dodecahedral shape)—there were substantial differences in their infrared spectra, which reflect their different impurity concentrations. The larger, brownish yellow piece had strong peaks due to nitrogen and moderate hydrogen peaks; however, the near-colorless piece showed moderate nitrogen and weak hydrogen absorptions. The nitrogen in both pieces had the same aggregation state, with approximately equal amounts of A and B aggregates. Much of the color in the brownish yellow piece was concentrated in a swirling cloud in the center, a distribution sometimes seen in hydrogen-rich diamonds (again, see the Fritsch and Scarratt reference cited above).

IR

Imitation Crystals

Since its introduction in the early 1970s, cubic zirconia (or "CZ") has revitalized the diamond simulant market. Its availability in nearly every shape and facet arrangement provides ample evidence of its popularity. We have occasionally reported on CZ being fashioned into carvings and shaped into diamond-like crystal forms. Some of these "crystals" have had very believable diamond-like features, such as engraved triangular depressions to simulate trigons, engraved parallel lines to simulate growth striations, and "frosted" surfaces (see Gem Trade Lab Notes, Fall 1982, p. 169, and Winter 1988, p. 241).

A good example of this deception was recently seen in the East Coast lab: five fashioned CZ "crystals" (figure 3) that very much resembled modified octahedra, a shape common in rough diamonds. For comparison, we photographed five diamond crystals of similar size (see figure 4) to show just how convincing in appearance the look-alikes really were. Not only was the overall resemblance in shape striking, but one of the imitations (at the upper right in figure 3) even had parallel lines engraved on a "face." These lines closely mimicked the striations often seen on dodecahedral faces of rough diamonds with modified octahedral habit (see the upper right stone in figure 4), which are occasionally found on the small natural surfaces sometimes left on polished diamonds.

The ersatz "diamond" rough was submitted to the lab because the observant dealer noted that the "heft" did not feel quite right for diamonds. The specific gravity (5.80 compared to 3.52 for diamond), hardness, and ultraviolet fluorescence of these "crystals" were all consistent with published values for cubic zirconia.

GRC and TM

Natural, with Unseen "Flaws"

Rarely is any gemstone examined as carefully for the presence of inclusions as is diamond. This is just as true for pieces of rough as for polished stones. A client submitted both partially polished halves of what was originally a 40+ ct crystal to the East Coast lab for examination. The two pieces were worked on a day apart. Both fractured spontaneously (figure 5) in the early stages of cutting.

The highly experienced owner was surprised and puzzled that this had occurred. His rough stones were routinely examined before manufac-

Figure 3. These five imitation diamond crystals (4.62–26.24 ct) are actually cubic zirconia.

Figure 4. Compare the appearance of these five diamond crystals, ranging from 5.27 to 8.67 ct, to that of the imitations in figure 3.

Figure 5. These two diamonds, a 16.48 ct blocked round and an 18.15 ct blocked square, were cut from the same piece of rough; both fractured due to strain.

Figure 6. Here the diamonds shown in figure 5 are oriented and repositioned to demonstrate their original crystallographic relationship.

turing, both with a microscope to detect visible inclusions and with a polariscope to detect any extraordinary strain or graining. Some diamond categories and colors, such as browns, are noted for their high degree of internal strain. In these diamonds, the presence of strain often influences how the crystal is fashioned. For example, manufacturers will sometimes opt to forgo traditional sawing and keep the stone "whole" to avoid damage. Other times, they may orient the stone so that the sawing does not intersect the center of strain.

We repositioned the two pieces in their original relative orientation to illustrate their relationship in the original piece of rough (figure 6). Figure 7 (taken with a polarizing microscope) shows the blue first-order interference color from residual strain that is present in both pieces. The fractures in both pieces related to a single area of strain that was present in the rough crystal. Also present was a linear strain pattern along the octahedral graining near both culets, but its gray interference colors indicated that this strain was significantly lower.

Whether strain in a rough diamond will lead to spontaneous fracturing during fashioning is a matter of chance, but the presence of localized strain is an indication for concern. Sawing is thought to be the most stressful event in diamond cutting; however, in this case the stone survived sawing perpendicular to the strain region, but the pieces fractured as faces were polished subparallel to the strain region. *TM and GRC*

Rare Color: Fancy Intense Pinkish Orange

Over the years, we have reported on a number of diamonds notable for their rare colors (see, for example, the Winter 1965–66 *Gems & Gemology*, p. 362, which illustrated a ring set with natural green, blue, and red diamonds; Winter 1982, p. 228, which showed a chameleon diamond with a dramatic color change; and Summer 1988, p. 112, with a grayish purple round brilliant cut).

Figure 7. First-order interference colors—shades of blue—seen here in the partly polished 18.15 ct piece were actually present in both halves, indicating the presence of residual strain. Magnified 10×.

The 3.40 ct heart-shaped diamond in figure 8 is another addition to this list. It was graded Fancy Intense Pinkish Orange and Internally Flawless. (For a description of the GIA Gem Trade Laboratory color-grading system, see "Color Grading of Colored Diamonds in the GIA Gem Trade Laboratory," by J. King et al., *Gems & Gemology*, Winter 1994, pp. 220–242.) Not only was the hue unusual for diamond, but the saturation was unusually high for such a color: In the rare instances when we have seen diamonds in this hue, the depth of color has been much weaker (less saturated). The rough reportedly came from Angola.

Infrared spectroscopy revealed that the stone was a type IIa diamond (i.e., lacking measurable amounts of nitrogen). The fluorescence was very strong orange to long-wave UV radiation and moderate orange to short-wave UV. The long-wave reaction further enhanced the color of the diamond when viewed in the daylight. The absorption pattern seen with a desk-model spectroscope consisted of a broad band centered at 550 nm.

TM and IR

A Suite of Treated-Color Pink-to-Purple Diamonds

The East Coast laboratory recently had the opportunity to examine six known treated-color pink diamonds borrowed from a local dealer. Although treated pink diamonds are relatively uncommon, we have seen and documented a number of them over the past 25 years. The diagnostic properties noted before (see *Gems & Gemology*, Summer 1976, p. 172; Summer 1988, p. 112; and Summer 1995, p. 121) were also observed in these diamonds; however this parcel provided a few surprises.

Two of the diamonds showed strikingly unusual colors, which are immediately apparent in figure 9. Although GIA GTL maintains a policy of not issuing color grades for stones of treated color, these stones were put through the color-grading process in order to locate their positions in color space and to compare them to the range of colors seen in natural-color pink diamonds. Treated pink diamonds are usually highly saturated, but dark in tone. The 0.05 carat orangy pink diamond, comparable to a grade of Fancy Vivid, was surprisingly light in tone for a treated-color pink, as well as being highly saturated. The pink-purple color of the 0.07 carat diamond is truly extraordinary, comparable to a grade of Fancy Vivid. Purple is an extremely rare color in diamond, and seldom has the lab seen a purple of this high saturation in either a treated- or natural-color diamond. The orangy pink stone is at least as saturated as any natural-color diamond we have seen of similar hue. The colors of the other four diamonds lie on the edges of the distribution we have seen for natural-color diamonds, with the high saturations and medium-to-dark tones that are typical of treated-color pink stones.

Figure 9. Among the colors displayed by this suite of treated diamonds are some that match or exceed the brightest natural pink colors seen in the lab to date. The 0.05 ct orangy pink and the 0.07 ct pink-purple stones, right, are particularly notable for their high saturation.

Figure 8. The Fancy Intense Pinkish Orange color of this 3.40 ct Internally Flawless heart shape is rare.

In a desk-model spectroscope, all six showed the diagnostic spectrum for treated-color pink (or purple or red) diamonds: sharp absorption lines at 575, 595, and 637 nm. Most of these diamonds showed emission lines at 595 and 637 nm as well. They also luminesced the characteristic strong, bright orange to both long-wave and short-wave UV that is associated with the 637 nm color center. Last, although graining was present in all six diamonds, it was phantom graining (for the meaning of this term, see "The Elusive Nature of Graining in Gem Quality Diamonds," by R. E. Kane, *Gems & Gemology*, Summer 1980, pp. 294–314) with no relationship to the distribution of color within the gems. (By contrast, most natural-color pink diamonds show most, or all, of their color as colored graining.) One stone had a "streaky" color distribution (figure 10), but magnification combined with immersion revealed that this color lacked the planar appearance of colored internal graining and was largely confined to the surface.

Although the face-up appearance of both natural- and treated-color pink, purple, or red diamonds can be similar, the causes of the color are entirely different. Natural-color pink diamonds are type Ia or IIa and show a smooth, broad band in the visible spectrum at about 550 nm. (See E. Fritsch and K. Scarratt, "Natural-Color Nonconductive Gray-to-Blue Diamonds," *Gems & Gemology*, Vol. 28, No. 1, Spring 1992, pp. 38–39, for a complete discussion of diamond type.) Treated-color pink diamonds must contain at least some type Ib component, and are sometimes pure type Ib. Their visible spectra show the three sharp lines mentioned

Figure 10. The streaky pink color seen in this 0.05 ct treated-color pink diamond might be confused with the pink graining seen in natural-color diamonds. Examination at 10× to while the stone was immersed in methylene iodide reveals that the color is largely confined to the surface.

above, with a broad feature formed from the overlap of their sidebands. Vacancies in the atomic structure are created in these diamonds by laboratory irradiation, and then mobilized during an annealing process. Some of the vacancies become trapped at single substitutional nitrogen atoms, creating the NV center with its strong absorption at 637 nm.

In examining these six stones, we found that four were type Ib, as expected, but one had some additional type IaA component and one of the paler stones had what appeared to be a pure type IaA spectrum and an H1b peak (due to a vacancy trapped at an A aggregate, a common feature in treated yellow diamonds; again, see the A. T. Collins reference cited in a previous entry). We had not seen such a mid-infrared spectrum in a treated pink stone before. Although the infrared spectrum implied that this diamond had only A aggregates, the visible spectrum showed the 637 nm peak, so there must have been at least some single substitutional nitrogen to trap the vacancies.

The nitrogen content of all six of these diamonds was extremely low, and some of the initial infrared results suggested that a few of them might have no nitrogen at all. For the stone that showed type IaA, it is probable that there was not enough single substitutional nitrogen to produce a detectable signal in the infrared spectrum. These diamonds demonstrate the time-honored gemological principle that identification must rely on *all* of the observed properties. A cursory examination might lead one to conclude that the paler stones are natural-color type IIa pink diamonds with orange fluorescence and faint pink graining. However, in our experience, such stones rarely show the 637 nm line, and never show the 595 nm line, in the hand spectroscope.

John King, Elizabeth Doyle, and IR

HERDERITE

In spring 1996, the West Coast lab received for identification a large (25.86 × 18.55 × 13.31 mm) pear-shaped stone that was transparent yellowish green (figure 11). The 38.91 ct stone proved to be an extraordinarily large herderite.

We recorded the following gemological properties for this stone: biaxial negative, with R.I. values of α = 1.580, γ = 1.611, and β between 1.600 and 1.606; S.G. (measured hydrostatically) of 3.04; no reaction (inert) to long-wave UV radiation, but faint yellowish green fluorescence to short-wave UV. With a desk-model spectroscope, we observed an absorption line at 585 nm.

Microscopic examination revealed a small feather under the table, as well as scattered "pinpoint" inclusions in the stone. However, the most pronounced feature seen with magnification was the strong doubling of the back facets visible through the table. This was not surprising given the strong birefringence (0.031) and the depth of the stone.

To satisfy our curiosity about this stone—and to characterize the material for our data files—we submitted it to energy-dispersive X-ray fluorescence (EDXRF) analysis. Calcium (Ca) and phosphorus (P) were the major elements found, along with minor manganese and trace amounts of lead, strontium, and yttrium. Gem herderite consists of material in the mineral series that has herderite, $CaBe(PO_4)F$, as one end-member and hydroxylherderite, $CaBe(PO_4)OH$, as the other. Because the elements beryllium (Be), oxygen (O), fluorine (F), and hydrogen (H) cannot be detected with our EDXRF system, we could not determine which end-member in the herderite-hydroxylherderite series is dominant in this stone. The manganese is probably responsible for the yellowish green color, which is similar to the color caused by manganese in some spodumenes. *MLJ*

Figure 11. This 38.91 ct faceted herderite is unusually large for this material.

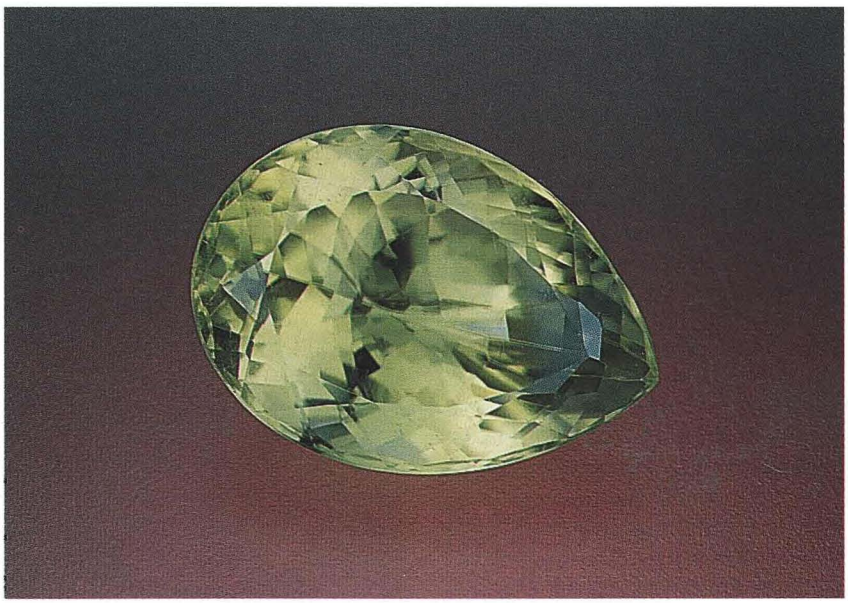

JADEITE

An intricately carved hairpin (figure 12) with a dragon motif was submitted to the East Coast laboratory to determine if it had been treated. Reportedly, this ornate piece was from the Chinese Qing dynasty (1644–1912), which popularized the use of jadeite jewelry and *objets d'art*.

Standard gemological tests revealed properties that were consis-

tent with jadeite jade. The strength of the "chrome" lines in the absorption spectrum varied with the intensity of the green color. There was no reaction with a Chelsea filter. Even with magnification, no visible reaction was observed when a "hot point" was brought near the surface. In addition, the carving revealed a compact intergrowth pattern very different from the "honeycomb" structure sometimes seen in bleached and impregnated jadeite. Infrared spectroscopy showed no evidence of impregnation.

Unlike the simple Western definition of "Imperial jade" (jadeite of uniform intense green color and exceptional translucency), Asian criteria are more complex and take into account a combination of factors, including the highest quality green color and translucency, as well as the carving's quality and style (see "Asian News Section: Jadeite Jewellery in the Qing Imperial Court," *Christie's International Magazine*, May 1996, p. 73). We suspect that this hairpin might be considered "Imperial" by either standard.

The difficulty in detecting that a piece of jadeite has been bleached and polymer impregnated, which is now a common practice in the marketplace, has made it necessary to test all important pieces, regardless of their purported history. *GRC and TM*

Figure 12. Reportedly from the Qing dynasty, this 20.3-cm-long jadeite hairpin showed no evidence of polymer impregnation.

OPAL, an Assemblage

An opaque gray free-form cabochon, displaying primarily green and blue play-of-color, was sent to the East Coast laboratory for identification. Since the stone was bezel set in a closed-back pendant mounting (figure 13), the client wanted us to determine if this opal was a quartz-top doublet or triplet, as is frequently encountered in the trade.

Visual examination showed that the top portion of the cabochon was obviously transparent. The play-of-color was not visible near the surface of the stone, but appeared to be confined to a deeper, somewhat opaque layer. The refractive index of the top, obtained by the spot method, was 1.52, which is lower than the 1.54–1.55 of quartz. Because of the irregular shape and the bezel mounting, it was difficult to determine an optic character between crossed polarized plates, but the transparent top appeared to be singly refractive with little anomalous double refraction. When exposed to long-wave UV radiation, the cabochon fluoresced a

strong bluish white with a distinct phosphorescence. However, when the stone was exposed to short-wave UV, we noticed a faint chalky yellow fluorescence, which is not characteristic of colorless quartz. These properties proved that the transparent top portion was not quartz, but a different material.

Magnification did not reveal any obvious inclusions. However, using standard overhead illumination, we did locate a tiny gas bubble deep inside the transparent layer. This confirmed that the top was glass. Further examination of the underlying colored layer with strong light showed the usual structure of natural opal. We did not find any evidence of cement planes, so we could not determine if the cabochon was a doublet or triplet without unmounting it. Therefore, we simply identified the piece as an assemblage, with a colorless glass top over natural opal.

KH

Figure 13. This assemblage, which measures about 30 × 22 mm, has a colorless glass top over natural opal.

Figure 14. Numerous thread-like "inclusions" were seen in these gray-blue assembled cultured blister pearls, which each measured about 6.35 mm in diameter.

Assembled Cultured Blister PEARLS, With Thread-Like Inclusions

Although gemologists do not expect to observe inclusions when examining pearls, staff members at the West Coast lab noticed some interesting internal features in cultured pearls that arrived last year for identification. The assembled cultured blister pearls, each of which measured about 6.35 mm in diameter, were an attractive light gray-blue. They were surrounded by old European brilliants, all set in a pair of earrings (figure 14).

The fact that these pieces were assembled was readily apparent with microscopic examination. Fiber-optic illumination revealed gas bubbles in the curved interface between the nacre and the half-bead nuclei. The flat bases of the cultured pearls had soft, wax-like backings attached. Not only was the gray-blue color unnatural, but fiber-optic illumination also revealed vivid color concentrations reflecting along hairline fractures in the nacre. Although these features indicated an artificial coloring process, we could not prove that one had been used.

The most interesting characteristic of these assembled cultured blister pearls were the thread-like inclusions in the nacre, which were again best observed with fiber-optic illumination. For the most part, these abundant inclusions appeared to be randomly oriented; they were long, curved, and continuous, with some shorter, more kinked threads splitting off to the sides (figure 15). The laboratory was unable to identify the composition or origin of these inclusions.

CYW

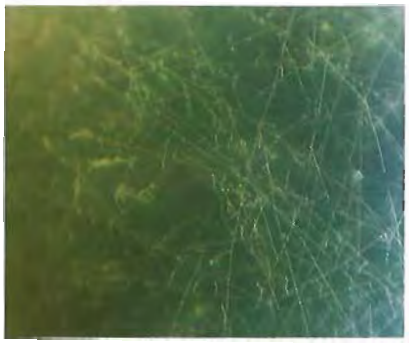

Figure 15. The long curved fibers in the assembled cultured blister pearls of figure 14 seemed, for the most part, to be randomly oriented. Magnified 25×.

QUARTZ, Single-Crystal Green

Last winter, the East Coast lab had the opportunity to examine a turn-of-the-century ring, stamped "Tiffany & Co.," set with an oval mixed-cut green quartz that was surrounded by fine-quality old-European brilliant cuts (figure 16). Both the setting and the company name indicated more respect for this gem than is typical today for similar single-crystal quartz of grayish green color. The ring may well represent an example of Tiffany's interest in promoting American gemstones, as green quartz was known at that time to occur in several localities (see G. F. Kunz, *Gems and Precious Stones of North America*, 2nd ed., 1968, Dover Publications, New York, pp. 120–122, 263). If so, it joins such American gems as Montana sapphires, chrome pyrope garnets, and American freshwater pearls, among others (see Gem Trade Lab Notes, Spring 1989, p. 37, and *The Tiffany Touch* by J. Purtell, 1971, Random House, New York).

This color of single-crystal quartz was rare until the mid-1950s, when it was discovered that amethyst from the Montezuma mine in Minas Gerais, Brazil, would turn green with

Figure 16. This turn-of-the-century ring from Tiffany features green natural quartz.

heat treatment. Such treated-color quartz is commonly known by the trade name "prasiolite." In recent years, the lab has also seen a few pieces of synthetic quartz with this grayish green color.

The stone in the ring proved to be natural quartz, as it demonstrated both Brazil twinning and parallel color zoning. However, it is not currently possible to distinguish naturally green quartz from heat-treated material. *GRC and IR*

SAPPHIRE,
Unusual Treated Natural Sapphire

In the Spring 1996 issue of *Gems & Gemology*, we reported on flame-fusion synthetic corundum oddities. Earlier this year, within a short period of time, the East Coast lab received two rather odd natural sapphires of treated blue color. The first was a 70.20 ct oval cabochon (figure 17) with an incised design on the back. Microscopic examination revealed numerous fluid-filled "fingerprints" and unidentified crystals that were altered in ways consistent with heat treatment. Exposure to long-wave UV radiation produced little reaction, but the stone fluoresced a patchy chalky blue to short-wave UV, further supporting the conclusion that it had been heat treated.

When examined with magnification in diffused light, several of the cavities and shallow fractures revealed blue color concentrations reminiscent of the effect sometimes seen in diffusion-treated stones (see, e.g., R. E. Kane et al., "The Identification of Blue Diffusion-Treated Sapphires," *Gems & Gemology*, Summer 1990, p. 124, figure 10). In this stone, the apparent color "bleeding" was actually a blue "dye," as was evident when the stone was immersed in methylene iodide (di-iodomethane; see figure 18). When we re-examined the stone with short-wave UV radiation and low magnification, the areas that luminesced corresponded to those with the blue dye. This treatment could easily have been confused with diffusion treatment because of the shallow penetration of the blue color in some areas.

The second stone (figure 19) was a diffusion-treated natural sapphire that had been quench crackled, making it more challenging to identify. Quench crackling, a relatively common procedure, is most often seen in quartz and beryl, which are quench crackled and then dyed green to imitate emerald. In the Summer 1996 Lab Notes section (pp. 125–126), however, we reported on a parcel of quench-crackled synthetic rubies. The crackling in this sapphire made it difficult to see the very small crystals and silk, which had been reduced from needles to lines of small unconnected dots. More importantly, it also disguised the surface diffusion treatment. Immersion again revealed the telltale outlined facet junctions and uneven surface coloration. *GRC and TM*

Figure 17. The color distribution in this 70.20 ct natural sapphire suggested some form of treatment.

Figure 18. Immersion in methylene iodide revealed both natural color zoning and evidence of a "dye" in the sapphire in figure 17.

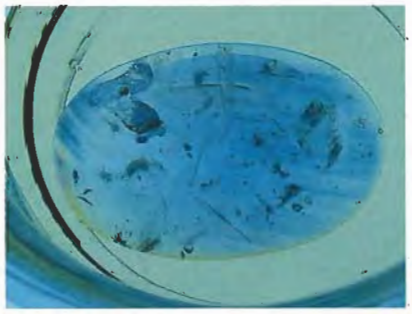

Flame-Fusion
SYNTHETIC SAPPHIRE

When GIA was founded in the early 1930s, gemology was relatively uncomplicated and most identifications could be made with basic instrumentation. However, then as now, the identification of synthetics was particularly worrisome. When we consider the primitive gemological microscopes available at that time, the great concern for the proper identification of Verneuil flame-fusion synthetics—the only type then available—is understandable.

Pioneering work in Europe had established that the main identifying features in these synthetic sapphires and rubies were curved striae or growth lines, as well as gas bubbles, large or small. One of the first indications that features believed to be characteristic of natural sapphires were also seen in synthetics was reported in 1920 by Mr. E. G. Sandmeier of Locarno, Switzerland, and confirmed by Mr. W. Plato of Frankfurt, Germany: the discovery of polysynthetic twinning in synthetic corundum. It is significant that one of the first gemological notes written

Figure 19. This quench-crackled natural sapphire owes its color to diffusion treatment. Magnified 10×.

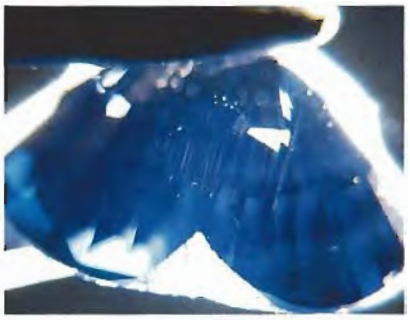

Figure 20. At first glance, the needle-like inclusions in this 4.18 ct heart shape seemed to indicate natural origin.

Figure 21. The curved growth lines easily seen with immersion in methylene iodide proved that the sapphire in figure 20 was synthetic.

by Robert Shipley Jr., in the second issue of the (then) new *Gems & Gemology*—March-April 1934—concerned his observation of nearly straight striae in a synthetic sapphire. Significant, too, is the fact that the very first (Summer 1942) of many well-illustrated feature articles in this journal by Dr. Eduard Gübelin addressed "Genuine Type Inclusions in New European Synthetic." Occasionally, other similarities between synthetic and natural gems have appeared in the gemological literature. More recently, synthetics with characteristics introduced to make them look natural, such as natural-appearing "fingerprints," have been seen on the market (see, e.g., J. I. Koivula, "Induced Fingerprints," *Gems & Gemology*, Winter 1983, pp. 220–227).

Another example of a natural-appearing inclusion in a synthetic stone was recently seen in the East Coast lab (figure 20). Needle-like inclusions near the cleft of this heart shape had convinced the client that the piece was natural. However, using only a loupe, he thought that he also saw curved growth lines. His suspicion proved to be well founded, as the curved growth lines were easily resolved when this synthetic sapphire was immersed in methylene iodide (figure 21). *GRC and TM*

PHOTO CREDITS

Figures 1 and 14 were taken by Maha DeMaggio. Nicholas DelRe supplied the pictures for figures 2–7, 9, 13, and 16–21. The photo in figure 8 is compliments of Laurence Graff. Shane Elen took figure 10. Shane F. McClure provided figures 11 and 15. Figure 12 is compliments of Christie's International.

BACK ISSUES OF GEMS & GEMOLOGY

Limited quantities of these issues are still available


Spring 1993


Spring 1994


Spring 1995

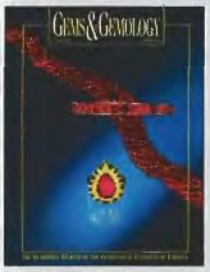
Summer 1993


Summer 1994


Summer 1995


Fall 1993


Fall 1994


Fall 1995


Winter 1993


Winter 1994


Winter 1995

Complete your back issues of Gems & Gemology NOW!

Single Issues*	$ 9.95 ea. U.S.	$ 14.00 ea. elsewhere
*Complete Volumes:** 1987, 1991,1992, 1993, 1994, 1995	$ 36.00 ea. vol. U.S.	$ 45.00 ea. vol. elsewhere
Three-year set	$ 99.00 U.S.	$125.00 elsewhere
Five-year set	$160.00 U.S.	$200.00 elsewhere

*10% discount for GIA Annual Fund donors at the Booster's Circle level and above.

TO ORDER: Call toll free (800) 421-7250, ext. 202 or (310) 829-2991, ext. 202
FAX (310) 453-4478 OR WRITE: G&G Subscriptions GIA
1660 Stewart Street, Santa Monica, CA 90404 USA

Spring 1987
"Modern" Jewelry: Retro to Abstract
Infrared Spectroscopy in Gem Identification
A Study of the General Electric Synthetic Jadeite
Iridescent Orthoamphibole from Greenland

Summer 1987
Gemstone Durability: Design to Display
Wessels Mine Sugilite
Three Notable Fancy-Color Diamonds
The Separation of Natural from Synthetic Emeralds by Infrared Spectroscopy
The Rutilated Topaz Misnomer

Fall 1987
An Update on Color in Gems. Part I
The Lennix Synthetic Emerald
Kyocera Corp. Products that Show Play-of-Color
Man-Made Jewelry Malachite
Inamori Synthetic Cat's-Eye Alexandrite

Winter 1987
The De Beers Gem-Quality Synthetic Diamonds
Queen Conch "Pearls"
The Seven Types of Yellow Sapphire

Summer 1988
The Diamond Deposits of Kalimantan, Borneo
An Update on Color in Gems: Part 3
Pastel Pyropes
Three-Phase Inclusions in Sapphires from Sri Lanka

Fall 1988
An Economic Review of Diamonds
The Sapphires of Penglai, Hainan Island, China
Iridescent Orthoamphibole from Wyoming
Detection of Treatment in Two Green Diamonds

Spring 1989
The Sinkankas Library
The Gujar Killi Emerald Deposit
Beryl Gem Nodules from the Bananal Mine
"Opalite:" Plastic Imitation Opal

Summer 1989
Filled Diamonds
Synthetic Diamond Thin Films
Grading the Hope Diamond
Diamonds with Color-Zoned Pavilions

Fall 1989
Polynesian Black Pearls
The Capoeirana Emerald Deposit
Brazil-Twinned Synthetic Quartz
Thermal Alteration of Inclusions in Rutilated Topaz
Chicken-Blood Stone from China

Spring 1990
Gem Localities of the 1980s
Gemstone Enhancement and Its Detection
Synthetic Gem Materials in the 1980s
New Technologies of the 1980s
Jewelry of the 1980s

Winter 1990
The Dresden Green Diamond
Identification of Kashmir Sapphires
A Suite of Black Diamond Jewelry
Emeraldolite
SOLD

Spring 1991
Age, Origin, and Emplacement of Diamonds
Emeralds of Panjshir Valley, Afghanistan

Summer 1991
Fracture Filling of Emeralds: Opticon and "Oils"
Emeralds from the Ural Mountains, USSR
Treated Andamooka Matrix Opal

Fall 1991
Rubies and Fancy Sapphires from Vietnam
New Rubies from Morogoro, Tanzania
Bohemian Garnet—Today

Winter 1991
Marine Mining of Diamonds off Southern Africa
Sunstone Labradorite from the Ponderosa Mine
Nontraditional Gemstone Cutting
Nontransparent "CZ" from Russia

Spring 1992
Gem-Quality Green Zoisite
Kilbourne Hole Peridot
Fluid Inclusion Study of Querétaro Opal
Natural-Color Nonconductive Gray-to-Blue Diamonds
Peridot as an Interplanetary Gemstone

Summer 1992
Gem Wealth of Tanzania
Gamma-Ray Spectroscopy and Radioactivity
Dyed Natural Corundum as a Ruby Imitation
An Update on Sumitomo Synthetic Diamonds

Fall 1992
Ruby and Sapphire Mining in Mogok
Bleached and Polymer-Impregnated Jadeite
Radiation-Induced Yellow-Green in Garnet

Winter 1992
Determining the Gold Content of Jewelry Metals
Diamond Sources and Production
Sapphires from Changle, China

Spring 1993
Queensland Boulder Opal
Update on Diffusion-Treated Corundum: Red and Other Colors
A New Gem Beryl Locality: Luumäki, Finland
De Beers Near Colorless-to-Blue Experimental Gem-Quality Synthetic Diamonds

Summer 1993
Flux-Grown Synthetic Red and Blue Spinels from Russia
Emeralds and Green Beryls of Upper Egypt
Reactor-Irradiated Green Topaz

Fall 1993
Jewels of the Edwardians
A Guide Map to the Gem Deposits of Sri Lanka
Two Treated-Color Synthetic Red Diamonds
Two Near-Colorless General Electric Type IIa Synthetic Diamond Crystals

Winter 1993
Russian Gem-Quality Synthetic Yellow Diamonds
Heat Treating Rock Creek (Montana) Sapphires
Garnets from Altay, China

Spring 1994
The Anahí Ametrine Mine, Bolivia
Indaia Sapphire Deposits of Minas Gerais, Brazil
Flux-Induced Fingerprints in Synthetic Ruby

Summer 1994
Synthetic Rubies by Douros
Emeralds from the Mananjary Region, Madagascar: Internal Features
Synthetic Forsterite and Synthetic Peridot
Update on Mining Rubies and Fancy Sapphires in Northern Vietnam

Fall 1994
Filled Diamonds: Identification and Durability
Inclusions of Native Copper and Tenorite in Cuprian-Elbaite Tourmaline, Paraíba, Brazil

Winter 1994
Color Grading of Colored Diamonds in the GIA Gem Trade Laboratory
Ruby and Sapphire from the Ural Mountains, Russia
Gem Corundum in Alkali Basalt

Spring 1995
Rubies from Mong Hsu
The Yogo Sapphire Deposit
Meerschaum from Eskisehir Province,Turkey

Summer 1995
History of Pearling in La Paz Bay
An Update on the Ural Emerald Mines
A Visual Guide to the Identification of Filled Diamonds

Fall 1995
Gem-Quality Grossular-Andradite: A New Garnet from Mali
Sapphires from Southern Vietnam
"Ti-Sapphire": Czochralski-Pulled Synthetic Pink Sapphire from Union Carbide

Winter 1995
A History of Diamond Sources in Africa: Part 1
A Chart for the Separation of Natural and Synthetic Diamonds

Some issues from the 1984–1986 volume years are also available. Please contact the Subscriptions Office for details.

ORDER NOW!

GEM N·E·W·S

DIAMONDS

Chatham synthetic "white" diamonds at JCK show. Three years ago, Tom Chatham of Chatham Created Gems, San Francisco, California, announced that he would be marketing "white" synthetic diamonds from Russia for jewelry use. Although it took longer than he originally anticipated, Mr. Chatham offered for sale a number of near-colorless synthetic diamond crystals at the June 1996 JCK show in Las Vegas, Nevada.

Mr. Chatham offered GIA Research a brief opportunity to examine about 100 of these synthetic diamond crystals (which ranged from about 10 points to almost a carat) before the show. Most were of small size and had too many inclusions for faceting. Research Associate Sam Muhlmeister and Research Gemologist Shane Elen focused their testing on four crystals of slightly better-than-average quality. These weighed between 0.41 and 0.51 ct, and were cubo-octahedral in crystal habit. All four had eye-visible metallic inclusions (figure 1), one had a typical white "cloud," one had relatively large stepped cavities (which resembled the hopper-growth cavities in, for instance, salt crystals, but are unusual in natural diamonds), and two had surface structures that looked like trigons. All four crystals were attracted to a strong magnet.

The crystals were inert to long-wave ultraviolet radiation, but fluoresced a very faint yellow or orange to short-wave UV. The UV fluorescence was typical, both in color and intensity, of that seen thus far in near-colorless synthetic diamonds; it is rare for a natural diamond to have a stronger fluorescence to short-wave than long-wave UV. However, no cross-shaped or octagonal pattern was visible in the UV fluorescence reaction—unlike the patterns reported previously for some synthetic diamonds (see, e.g., J. E. Shigley et al., "A Chart for the Separation of Natural and Synthetic Diamonds," Winter 1995, pp. 256–264). The crystals phosphoresced blue for at least one minute after exposure to short-wave UV; phosphorescence was much fainter in one than in the other three.

On the basis of their infrared spectra, we determined that these four samples were all type IIa (essentially nitrogen-free) synthetic diamonds. Near-colorless synthetic diamonds are typically type IIa or mixed type IIa plus other types, whereas type IIa near-colorless natural diamonds are relatively rare.

Energy-dispersive X-ray fluorescence (EDXRF) spectroscopy disclosed both iron (Fe) and germanium (Ge) in all four crystals. GIA Research had not previously detected germanium in any diamond, natural or synthetic. They suspect that Ge is being added to the growth environment of these crystals to prevent nitrogen from incorporating into the crystal structure of the synthetic diamonds, as the nitrogen would color them yellow.

Although all of these properties indicated that these samples were synthetics, conclusive proof was provided most readily by the metallic inclusions, which were eye-visible in all four samples, and were easily identified with magnification. All four proved to be magnetic. The presence of Ge in these samples also provides proof of synthesis, but trace-element determination requires the use of equipment beyond the reach of the average gemologist. Mr. Muhlmeister and Mr. Elen cautioned that this preliminary study involved only four crystals; the properties of other Chatham synthetic "white" diamonds may differ.

Figure 1. Chatham "white" synthetic diamonds were recently offered for sale at the Las Vegas JCK Show. Note the numerous metallic inclusions—characteristic of synthetic diamonds—in this 0.51 ct example. Photo by Shane Elen.

Figure 2. This 2.14 ct diamond (9.40 × 8.46 × 5.26 mm) is an example of the "Buddha Cut." Photo by Maha DeMaggio.

Diamond novelty-cut as a seated Buddha. New forms of fashioned diamonds are designed either for novel light-transmission and weight-retention properties, or to resemble other items. Examples of the former cuts include the "Flanders Brilliant" (Gem News, Summer 1993, pp. 130–131) and the "Context" and "Spirit Sun" cuts (Gem News, Spring 1995, pp. 59–60). Examples of the latter include diamonds cut to resemble dice (Lab Notes, Fall 1985, p. 172) and letters of the alphabet (Lab Notes, Spring 1986, p. 47). We recently had the opportunity to examine a new cut, the "Buddha Cut" (figure 2), which is being marketed in the United States by J. Kleinhaus and Sons of New York City. The distribution of facets was reminiscent of triangular modified brilliants, with 33 crown facets and 21 pavilion facets (no culet). The girdle was also faceted; two GIA Gem Trade Laboratory (GTL) graders assessed the girdle as thick to extremely thick.

Some consumers wear "Buddha Cut" diamonds in necklaces, while others treat them as *objets d'art*, according to a J. Kleinhaus spokesperson. (The unmounted sample we examined did "sit up" by itself.) Because of the potential religious implications, the cutter reportedly has strict criteria governing cut symmetry and what constitutes a diamond appropriate for this cut. For example, the "head" region should be free of unsightly inclusions.

COLORED STONES

Nonphenomenal vanadium-bearing chrysoberyl. Attractive examples of green chrysoberyl, lacking change of color, were seen at the February 1996 Tucson gem shows; some material was marketed as "mint" chrysoberyl. Six months earlier, the editors had examined a 3.48 ct stone cut from similar material. The gemological properties (see below) confirmed that this cushion-shaped modified brilliant cut was a natural chrysoberyl. We were somewhat surprised that there was no perceptible change of color (alexandrite effect) between incandescent and fluorescent light in a stone of such saturated green. With magnification, we noted a small brown-red crystal in the pavilion and growth zoning. EDXRF spectroscopy showed that the stone contained Al, Fe, V, Ti, Ga, and Sn. We had seen synthetic nonphenomenal green chrysoberyls colored by vanadium, but we had not previously examined natural vanadium-bearing chrysoberyls.

For comparison, we borrowed from Malhotra Inc., New York City, four faceted nonphenomenal green chrysoberyls (figure 3) that reportedly had been mined in Tanzania. Three had properties similar to the chrysoberyl in question. These included: pleochroism—trichroic colors of bluish green to blue-green/yellow-green to green/near-colorless to yellow; optic character—biaxial positive; color-filter reaction—none to faint pink; refractive indices—1.742 and 1.750–1.751; birefringence—0.008–0.009; specific gravity—3.71–3.72; luminescence to UV radiation—inert to faint orange (long wave) and inert to faint yellow (short wave); no luminescence to visible radiation; absorption spectrum in the desk-model spectroscope—440–445 nm band; infrared spectrum—strong features at 3225 and 2975 cm^{-1}, weaker features at 3140, 2850, and 2650 cm^{-1}; UV-visible spectrum—bands at 415 and 608 nm, peaks at 318, 366, 375, and 380 nm. Again, EDXRF spectroscopy revealed Al, Fe, V, Ga, and Sn. The fourth stone (1.47 ct), which was bluish green, showed additional features typically associated with chromium (including a red reaction to the Chelsea color filter; moderate red luminescence to

Figure 3. These four vanadium-bearing chrysoberyls (1.47–13.52 ct) are reportedly from Tanzania. The smallest contains chromium as well as vanadium, but none shows change of color. Photo by Maha DeMaggio.

Figure 4. Electron microprobe analyses revealed significant differences in chemical content between this natural 11.14 ct bluish green vanadium chrysoberyl from the Tunduru area in southern Tanzania and the two synthetic chrysoberyls (right, 1.00 and 1.12 ct) produced in Russia. The natural stone is courtesy of W. Spaltenstein, Bangkok; photo courtesy of SSEF.

visible light; and a 590–665 nm absorption—and 670 nm emission line—seen with the handheld spectroscope, as well as Cr in the EDXRF spectrum); however, there still was no perceptible change-of-color.

Contributing editor Henry A. Hänni had the opportunity to examine an 11.14 ct "intense" bluish green chrysoberyl (figure 4) that was reportedly from Tunduru, Tanzania. An associate at the University of Basel, M. Krzemnicki, performed electron microprobe analyses on this stone and on two samples of Russian hydrothermal synthetic nonphenomenal chrysoberyl that had been purchased at Tucson. The natural stone contained 0.4 wt.% V_2O_3, 0.2 wt.% Fe_2O_3, and trace amounts of Cr, Sn, and Ga; whereas the synthetic chrysoberyls revealed more vanadium (1.8 wt.% V_2O_3), more chromium (0.2 wt.% Cr_2O_3), and no appreciable Fe, Sn, or Ga.

Large faceted chrome diopsides. At one of the 1996 Tucson shows, Alex Grizenko, of the Russian Colored Stone Company, Genesee, Colorado, showed an editor two dark green oval modified brilliants: chrome diopside from the Inagly mine, Yakutsk, Siberia, north of Lake Baikal. The larger oval, at 26.17 ct, may be the largest known example of this faceted material; however, the 25.33 ct stone (figure 5) was brighter. Although this is not a new find (the rough for these pieces was probably mined 30–40 years ago), this material is increasingly popular in the colored stone market. Mr. Grizenko kindly loaned us these samples for closer examination.

We recorded the following gemological properties for the two diopsides: color—dark green, with even distribution; pleochroism—weak, green to brownish green; diaphaneity—transparent; optic character—biaxial positive; Chelsea filter reaction—none. Refractive indices for the 25.33 ct stone were $\alpha = 1.670$, $\beta = 1.680$, and $\gamma = 1.699$, with a birefringence of 0.029; for the 26.17 ct stone, β was not determined, but $\alpha = 1.672$, $\gamma = 1.700$, and birefringence was 0.028. Both stones had an S.G. of 3.30, were inert to both short- and long-wave UV radiation, and had very dark spectra as seen with a handheld spectroscope: The cut-off was at about 520 nm, with "chrome bands" at 630, 660, and 690 nm. Both stones contained scattered small crystals and "fingerprints," visible with magnification but not particularly distinctive. EDXRF spectra of the two stones showed major Mg, Al, and Ca, with smaller amounts of Fe, Cr, Ni, Ti, and Sr.

"Rose"-colored plagioclase-corundum rock from Sri Lanka. In March 1995, contributing editor Henry Hänni received two small "rose" pink translucent pebbles (figure 6) that each had one small polished face. These stones reportedly came from a locality near Pallebedda, Ratnapura district, Sri Lanka. The sender could not identify them on the basis of the R.I. (1.576) and S.G. (2.98) values that he determined. He also noted weak chromium lines in the absorption spectrum.

At the SSEF in Basel, microscopic observation of the surface in reflected light revealed a granular groundmass (90%) with occasional interspersed aggregates of idiomorphic crystals, which ranged from 20 to 70 microns (10%). The pink crystals had a hardness greater than that of the groundmass, as seen by their relatively higher relief. EDXRF analysis of the entire pebble indicated that Si, Al, and Ca were the main constituents, with Cr, Fe, and Sr present as trace elements. On the basis of SEM-EDS analysis of individual mineral grains within the pebbles, the main (groundmass) mineral component was identified as Ca-rich plagioclase feldspar, and the interspersed harder grains were identified as corundum. The Cr was contained in the corundum, which explained the rock's pink

Figure 5. The Inagly mine, Yakutsk, Siberia, is the source of this 25.33 ct (22.10 × 15.95 × 9.43 mm) chrome diopside, one of the largest such stones ever seen by the editors. Stone courtesy of the Russian Colored Stone Company; photo by Shane F. McClure.

Figure 6. Mixtures of feldspar and corundum, these two pebbles from Sri Lanka have some gem properties common to both materials. The largest pebble is about 1 cm across. Photo courtesy of SSEF.

color and the Cr spectrum. The higher density of the pebbles—about 2.98, compared to 2.76 for anorthite (plagioclase)—is also explained by the admixture of corundum.

Dr. Hänni doubts that this material will have great gemstone potential, but he considers it an interesting gemological puzzle: As a mixture of feldspar and corundum, it has the R.I. of one, the spectrum of the other, and an S.G. intermediate between the two.

Quartz-magnesite rock, so-called "lemon chrysoprase," from Australia. In past Gem News items, we have reported on various yellow-green materials from Australia, including the cryptocrystalline quartz variety chrysoprase (Summer 1994, pp. 125–126; Fall 1994, pp. 193–194), colored by nickel, and the nickel-carbonate mineral gaspeite (Summer 1994, pp. 125–126), sometimes marketed as "Allura." Another Australian material was seen throughout the 1996 Tucson gem shows, marketed as "lemon chrysoprase." After a cursory initial inspection, the curiosities of contributing editors Dino DeGhionno and Shane McClure were piqued; they decided to investigate further.

They acquired several samples, including a strand of 7 mm beads and a heart-shaped pendant (figure 7), and selected one 2.27 ct bead for detailed examination. The semi-translucent light yellowish green bead had a specific gravity of 2.83 and refractive indices of 1.51–1.68, with a pronounced carbonate "blink." Fluorescence to both long- and short-wave UV radiation was unevenly distributed—weak yellow in scattered areas. The absorption spectrum viewed with a desk-model spectroscope showed a lower wavelength cutoff at 450 nm; a dark band between 490 and 510 nm; lines at 600, 615, and 630 nm; and an upper-wavelength cutoff at 640 nm. With magnification, distinct areas of a lighter colored, more opaque material and a brighter yellowish green, more translucent material could be seen in the bead; the more opaque material had higher relief (that is, it was harder than the greener material).

EDXRF analysis revealed silicon, magnesium, and nickel. X-ray diffraction powder patterns were consistent with two phases being present: quartz and a carbonate with the calcite structure. The unit-cell spacings determined for the carbonate mineral were consistent with magnesite ($MgCO_3$) rather than gaspeite ($NiCO_3$); however, there is a solid solution between these two minerals, so that a phase can have up to 50% gaspeite and still be considered magnesite mineralogically. One identification question remained: Was the quartz material colored green by nickel (that is, was it chrysoprase?), or was it merely intergrown with the yellow-green carbonate? To answer this, the bead was submerged in a hydrochloric acid solution: The bead was selectively dissolved and turned white; a diffraction pattern showed only quartz. Consequently, we concluded that the "lemon chrysoprase" was not chrysoprase at all, but rather a rock consisting of (white) quartz and (yellowish green) magnesite.

Update on Madagascar sapphires. The Summer 1996 *Gems & Gemology* featured an article on sapphires from Madagascar's Andranondambo region (by D. Schwarz et al., pp. 80–99). Since then, we have received additional information about significant discoveries of sapphire elsewhere in this region. Thomas Banker, of Gem Essence Co., Bangkok, Thailand, writes that large quantities of sapphires have also been found at Antsiermene, about 10–12 km north of Andranondambo. The "sapphire rush" at Antsiermene began not long before Mr. Banker's April 1995 visit. Mining resembled that at Andranondambo, with each individual digging accompanied by its own small tailings pile of white plagioclase-rich rock. By his second visit in November 1995, a considerable shanty town (with about five streets) had developed next to the diggings (figure 8): Mr. Banker estimated

Figure 7. This "lemon chrysoprase" is really a quartz-magnesite rock. Photo by Maha DeMaggio.

Figure 8. By November 1995, a large shanty town, with a population in the thousands, had grown up adjacent to the Antsiermene sapphire diggings. Photo courtesy of Thomas Banker.

that 2,000–3,000 miners inhabited this town at the time of his visit, and others commuted from Andranondambo. The diggings covered about 3–5 km^2.

Madagascar is also the source of a large (17.97 kg; 29 × 19 × 16 cm) crystal that was recovered late last year from an undisclosed region. The deep blue crystal (figure 9) was the subject of a short report in the June-July 1996 *JewelSiam* ("The Find of a Lifetime," pp. 86–87).

Figure 9. This 89,850 ct blue sapphire crystal, here held by gem dealer Jeffrey Bergman, was found in Madagascar late last year.

Spessartine from Pakistan. Late last year, the Gem News editors were loaned samples of spessartine from a relatively new locality, Azad Kashmir, in northeastern Pakistan. Dr. Lon C. Ruedisili of Ruedisili Inc., Sylvania, Ohio, provided a 22.31 ct rough crystal and four faceted examples (figure 10) of this garnet, which is being marketed as "Kashmirine." Gemological investigation of the faceted stones revealed: color—slightly yellowish orange to brownish orange or red-orange; diaphaneity—transparent; color distribution—even; optic character—singly refractive, with weak anomalous double refraction; color filter reaction—orange; refractive index—1.800; specific gravity (measured hydrostatically)—4.19 to 4.20; inert to both long- and short-wave UV radiation; and a typical spessartine absorption spectrum, with bands at 410, 420, and 430 nm visible with strong transmitted light in a desk-model spectroscope. Using magnification (and for some stones, polarized light), we saw internal growth zoning (figure 11) in all samples. In addition, the 2.31 ct stone contained acicular inclusions, possibly birefringent (figure 12), and the 1.91 ct stone contained two small "fingerprint" inclusions. Dr. Ruedisili also provided UV-visible absorption spectra of some of this material—obtained by Dr. Eric Findson of the University of Toledo, Ohio—which showed absorption maxima at 408.5, 422, 430, 461, 482.5, 504.5, 522.5, 563.5, and 611 nm. These gemological properties are similar to those given in a short article on this material by Dr. U. Henn ("Spessartine aus Pakistan," *Zeitschrift der Deutschen Gemmologischen Gesellschaft*, Vol. 45, No. 2, 1996, pp. 93–94). Dr. Henn reports the composition of one stone (determined by electron microprobe analysis) as 85.26 mol.% spessartine, 10.13 mol.% almandite, and 4.61 mol.% grossular garnet.

According to Dr. Ruedisili, this material first became known when a 19.30 gram specimen was discovered in the summer of 1993. A representative of the Remmy Company, Pakistan (partners with Ruedisili Inc.), saw some of the material at the Mineral and Industrial Development Corporation (MIDC), Azad Kashmir, government auction in April 1994. The "Kashmirine" garnets are found in a pegmatite in the Janwai-Folawai region (Neelum Valley) of Azad Kashmir. The deposit is about 177–200 km (110–124 miles) northeast of Muzaffarabad. Seven pegmatites are being explored for garnets and other gem materials. The main mine is in Jandranwala Nar pegmatite no. 1, which lies about 1.5 km northeast of Folawai Village, at an altitude of 2,590 m. The pegmatite occurs in a migmatite complex, and averages 15 m by 2 m; so far, 143 m^3 have been excavated. In addition to the spessartines, quartz and greenish black tourmaline have been found in the gem zone of this pegmatite. These same minerals occur in the neighboring Donga Nar pegmatite, but the spessartine is not of gem quality.

Thirteen kilograms of spessartine were mined in 1994, and 16 kg in 1995. Approximately 20% of this production was suitable for cutting as cabochons or faceted stones. Most of the fashioned "Kashmirines" seen to date are in the 0.75–7.50 ct range, with a very few stones above 7.5 ct. The largest to date is about 30 ct. A joint venture between Ruedisili Inc., the Remmy Company, and the Azad Kashmir MIDC is being planned, in order to exploit the spessartines and other gem materials—including morganite, aquamarine, "mint green" and bicolored tourmaline, and topaz—from pegmatites in this region.

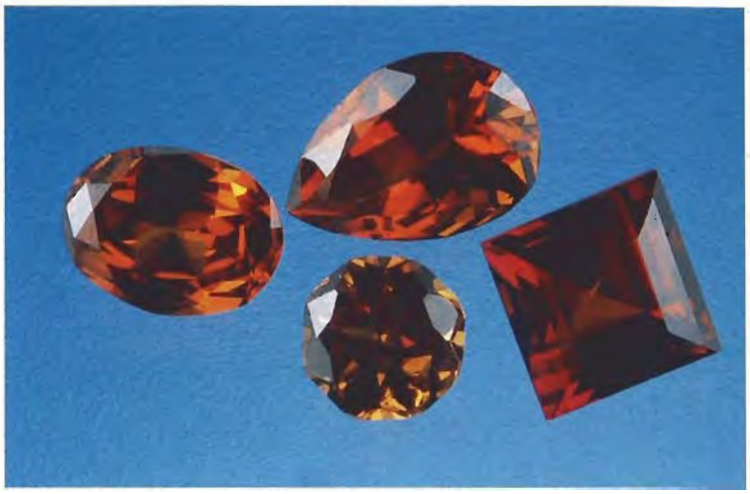

Figure 10. These four spessartines (0.69–2.31 ct) are from Azad Kashmir, Pakistan. Photo by Maha DeMaggio.

Activity continues at the Capão do Lana "Imperial" topaz mine. Two mining sites near the historic city of Ouro Prêto in Minas Gerais, Brazil, are famous for their production of fine Imperial topaz: Capão do Lana and Vermelhão. Currently, operations at the Vermelhão/HCC/Alcan mining complex, on the outskirts of Ouro Prêto, are temporarily halted because of a landslide on the boundary between two concessions, according to geologist Daniel Sauer, of Amsterdam Sauer, Rio de Janeiro, Brazil. However, the Capão do Lana mine, in the Rodrigo Silva district, is fully operational.

Figure 11. Internal growth zoning is visible with transmitted light in this 1.10 ct spessartine garnet from Pakistan. Photomicrograph by John I. Koivula; magnified 30×.

Figure 12. When examined with polarized light, these needle-shaped inclusions in a 2.31 ct spessartine garnet from Pakistan appeared to be birefringent. Photomicrograph by John I. Koivula; magnified 25×.

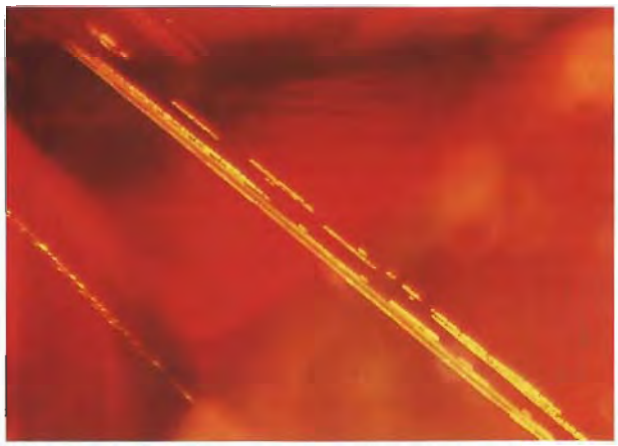

Figure 13. Draglines stretch across the large open pit at the Capão do Lana Imperial topaz mine. Large buckets suspended from the two lines scoop up the gem-bearing slurry from the bottom of the pit and drag it to the top for processing. Photo by Daniel A. Sauer, Amsterdam Sauer, Rio de Janeiro.

During an August 1996 visit to Capão do Lana, Mr. Sauer and *Gems & Gemology* editor Alice Keller observed the mining operations at what are now two large open pits (approximately 30 m at the deepest point, covering a total area of about 5 ha, or 12 acres) next to one another in the 800–1,000 ha (2,000–2,500 acre) concession area. Using draglines (figure 13), bulldozers, and water cannons, miners recover an average of 11,000 m^3 of mineralized rocks a month, which are processed to yield about 100 kg of topaz crystals. The estimated yield of fashioned stones from this material is 5,500 ct. Approximately 50 people are currently involved in mining and processing the ore.

Typically, the material is heavily included, so totally clean crystals are quite rare. At the mine office, Mr. Sauer and Ms. Keller saw topazes in a wide range of colors—light yellow, orange-yellow, brownish orange, pinkish orange ("salmon" or "peach"), pink, reddish orange, orange-red, and purple or violet (figure 14)—all of which

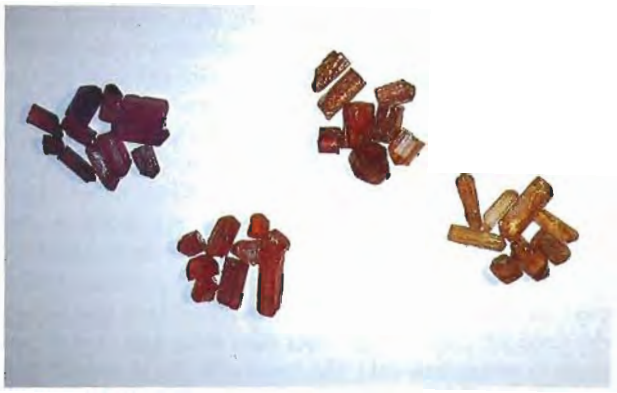

Figure 14. Topaz occurs in a wide range of colors at Capão do Lana, as these groups of natural-color crystals seen at the mine office in Rodrigo Silva demonstrate (the largest crystal is 180 ct). Red and purple are the rarest colors. Photo by Daniel A. Sauer.

are marketed as Imperial topaz. The most sought-after are the intense pink, red, and purple stones, which—according to mine director Wagner Colombaroli—represent less than one-half of one percent of the total cuttable material. Although these colors occur naturally, many of the pink and red stones on the market today were produced by heat treating the original rough to remove the yellow component.

An article on gem topaz from the Capão do Lana deposit is in preparation for an upcoming issue of *Gems & Gemology*.

Gem materials from Vietnam. Items on gems from Vietnam regularly appear in Gem News (see, e.g., Winter 1992, pp. 274–275; Summer 1993, p. 134; Fall 1993, pp. 211–212; Winter 1993, p. 285; and Fall 1994, p. 197). Vietnamese gems from many provinces were available at the 1996 Tucson shows. Mary Nguyen of Van Sa International, Marina del Rey, California, showed one of the editors (MLJ) several examples of gem rough from Vietnam, including: aquamarine and topaz from Thanh Hoa; topaz from the Darlac Plateau; ruby and sapphire rough from Luc Yen; zircon and opal from Pleiku; amethyst and citrine from Phan Thiet; and several materials from Lam Dong, among them tourmaline, peridot, petrified wood, chalcedony, and tektites. This extensive assortment suggests that Vietnam—a region with little previous history or lore in gemology—promises to be a rich source of gem materials for many years to come.

TREATMENTS

Coated quartz in "natural" colors. One of the techniques commonly used to change the apparent color of gems is that of coating the sample with a colored material (see, e.g., "'Tavalite,' cubic zirconia colored by an optical coating," Summer 1996 Gem News, pp. 139–140). The most prominent example of this technology is so-called "aqua-

aura" quartz, which owes its blue color to a thin surface coating of gold (Gem News, Winter 1988, p. 251; Fall 1990, pp. 234–235). At one of the 1996 Tucson shows, mineral dealer Rock Currier of Jewel Tunnel Imports, Baldwin Park, California, showed one of the editors (MLJ) several examples of coated quartz crystals in colors resembling natural quartz varieties. Four samples (figure 15) were borrowed for further study; these resembled amethyst, citrine, green "prasiolite" (heated amethyst), and red "strawberry quartz." The coatings contained gold, bismuth, lead, chromium, titanium, and lesser amounts of calcium, potassium, and iron, as determined by EDXRF spectroscopy. As with the "aqua-aura" quartz, the coatings on these samples were too thin to affect the 1.54 R.I. value expected for quartz.

Figure 15. These four quartz clusters (32.3–68.17 mm long) owe their colors to thin coatings of gold, bismuth, lead, and other elements. Photo by Maha DeMaggio.

SYNTHETICS AND SIMULANTS

Flexible "crystal" fabric. A new product from the Swarovski Company of Wattens, Austria, is a flexible mesh fabric of faceted glass "crystals" (figure 16). The editors recently examined a sample of this "Crystal Mesh," which consisted of 238 mounted foil-backed single-cuts, each about 2.7–2.8 mm in diameter, which (in our sample) occurred in three colors:

- Near-colorless (which had a weak-to-moderate, even light blue fluorescence to long-wave UV radiation, and a moderate-to-strong, even whitish yellow fluorescence to short-wave UV radiation)
- Light blue (fluorescing a slightly chalky, weak-to-moderate, even yellow-orange to long-wave UV and a moderate-to-strong, even light blue to short-wave UV)
- Medium dark blue (fluorescing a weak-to-moderate, even blue to long-wave UV and a moderate-to-strong, even blue to short wave UV)

All had the same refractive index, 1.578. When examined with the microscope, these single-cuts were mostly free of inclusions, although some contained scattered gas bubbles. Each single-cut was foil-backed and

Figure 16. This 43 × 52 mm flexible swatch of "Crystal Mesh" contains 238 single-cut glass "crystals." Photo by Maha DeMaggio.

Figure 17. The single-cuts in the "Crystal Mesh" sample shown in figure 16 are mounted in black cups, which are connected by prongs through black rings; the prongs are cemented closed. View from the back side, magnified 2×. Photomicrograph by John I. Koivula.

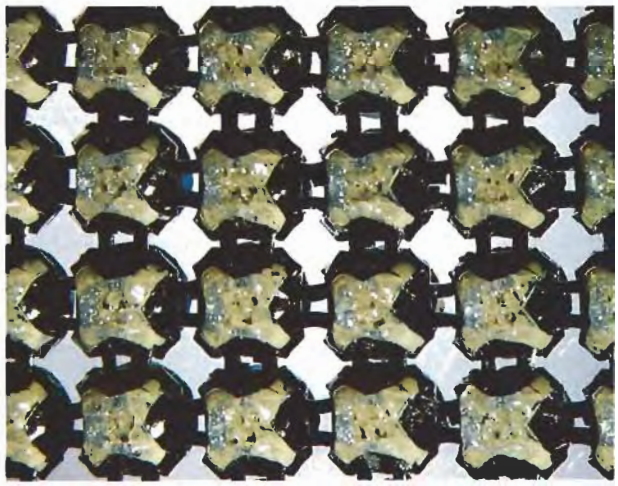

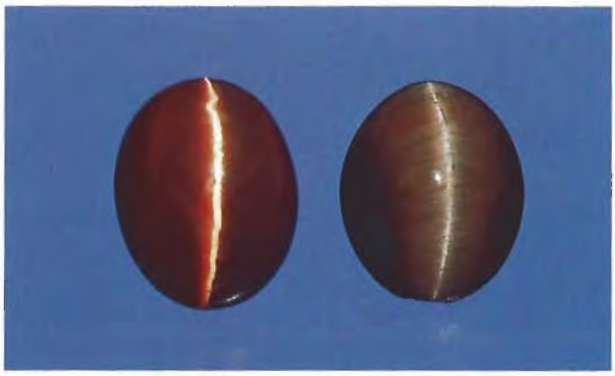

Figure 18. Optical fiber glass—like the 2.85 ct cabochon (10.03 × 7.86 × 4.09 mm) on the left—is being produced in colors such as this specifically for gem use. A natural (heat-treated) tiger's-eye cabochon (1.83 ct, 9.61 × 7.96 × 3.67 mm) is shown on the right for comparison. Photo by Maha DeMaggio.

fastened with black glue into a black-painted metal cup; these cups alternated with black-painted metal rings, with one of four prongs on each cup folded through the adjacent rings and then glued shut with a brown rubbery material (figure 17). According to product information supplied by the manufacturer, "Crystal Mesh" can be machine-washed but not dry cleaned. Additional colors and patterns are available, and "Crystal Mesh" is available in pieces as large as 20 × 50 cm (about 8 × 20 inches).

Figure 19. A stickpin mounted with a tourmaline attaches this woven 18K gold brooch to the wearer's jacket or dress; other stickpins can be used to change the appearance of the piece. Gold wire-, diamond-, and pearl-mounted pins are shown; the brooch is about 5 cm in diameter. Pieces made by Barbara Berk; photo © Harold and Erica Van Pelt, Los Angeles.

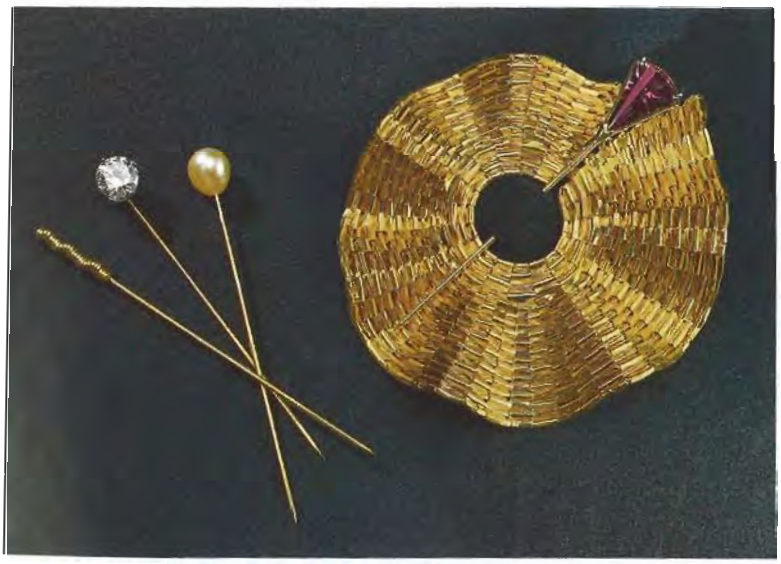

Fiber-optic glass imitation of tiger's-eye. Entries on fiber-optic glass (marketed under the names "Catseyte," "Cathaystone," and "Fiber Eye") appeared in the Summer 1991 and Summer 1994 Gem News sections. In the latter section, gray fiber-optic glass was discussed as a simulant of cat's-eye sillimanite from Orissa, India. Fiber-optic glass, which is most often oriented in fashioning to produce an extremely sharp chatoyant band, has been commercially available for some time in two colors: white and brown.

During the last few years, we have seen additional colors on the market: saturated yellow, pink, purple, black, and blue, as well as a more subdued "gunmetal" grayish blue that yields cabochons reminiscent of hawk's-eye quartz, a bright green similar to some cat's-eye diopside now coming from India, and a reddish orange similar to some heat-treated tiger's-eye (figure 18). The most recent material seen was "striped" in red/white/green, red/blue/green, and red/white/blue. According to a representative of Teton Gems, Boise, Idaho, the white and brown material previously available had been produced and rejected for laser or other technical applications. The newer colors, however, were produced specifically for their gem potential.

Gemological investigation of the 2.85 ct reddish orange glass cabochon shown in figure 18 revealed: 1.55 spot R.I.; 3.09 S.G.; moderate red appearance through the Chelsea filter; weak, dull red fluorescence to long-wave UV and strong, chalky whitish yellow fluorescence to short-wave UV. Magnification revealed that the optic fibers have hexagonal outlines with a "honeycomb-like" structure similar to that seen in other fiber-optic glasses. Also seen, when looking parallel to the fibers, was a "speckled" color appearance, apparently the result of orange fibers intermixed with colorless ones.

Some of the cabochons displayed a somewhat less distinct chatoyant band than what has typically been encountered. According to the vendor, these stones had been cut as lower-domed cabochons to give the "eye" a more natural appearance.

MISCELLANEOUS

Versatile jewelry. A recurring trend in jewelry design is that of creating pieces in which the stones are interchangeable, enabling the wearer to adjust color schemes or "looks" with minimum effort. One attractive contemporary example of this trend is a brooch and stickpin combination (figure 19) designed by Barbara Berk, of Foster City, California. With this set of combination jewelry, the overall appearance can be easily altered by changing stickpins; in addition to the tourmaline, diamond, pearl, and gold wire pins pictured, the set that we saw contained citrine- and onyx-headed stickpins. Virtually any gem material could be adapted for this use.

BOOK Reviews

SUSAN B. JOHNSON AND JANA E. MIYAHIRA, EDITORS

THE DEALER'S BOOKS OF GEMS & DIAMONDS

*By Menahem Sevdermish and Albert Mashiah, 1004 pp., illus., Kal Printing House, Israel, 1996. US$98.00**

This two-volume work was first published in Hebrew in 1986 by Mada Avanim Yekarot Ltd.; a second revised edition in the same language was issued in 1995. This is the first English edition.

Menahem Sevdermish is a Fellow of the Gemmological Association of Great Britain, a founder and president of the Gemological Association of Israel, and the owner of a gemstone manufacturing and trading company. He has particular expertise in gemstone cutting and selling. Coauthor Albert Mashiah also has impressive credentials: A long-time member of the Israeli precious stones industry, he has been a vice-president of the Israel Precious Stones and Diamonds Exchange, as well as vice-president of the Israel Emerald Cutters Association and the Gemological Institute for Precious Stones and Diamonds.

This book presents an interestingly different approach to a gemological text, in that it is written from the gem dealer's point of view. The authors seem totally at home with the business aspects of diamonds and colored stones, as well as with assessing rough and cutting it for the market. In general, however, the two volumes of this work differ in effectiveness and value. The chapters on diamond are up-to-date and probably the best exposition of current practices in diamond cutting to be found anywhere in book form. The chapters on diamond grading and on judging value in colored-stone rough are very well planned and executed. However, the chapters on colored-stone identification leave something to be desired. Although many of the comments made from a dealer's viewpoint are germane and useful to the reader, these chapters suggest that the authors have had little experience in colored-stone identification in a laboratory—or that the copyediting and proofreading were inadequate.

For example, in a discussion of spinel identification, the authors mention that glass would be distinguished because it is amorphous and, thus, isotropic. As I am sure the authors are aware that both spinel and glass are isotropic, this is undoubtedly a fault of inadequate proofreading. They also state that "it is sometimes very difficult to decide if a stone is peridot or sinhalite, and only a chemical test will distinguish between them." It is true, certainly, that for many years sinhalite was thought to be brown peridot, but the difference in spectra and the nature of the birefringence readily separates the two. In the identification table for the peridot section, they list the birefringence of sinhalite—which they refer to as DR—as exactly the same as peridot, and they also give the refractive indices, specific gravity, and hardness of the two as identical. Both the R.I. and S.G. for sinhalite are higher than those for peridot, and the beta index is closer to that of gamma.

Elsewhere, the explanation of what causes play-of-color in opal leaves the reader bewildered. It states, in referring to the silica spheres, "When the spheres are uneven in size, the light reaching them is dispersed differently in each sphere, so that different colors are reflected. But, since the human eye is unable to see the minute spheres, the color coming from this layer will appear white because the human eye interprets a mixture of the spectrum as white." These are just a few of a significant number of examples where careful editing would have been useful. Editing in the chapters related to diamond seems to have been more rigorous.

Yet there are also interesting chapters on subjects not found in other gem books, such as "A Commercial Analysis of the Gemstone" and "A Pre-purchase Cost Analysis." In addition, there is a lucid account of the ingenious Robogem, a new instrument that analyzes rough to obtain maximum yield.

On the whole, the book is useful because it offers not only the exceptionally good diamond chapters, but also unique insights into other areas of the gem field. Although slightly flawed, the book seems, to this reviewer, a very worthwhile addition to any gemological library.

RICHARD T. LIDDICOAT
Chairman of the Board
Gemological Institute of America
Santa Monica, California

NEW FRONTIERS IN DIAMONDS—THE MINING REVOLUTION

*By David Duval, Timothy Green, and Ross Louthean, 175 pp., illus., publ. by Rosendale Press, London, 1996. US$55.00**

History has shown that no single factor—other than the world economy—has affected the orderly functioning of the diamond industry more

*This book is available for purchase through the GIA Bookstore, 1660 Stewart Street, Santa Monica, CA 90404. Telephone: (800) 421-7250, ext. 282; outside the U.S. (310) 829-2991, ext. 282. Fax: (310) 449-1161.

than the production and availability of rough. Today, exploration for diamonds is proceeding at a feverish pace on all continents except Antarctica. In addition to De Beers, dozens of mining companies have entered the arena These include some of the world's largest, who traditionally have been involved primarily with metals. A very few appear to have been eminently successful, as evidenced by the anticipated 3 to 5 million carats of production from one major new mine (BHP/Dia Met) in Canada by the end of this century.

Responding to the interest that all of this activity has generated, three prominent resource journalists—from three widely separated parts of the world—have teamed up to review the highlights of diamond exploration during the last decade. The result is this small book, which is divided into four parts. Information is remarkably current, as the February 1996 "agreement" between De Beers and Russia is mentioned several times.

Part 1 (Green, London), "The Global View," reviews the special and essential role of De Beers in the diamond industry. It then proceeds to summarize the history and current status of mining and production. The main focus is on Africa (which is still the world's most important diamond producer, with—according to 1994 data—46% by weight and 69% by value of world production). There are many interesting statistics and facts; for example, a ship looking for marine diamonds off Namibia can "mine" 0.25–0.40 km^2 of ocean bottom per year. However, there are also occasional errors—such as the area of the Mwadui mine (Tanzania) given as 13 km^2, when its surface area is actually 146 hectares, or 1.46 km^2. The chapter concludes with a discussion of production from Russia, followed by brief comments on exploration in Finland, Brazil, and India.

Part 2 (Duval, Vancouver), "Canada: Joining the Big League," is a narrative-style review of the history of diamond exploration in the Northwest Territories, which led to the discovery of the Lac de Gras kimberlite field by Charles Fipke in 1991. From Duval's discussion of the current exploration activity by about a dozen companies (most small and speculative), it is clear that only the BHP/Dia Met mine mentioned above approaches commercial viability at this time. The difficulties of exploring for diamonds—especially the heavy investments in time and money required—become evident in this chapter and the next.

Part 3 (Louthean, Perth), "Australia: Any Heirs to Argyle?," is similar in scope to Part 2, except that it places heavy emphasis on the Argyle mine (its discovery, development, corporate structure, marketing strategies, and the crucial question of whether it will be able to operate after about 2003). Also discussed are many of the companies presently exploring in Western Australia, New South Wales, and offshore, where rivers draining the Argyle region empty into the sea. Brief mention is also made of exploration in Kalimantan, on the island of Borneo. However, the question as to who (if anyone) will be Argyle's heir is not answered.

Part 4 (Green, London), "Who Will Buy My Beautiful Diamonds?," is a short, statistics-based discussion of the world retail trade (there is a seemingly relentless rise in diamond jewelry sales). Green concludes that the markets for diamonds in the United States and Japan have matured. Future additional production will be consumed in East Asia (Taiwan, South Korea, Thailand, eventually China, and—it is hoped—India).

It must be noted that every major topic in this book (including most of the figures and all three tables) can be found in articles that have appeared recently in such sources as *JCK*, *Diamond International*, *Northern Miner*, literature available from two investment (securities) companies, and this journal (*Gems & Gemology*). Those gemologists and jewelers who have kept abreast of the professional literature will have a sense of *déjà vu* when they read this fairly expensive review. Nevertheless, this conveniently sized compendium will be appreciated by those who are just entering the field or have not kept up with recent events.

ALFRED A. LEVINSON, PH.D.
University of Calgary
Calgary, Alberta, Canada

PHOTOGRAPHING MINERALS, FOSSILS AND LAPIDARY MATERIALS

*By Jeffrey A. Scovil, 224 pp., illus., Geoscience Press, Tucson, AZ, 1996. US$40.00**

This important "how-to" book will be useful to anyone—beginner or professional—who wants to improve their photography of gems and minerals. It explains in plain language, for those not trained in this type of photography, the equipment and procedures necessary. Line illustrations and photographic examples clearly illustrate these lessons.

Specifically, the book describes techniques for cameras that use a film size from 35 mm up to 4 × 5 inches. This includes selection of lenses, films, lighting, filters, and backgrounds. Also explained and illustrated are special approaches to magnification in photomicrography, macro images, stereo views, and photographing fluorescence.

Authors who intend to travel to mines or other locations can improve the quality of their photos by following Mr. Scovil's guidelines. They can also learn important tips on packing photo equipment for various modes of transportation, as well as how to prevent equipment loss or theft during international travel.

Of help to lecturers are the techniques Mr. Scovil gives for presenting slide shows and his advice on how to copy artwork and line drawings. Writers can also improve their presentations by using the reproduction procedures and instructions available in this valuable book.

Overall, this publication is a useful addition to the library of amateur and professional photographers alike.

HAROLD VAN PELT
Van Pelt Photography
Los Angeles, California

GEMOLOGICAL ABSTRACTS

C. W. FRYER, EDITOR

COLORED STONES AND ORGANIC MATERIALS

Cretaceous mushrooms in amber. D. S. Hibbett, D. Grimaldi, and M. J. Donaghue, *Nature*, October 12, 1995, p. 487.

Recently, two mushrooms were discovered in amber of Turonian age (90–94 million years old, mid-Cretaceous) in central New Jersey. One specimen is nearly complete, with an intact cap, distinct gills, and a central stalk (it is the oldest known such mushroom, by about 60 million years); the other is a wedge-shaped fragment of a mushroom cap. Both mushrooms resemble modern common leaf-litter and wood-decayer species, and both were growing on a cedar (a member of the Cupressaceae family). *MLJ*

Opal. *extraLapis*, No. 10, 1996, 96 pp. [In German].

Opal is the subject of another *extraLapis*, an issue of *Lapis* magazine that is devoted entirely to one gemstone. Following a comprehensive introduction by Edward Gübelin, a series of articles provide information on all important aspects of this colorful gem.

An article by Max Weibel explains the origin of play-of-color. Two other papers describe Queensland's boulder opals, their forms, production, and prospecting methods (Wilson Cooper and Barry J. Neville); and the geologic setting and processes that led to opal formation in the sediments of Australia's Great Artesian Basin (Jack Townsend). In disagreement with traditional theories of opal formation, Len Cram offers a surprising new model, based on ion exchange, that he demonstrated by growing synthetic opal out of "opal dirt" in a bottle in just three months. Jürgen Schütz describes the long history of Mexican opals, their varieties, and the present mining situation. Jochen Knigge recounts the history and production of opals from Pedro II, Piauí, Brazil. Klaus Eberhard Wild portrays another important locality—Kirschweiler, near Idar-Oberstein—which was (and perhaps still is) one of the most important centers of opal fashioning and trade worldwide.

Jürgen Schütz explains the factors that determine the price of an opal (locality of origin, body color, play-of-color,

This section is designed to provide as complete a record as practical of the recent literature on gems and gemology. Articles are selected for abstracting solely at the discretion of the section editor and his reviewers, and space limitations may require that we include only those articles that we feel will be of greatest interest to our readership.

Inquiries for reprints of articles abstracted must be addressed to the author or publisher of the original material.

The reviewer of each article is identified by his or her initials at the end of each abstract. Guest reviewers are identified by their full names. Opinions expressed in an abstract belong to the abstracter and in no way reflect the position of Gems & Gemology *or GIA.*

pattern, cut, size). Even with these criteria, it remains difficult to know how much a harlequin opal is really worth. Three additional articles provide information on opal nomenclature (Jürgen Schütz and Manfred Szykora); doublets, triplets, and opal mosaics (Karl Fischer); and synthetic opals and opal simulants (Manfred Szykora). The volume concludes with a description of opalized fossils: snails, mussels, belemnites, and even dinosaurs (Alex Ritchie and Brigitte Szykora).

This *extraLapis* also contains short descriptions of smaller opal sources (Denmark, Honduras, Indonesia, Mali, Saxony, Slovakia [formerly Hungary], Turkey, and the United States); an opal glossary; and the stories of the Hope and *El Águila Azteca* opals (by John S. White). Also described is an extraordinary opal necklace that Queen Elizabeth II was *not* given as a coronation present (by Helmut Weis). Two stories tell us how Australian aborigines explain the origin of opals.

A volume about opals with words only (in this case, German) would be utterly frustrating. In this edition, however, the stunning beauty and incredible variability of opals is illustrated throughout the entire volume by wonderful color photographs. *RT*

Zur Entstehung der sternfoermigen Achate in sauren Vulkaniten. Eine modifizierte Bildungstheorie (The origin of star-shaped agates in acidic vulcanites. A modified theory of formation). R. Rykart, *Der Aufschluss*, Vol. 46, 1995, pp. 33–36.

It has generally been believed that agate formation in rhyolites and porphyries takes place at high temperatures. Recent research by M. Landmesser has shown that agate may form in other types of rocks at lower temperatures. In this article, Mr. Rykart proposes a new theory for the formation of star-shaped agates in lithophysae (e.g., thunder eggs) in rhyolitic vulcanites. The basic idea is that the gaseous bubbles in the magma contract to form polygonal cavities because of dropping gas pressure during cooling near the Earth's surface. Subsequently, monomer H_4SiO_4, dissolved in the water that invades the cavities, fills them with chalcedony and quartz. The surrounding rhyolite devitrifies and hardens, forming the well-known quartz porphyry balls. *RT*

DIAMONDS

Aber Resources Ltd. *Diamond Industry Week*, February 26, 1996, p. 3.

Aber Resources has announced results from drill cores at A-418, one of their kimberlite pipes in the Northwest Territories, Canada. Nineteen tons of ore in a large-diameter (6 inches, about 15 cm) core drilled through 367 m of kimberlite yielded 83.1 carats of diamonds—4.3 carats per ton of ore—with individual stones between 0.025 and 3 carats. The largest "gem" diamond weighed 2.2 carats. The A-418 pipe is estimated to contain 15 million tons of ore to 650 m depth; the grade is similar to that of the A-154 South kimberlite, which showed 4.5 carats per ton of ore, at a valuation of $58.17 per carat. Bulk sampling is proceeding at the A-154 South, A-154 North, and A-21 kimberlites. *MLJ*

Diamonds everywhere. C. Koeberl, *Nature*, November 2, 1995, pp. 17–18.

On Earth, diamonds usually occur in rocks derived from the mantle. They are thought to have formed from fluids or melts in the upper mantle at "immense" temperatures and pressures, probably—according to Mr. Koeberl—during several diamond-forming events early in the Earth's history. Diamonds have also been produced, directly on the Earth's surface, during meteorite impacts; such diamonds may have formed, at least in one case (Ries Crater), from the vapor phase. Diamonds found in iron meteorites and ureilites (another variety of meteorite) were formed by shock from graphite or amorphous carbon, probably in the meteorite and not after it arrived on the Earth. Nanometer-size diamonds have been found in chondritic meteorites, associated with noble gases (xenon, argon, etc.) with unusual isotopic compositions; these came from interstellar or presolar events very early in the history of the solar system. Small diamonds have also been found in clays marking the boundary of the Cretaceous and Tertiary periods, which has evidence of a large impact; their carbon and nitrogen isotopes point to an origin within the impact event or the resulting fireball. Polycrystalline diamonds up to 1 cm, discovered in impactites at a few Russian and Ukrainian impact structures, also appear to be crustal in origin. Impact-produced diamonds are very different from microdiamonds found in high-grade metamorphic rocks.

Also rare and unusual are polycrystalline black diamonds, called carbonados. No carbonado diamond has ever been found *in situ* in a rock. Possible origins include carbon subduction in the mantle, shock metamorphism during impact, or irradiation of organic matter; vapor-deposition may also be a candidate. MLJ

Diamonds: Wyoming's best friend. *Geotimes*, Vol. 41, No. 2, February 1996, pp. 9–10.

The first diamond mine in Wyoming is about to begin production, and many more kimberlites and lamproites in the region may contain diamonds, according to W. Dan Hausel of the Wyoming State Geological Survey. Redaurum Red Lake has just finished construction of a 140-ton-per-hour ore-processing mill for the company's Kelsey Lake diamond property, along the Colorado-Wyoming state line; several gem diamonds, up to 14.2 ct, already have been recovered from this property. The Colorado-Wyoming kimberlite province includes more than 100 kimberlite intrusives, one of the world's largest lamproite fields, and dozens of unexplored geophysical and geochemical anomalies. More than 120,000 diamonds have been recovered from this area in the last 20 years.

No history of diamond mining in Wyoming is complete without mention of the "Great Diamond Hoax of 1872." A

sandstone outcrop was salted with 10 pounds of uncut diamonds and rubies (purchased in London), plus another 50 pounds of garnets and chrome-rich diopsides from Arizona. (At the time, sandstone was thought to be a host rock for diamonds, no doubt based on the many alluvial diamond sources then known.) This hoax helped provoke passage of the Mining Law of 1872, which established the first mine-patenting regulations in this country. Full details of the story may be found in the Wyoming Geological Association's *1995 Field Conference Guidebook*. *MLJ*

Are euhedral microdiamonds formed during ascent and decompression of kimberlite magma? Implications for use of microdiamonds in diamond grade estimation. D. R. M. Pattison and A. A. Levinson, *Applied Geochemistry*, Vol. 10, 1995, pp. 725–738.

The authors answer this question with "Yes, quite likely in some cases." Before they proceed with their explanation, they first state clearly that this paper only discusses transparent, well-crystallized, euhedral octahedral stones smaller than 1 mm (so-called microdiamonds), which show little or no signs of resorption. No broken stones, fragments, or crystal shards are considered.

In a detailed review of several theories about the origin of euhedral microdiamonds (break-up of peridotitic or eclogitic xenoliths, resorption of larger diamonds, precipitation from melts of metasomatic events), the authors show that none of these satisfactorily explains the presence of both resorbed macrodiamonds (larger than 1 mm) and euhedral microdiamonds in a single kimberlite pipe. They argue that if diamonds are resorbed in a kimberlite magma, the microdiamonds would be resorbed more, possibly to extinction, and there would be no euhedral microdiamonds. The authors propose a hypothesis: Varying pressure-temperature and oxidation conditions generate (at different times) resorption of existing macro- and microdiamonds, followed by crystallization of euhedral microdiamonds from carbon dispersed in the magma and, to a lesser extent, from carbon released by the resorption of pre-existing diamonds. The process can be multistage and can produce different mixtures of stones in different pipes, ranging from the extremes of only rounded resorbed macrodiamonds and no microdiamonds to no macrodiamonds (resorbed to extinction) and only euhedral microdiamonds. Thus, the relationship between the population of macrodiamonds and that of euhedral microdiamonds is not simple and direct.

The implication is that the use of microdiamonds in estimating the overall diamond content in a pipe (which is widely done in Canada, where pipes are buried and only drill core samples are available for testing) is not straightforward. In several cases, this method can give an incorrect answer. Diamond exploration companies' arguments that the method does work rest on their use of the ratios of euhedral, resorbed, and cubic microdiamonds, as well as broken and fragmented crystals. However, this privileged information is not available in published form, so it is impossible to confirm their arguments.

The authors note the paucity of published research into nitrogen content and the aggregation and carbon-isotope composition of microdiamonds, by which their hypothesis could be tested. Very recently, a number of papers (by researchers such as Milledge, Mendelssohn, Taylor, and Pillinger, among others) have addressed these subjects, but not the specific issue of euhedral microdiamonds. However, this interesting review and thought-provoking hypothesis may give a welcome impetus to the release of more information on microdiamonds and their usefulness in estimating diamond content. *Bram Janse*

French Guiana diamonds. *Mining Journal, London*, March 22, 1996, p. 212.

Diamonds have been found in a metamorphosed ultramafic rock in the Dachine permit area, Inini, French Guiana. Golden Star Resources, Guyanor Resources SA, and Lakefield Research have recovered 3,748 microdiamonds from over 113 kg of host rock; also, 8 macrodiamonds (the largest being 2.4 mm) have been recovered from 1.8 tons of rock altered to saprolite. *MLJ*

ODM: Namibian gem. *Mining Journal, London*, March 15, 1996, p. 205.

Several companies have licenses to mine the diamond-rich offshore deposits along the Namibian and South African coasts: De Beers Marine (which produces the most stones at this time, about 0.5 million carats), Namibian Minerals Corp., Diamond Fields Resources, BHP, and Ocean Diamond Mining (ODM), plus a few others. Capetown-based ODM is an "important, but underreported" company operating in the region. ODM currently works in two main areas: It has production around the 12 Penguin Islands, and exploration along South African concession 7b and deep-water concessions 6c and 14c (in a joint venture with Benguela Concessions). Production in fiscal 1995 was about 40,000 carats at an average price of US$200 per carat. *MLJ*

GEM LOCALITIES

Alkali basalts and associated volcaniclastic rocks as a source of sapphire in eastern Australia. G. M. Oakes, L. M. Barron, and S. R. Lishmund, *Australian Journal of Earth Sciences*, Vol. 43, No. 3, 1996, pp. 289–298.

The major sapphire deposits in eastern Australia are alluvial; they occur in recent drainage systems where Tertiary alkali basaltic volcanic rocks dominate the present surface. As a result, it has been generally accepted that these basalts are the immediate source of the sapphires. The enigma is that sapphires are only rarely found in these rocks. This paper discusses recent developments in the understanding of sapphire occurrences in eastern Australia and reviews several possible origins for these deposits.

During field studies, it was observed that the sapphires are associated with volcaniclastic rock units, now mostly altered to clay minerals, that are common within

the main basaltic sequences. (*Volcaniclastic* means a rock composed of volcanic fragments, and includes such rock types as ash, tuff, or breccia). The volcaniclastic units are laterally extensive, but they are thin, easily eroded, and generally poorly exposed. In some locations, however, extraordinary concentrations of sapphires (up to 12 kg per cubic meter) have been observed within these units. These volcaniclastic rocks are the products of the early explosive stages of the basaltic volcanic episodes of eastern Australia, and they are chemically distinct (i.e., "more fractionated") from the surface basalts that are products of quieter episodes.

The Tertiary volcaniclastic rock units constitute prime exploration targets for alluvial sapphires (and associated minerals such as zircon and spinel) in eastern Australia and possibly in similar geologic provinces elsewhere (e.g., Southeast Asia). *AAL*

Alkaline rocks and gemstones, Australia: A review and synthesis. F. L. Sutherland, *Australian Journal of Earth Sciences*, Vol. 43, No. 3, 1996, pp. 323–343.

Valuable gemstones that occur in Australian alkaline rocks include diamonds in lamproites and kimberlites; sapphires, zircons, and rubies in alkali basalts; and one gem zircon prospect in carbonatite. This paper reviews the tectonic settings and origins of Australia's gem-bearing alkaline rocks.

There are marked contrasts between diamond and sapphire-zircon associations across the continent. Most western cratonic areas exhibit episodic, sparse, deep alkaline activity from the diamond zone (2 billion–20 million years [My] old). However, in eastern fold-belt areas, prolific Mesozoic/Cenozoic basaltic volcanism carried up considerable amounts of sapphire and zircon (since 170 My). Some South Australian Mesozoic kimberlitic diamond events (180–170 My) represent ultra-deep material rising through the mantle transition zone. Eastern Australian diamonds are unusual; at present, their origin is in dispute. Several different models compete to explain sapphire/zircon formation in eastern Australia. These range from eruptive plucking of metamorphosed subducted materials to crystallization from felsic melts to carbonatitic reactions. Pb-U isotopic zircon ages favor formation during Phanerozoic basaltic activity and not during earlier Paleozoic subduction or granitic-intrusion events. A problem for the theory that zircon crystallized from fractionated basaltic melts is negligible Eu depletion in rare-earth-element patterns.

The authors propose a model that favors sapphire/zircon crystallization from relatively small-volume, little-evolved, felsic melts that are generated from metasomatized mantle as the lithosphere overruns subdued hot spot systems, initiated at Tasman–Coral Sea margins. A unique ruby, sapphire, sapphirine, spinel assemblage from the Barrington basalt shield in New South Wales marks a separate ruby/pastel-colored-sapphire genesis. *RAH*

Country summaries. *African Mining Supplement to Mining Journal, London*, January 26, 1996, pp. 7, 9, 13, 15, 17, 19, 21, 23.

This article summarizes mining activities, by country, for African nations in 1994. Reports relevant to gemstones—primarily diamonds—include those for:

- Angola, where only state-owned Endiama, or its joint ventures, can hold diamond-mining rights. Alluvial mining totaled 1.25 million carats (Mct) in 1992, but official production has collapsed since.
- Botswana, the second biggest producer of gem diamonds after Russia. Recovery from Jwaneng, Orapa, and Letlhakane rose 6%, to 15.5 Mct in 1994. The value of diamond exports rose 1%, to US$1.4 billion.
- The Central African Republic, with official production figures of 530,000 carats annually.
- Congo, where traces of diamonds were found near the border with the Central African Republic and on the island of M'bamu, near Brazzaville.
- Ivory Coast, where two diamond mines, at Tortiya and Séguéla, produce about 15,000 carats annually.
- Ghana, which produced about 750,000 carats of diamonds in 1994.
- Guinea; production at Aredor's diamond mine at Banankoro was suspended in 1994.
- Liberia, where illicit gold- and diamond-mining activity continued around the Lofa River, on the border with Sierra Leone.
- Malawi, which continues to have "extremely limited" production.
- Mali; 20 kimberlite pipes have been found in the southwest, but no production has begun.
- Namibia, a major diamond producer (over one-third of its export income comes from diamonds). Production from onshore and offshore deposits rose 15% in 1994, to 1.31 Mct (95% of which was gem quality), mostly from Namdeb (or its predecessor Consolidated Diamond Mines).
- Sierra Leone; diamond production from the eastern Kono region generated 255,000 carats of exported diamonds, valued at US$30.2 million. Civil unrest disrupted mining in most other areas.
- South Africa, which produced 10.8 Mct of diamonds in 1994, split 90%-9%-1% among kimberlites, alluvial mines, and offshore production.
- Swaziland; the Dolokwayo mine processes 600,000 tons of diamond ore per year (but no production figures were given).
- Tanzania, where production at the dilapidated Williamson mine fell to 22,567 carats in 1994. However, changes in ownership may lead to overhaul, and exploration continues.
- Zaire, where 16 Mct of diamonds were produced—11 Mct from artisanal working and 5 Mct from the Bakwanga (Miba) mines. Coffee is now the leading export.
- Zimbabwe; Auridiam produced 15,000 carats from the River Ranch deposit. Two-thirds of the country is covered with prospecting orders, mostly for diamonds. *MLJ*

An evaporitic origin of the parent brines of Colombian emeralds: Fluid inclusion and sulphur isotope evidence. G. Giuliani, A. Cheilletz, C. Arboleda, V. Carillo, F. Rueda, and J. H. Baker, *European Journal of Mineralogy*, Vol. 7, No. 1, 1995, pp. 151–165.

This paper presents the results of microthermometry, SEM, and Raman probe examination of emeralds and gangue minerals, as well as the first sulfur isotopic data on pyrite, from seven Colombian emerald deposits. Also discussed is the origin of the hydrothermal fluids that formed the carbonate-pyrite-emerald vein mineralization in Colombia.

The fluid-inclusion study shows the presence of homogeneous and hypersaline brines; the isotope study suggests a uniform sulfur isotopic composition for the fluids and a heavy, probably unique, sulfide-sulfur source for emerald deposits of both the western and eastern emerald zones. Considering the presence of salt diapirs and gypsum diapirs in the area, the authors conclude that "the only likely and unique source of sulphur might be derived from evaporites through a sulphate reduction process at the site of mineral precipitation." These results, together with those of previous studies, support the interpretation of hydrothermal emerald mineralization in a sedimentary environment. In that respect, the Colombian emerald deposits differ dramatically from almost all other emerald sources. *RT*

Opal safari. J. F. Watson, *Australian Gold Gem & Treasure*, Vol. 11, No. 2, February 1996, pp. 27–31.

Mining for black opals continues in the area of New South Wales, Australia. Although Lightning Ridge proper is the most popular tourist destination, the author visited the more remote opal fields at Grawin, Glengarry, and Sheep Yards. Most of the miners in the Grawin and Sheep Yards area dig down 9–12 m to reach the working level. Prospecting entails two stages: A drilling rig makes a 17.5-cm-diameter test hole down to the working level; if the hole looks promising, a 1-m-diameter shaft is drilled after the claim is registered.

Most of the opal mined is "potch," or common opal, usually gray, "amber," or black; a black-and-white variety is known locally as "magpie" potch. Only 5% shows play-of-color, and only 5% of that (0.25% altogether) is classified as "precious gem quality" opal. Gem opal sitting on black potch is the most desirable.

The Grawin opal fields were discovered in 1907, and all three opal fields (Grawin, Glengarry, and Sheep Yards) have been extensively mined. However, amateur collectors continue to find opals in the "mullock heaps" (dumps). The author warns the unwary of the area's many unmarked mine shafts; a fall down one is almost certainly fatal. In nearby Cumborah, "crystal clear" quartz and petrified wood can be collected. *MLJ*

Vietnam's illegal miners. *Mining Journal, London*, April 5, 1996, p. 252.

Vietnam's National Assembly passed a new mining law, scheduled to take effect in September 1996, that grants foreign investors the right to exploit certain mineral resources, including gemstones. The law gives foreign companies the right to "store, transport, consume domestically and export minerals they exploit." However, the first enforcement activity is expected to be aimed at small-scale operations in regions overrun by fortune seekers: In particular, the conditions of child laborers in mining camps—primarily gold mining camps—in the north of the country will be addressed. *MLJ*

INSTRUMENTS AND TECHNIQUES

Scanning near-field optical microscopy (SNOM) and its application in mineralogy. W. Gutmannsbauer, T. Huser, T. Lacoste, H. Heinzelmann, and H.-J. Güntherodt, 1995, *Schweizerische Mineralogische und Petrographische Mitteleitung*, Vol. 75, pp. 259–264.

The technique described uses visible radiation (light) to observe sub-micron-sized features in mineral samples. Bluish green light from an argon-ion laser is transmitted though an optic fiber with a very narrow tip (around 50 nm in diameter); the tip is scanned across the sample, and light transmitted through the sample is collected and displayed as a function of position. The resulting two-dimensional image has a resolution on the order of 0.5 micron or better.

The authors examined 25-micron-thick transparent thin sections (with parallel front and back faces) for this paper, but they believe that reflected light could also be collected, enabling study of opaque samples. The technique could be adapted to multi-wavelength (color) observation if a tunable laser were used; it should also be adaptable for fluorescence, cathodoluminescence, Raman spectroscopy, and infrared spectroscopy. As described in this paper, however, the potential usefulness of this technique in gem testing is very limited, as the sample must be a transparent, well-polished thin section. *MLJ*

JEWELRY RETAILING

Saleroom report: June results buoy London market. *Retail Jeweller*, July 11, 1996, p. 8.

June was a bumper month for London jewelry sales; Christie's and Phillips both did well. Christie's June 19 sale was the greater success, with a £4,299,975 total. Buyers from 26 countries competed actively on the phone, in the room, and in the book; more than 60% were private clients.

A pair of rare antique Indian diamond briolettes more than doubled their estimate, to sell to the trade at £115,500. An antique emerald, diamond, and pearl necklace, estimated at £30,000–£35,000 brought in £89,500, and a fancy intense yellow diamond ring—estimated at £40,000–£50,000—sold to an anonymous buyer for £122,500. A typical Belle Epoque garland-style diamond necklace brought an extraordinarily high £73,000. The overflow from these refined Christie's sales goes to the ever-popular Christie's South Kensington, which boasted its best-ever sale on June 18.

Phillips's fine jewelry sale on June 27 was highlighted by a group of 19th-century jewels by French gothic-revival goldsmith Louis Wiese. A heavy neo-gothic bangle, mounted with a large cabochon sapphire and flanked by leopard heads, went above estimate for £21,850. A gold lozenge-shaped brooch with matching ring, again set with cabochon sapphires and with pearls, sold for £6,670. A heavy neo-Renaissance gold, cameo, and pearl locket and chain made £26,450. Buyers also showed a good appetite for old-cut Victorian diamonds. A diamond rivière necklace from about 1880 sold for £10,350, more than doubling its estimate. A late-Victorian pearl and diamond bangle, estimated at £1,200–£1,500, sold for £3,220. Solitaire diamond rings sold particularly well to private buyers. *MD*

SYNTHETICS AND SIMULANTS

Harder than diamond? R. W. Cahn, *Nature*, March 14, 1996, pp. 104–105.

Theorists have predicted a structure of carbon nitride that should be harder than diamond, and experimentalists are trying to make it. The predicted material, cubic C_3N_4, has the same structure as Si_3N_4. Attempts to make this compound by vapor deposition have been hampered by the difficulty in getting enough nitrogen into the material; graphite-like structures and films with triple-bonded (acetylene-like) carbon form instead. Annealing of the latter gets rid of the triple bonds and produces a film that has diamond-like electrical properties but much lower hardness than diamond thin films. It is possible that "superhard" C_3N_4 can be produced by high-pressure synthesis methods. *MLJ*

Metastable diamond synthesis—Principles and applications. C.-P. Klages, *European Journal of Mineralogy*, Vol. 7, No. 4, 1995, pp. 767–774.

Chemical vapor deposition (CVD) of diamond films from activated gas phases was first achieved in 1952–53, but only since 1983 has it become an important and rapidly developing field of research. This paper summarizes the principles, results, and perspectives of CVD technology. It starts with a description of the conditions in which diamond thin films crystallize from gas phases and the many deposition processes now available. The growth of textured and hetero-epitaxial diamond films on different substrates, especially silicon, is discussed and illustrated with scanning electron micrographs. The author then outlines the many applications of diamond films (from high-frequency electronic devices to optical filters to membranes for loudspeakers) and gives an outlook on their future potential.

Although not mentioned in this comprehensive article, the possible consequences for gemology (e.g., the coating of gems, especially diamond simulants) should be kept in mind. *RT*

UF engineers' patented process makes world's largest synthetic diamond. *Diamond Industry Week*, February 12, 1996, p. 1.

Researchers James Adair and Rajiv Singh at the University of Florida (and their coworkers and industrial collaborators) have made the largest synthetic diamond known to date—about 1600 ct. It was grown by a low-temperature (to as low as 500°C) vapor-deposition technique; color and clarity were not specified, but its dimensions (11 inches [about 28 cm] in diameter and 1.5 mm thick) would seem to preclude any gemstone application. The prospects for large-scale diamond coatings look very promising, however. *MLJ*

TREATMENTS

A fact of life: Treatments are forever. *Mazal U'Bracha*, No. 79, June 1996, pp. 33–40.

Highlights of the 27th World Diamond Congress in Tel Aviv included the general agreement that a standard nomenclature must be devised to cope with the rising numbers of fracture-filled, enhanced, and treated diamonds entering the market. Some congress members expressed concern about fracture-filled rough; Howard Vaughan of De Beers said that the CSO would never sell treated or filled rough. He added, however, that De Beers could not prevent manufacturers from treating or filling rough they had purchased from De Beers.

In other action, a trade development committee of international diamond dealers was formed to promote "exchange" (presumably an exchange of ideas, although the article does not say specifically) with developing Asian markets. The World Federation of Diamond Bourses agreed to look into the feasibility of creating a computer network.

Addressing the Israeli Diamond Manufacturers Association, Yvegeny Bychkov, head of the Association of Russian Diamond Manufacturers, noted that Russia is the only country that both mines (about US$1.4 billion in 1995) and cuts a substantial amount of diamonds. Twenty-five percent of all diamonds mined are Russian, and 7,000 people are employed by Russia's 60 manufacturers. Although Mr. Bychkov predicted that Russia would expand its cutting operations, he also warned that the fledgling industry could be strangled by "hard conditions imposed by De Beers." *AC*